Linking Metabolic Rates with the Diversity and Functional Capacity of Endolithic Microbial Communities within Hydrothermal Vent Structures

Linking Metabolic Rates with the Diversity and Functional Capacity of Endolithic Microbial Communities within Hydrothermal Vent Structures

A dissertation presented
by

Kiana Laieikawai Frank

to
The Department of Molecular and Cellular Biology

in partial fulfillment of the requirements
for the degree of
Doctor of Philosophy
in the subject of
Biology

Harvard University
Cambridge, MA

August, 2013

Dissertation Advisor: Professor Peter R. Girguis Kiana L. Frank

Linking Metabolic Rates with the Diversity and Functional Capacity of Endolithic Microbial Communities within Hydrothermal Vent Structures

ABSTRACT

At hydrothermal vents, thermal and chemical gradients generated by the mixing of hydrothermal fluids with seawater provide diverse niches for prokaryotic communities. To date, our knowledge of environmental factors that shape bacterial and archaeal community composition and metabolic activities across these gradients within the active sulfide structures is limited. While many studies have laid the foundation for our understanding of the extent of diversity in relation to varying hydrothermal settings, few studies exists regarding the detailed spatial relationships between vent geochemistry and the abundance, distribution, and metabolic characteristics of the endolithic hosted communities. Even fewer data have been generated on the magnitude of metabolic rates and factors controlling the kinetics of these reactions have not been well constrained.

The overarching goal of this thesis is to better understand microbially mediated sulfur cycling at hydrothermal vents by allying phylogenetic identity to metabolic potential and rates of sulfur metabolism within hydrothermal chimneys. This work features the use of an *in situ* sulfide microbial incubator to characterize *de novo* endolithic prokaryotic communities with spatially co-registered temperature within a hydrothermal vent chimney, as well as laboratory studies of communities using radioisotopic ^{35}S-tracer techniques to elucidate their metabolic activities. Based on analyses of taxonomic and metagenomic data, the observed differences in

community composition reflect the physiological tolerances of specific microbial taxa, as well as the net metabolic capacities of each community. The rates of sulfate reduction presented here further suggest that-within anaerobic niches of hydrothermal deposits-heterotrophic sulfate reduction may be quite common and can contribute substantially to secondary productivity, underscoring the potential role of this process in both sulfur and carbon cycling at vents. Direct metabolic rate measurements, in particular of sulfate reduction, will in conjunction with the *in situ* incubations facilitate defining key environmental and energetic parameters for microbial community colonization in hydrothermal sulfide. Better understanding of the metabolic and taxonomic relationship of these endolithic communities in the geochemical context of hydrothermal vents will help to constrain the microbial impact on global biogeochemical cycling.

TABLE OF CONTENTS

LIST OF TABLES

LIST OF FIGURES

Figure

DEDICATION

to the woman who made me who I am today, inspired me to pursue my passions and supported me since the beginning

ACKNOWLEDGEMENTS

I am sincerely grateful to all the people who encouraged my passions, provided constant support and played a unique role in shaping the person and scientist into whom I have evolved. The love and support of my family, friends, mentors and colleagues helped see me through some of the roughest moments of my life and encouraged me to finish my PhD with my best foot forward.

First and foremost I would like to thank my advisor Peter Girguis who gave me the guidance, support, freedom and tools allowing me to grow as a scientist and individual, find my bearings when I got off track and jimmy rig a piece of equipment with limited supplies. Not only did Pete help to develop me into a better scientist, but he especially helped to refine my communication skills giving me the capacity to package my science in the most accessible form and deliver it with a bang. I would also like to thank my committee members Colleen Cavanaugh, Andy Knoll and Briana Burton for their constant support and constructive feedback on my research and their helpful advice on achieving my career goals.

I am incredibly fortunate to have been a member of such a wonderful and diverse group of Girgoyles. The diverse background of my lab mates and collaborative nature our lab provided me with unique perspectives on my research and opportunities to learn new. I am so lucky that my lab mates are not just my colleagues, but my friends and family who will throw down at lab dance battles, pig out at pie palloozas, class it up at lunch club and spend 24/7 on a boat doing smelly science with me. I am especially grateful to my MVPD's (most valuable post docs) Mark Nielsen and Dan Rogers, who pulled me through my qualifying exams, helped me with fellowship proposals, read almost every draft I've ever written, edited my slides, explained

difficult papers and concepts and calmed my nerves during those times of existential grad school life crisis. I am also eternally indebted to Roxie Beinart, Heather Olins and John Skutnik for being the backbone support of my graduate career- my daily partners in science, sounding board for ideas and questions, copy editors, muscle and on many occasions' personal chiefs and therapists.

I would furthermore like to thank Steve Sansone, Julie Hanlon and Joe Ring for helping me with the technical aspects of physically doing the type of science that I did. I would like to thank collaborators Dave Johnston, Deb Kelley, Geoff Wheat, Beth Orcutt, Karyn Rogers, Matt Schrenk and Brian Glazer for providing opportunities, feedback and support throughout my graduate career. I am also especially grateful for the hard work and dedication of Mike Lawrence and Debbie Maddalena who made navigating the graduate processes easy and served as some of my strongest advocates for fellowships.

Finally I would like to thank my parents Francine and Stephen and my siblings Kainoa, Keoni and Kalae for their undying support, love and guidance. I am incredibly proud to be their daughter and sister. Everything that I am and everything that I have accomplished is due to their encouragement, sacrifice and aloha.

This work was supported by an NSF and C-DEBI graduate research fellowship, and grants Nation Science Foundation (OCE-0838107 and OCE-1061934 to P.R. Girguis and OCE-0838107 and OCE-0426109 to D.S. Kelley), and the National Aeronautic and Space Administration (NASA-ASTEP NNX09AB78G to C. Scholin and P. R. Girguis and NASA-ASTEP NNX07AV51G to A. Knoll and P. R.Girguis).

CHAPTER ONE:

Endolithic microbes at hydrothermal vents: detection and metabolic diversity

1.1 Introduction

Deep sea hydrothermal vents are one of our planet's most extreme environments. Sites of ocean crust formation, plate separation and global heat loss, hydrothermal vents are ubiquitous along the mid-ocean ridge system and also occur in other locales, e.g., back-arc basins and seafloor volcanoes. Hydrothermal vents play a significant role in (bio)geochemical cycles, as it is estimated that the entire volume of the global ocean circulates through these systems once every 70,000 to 200,000 years (Wheat *et al.* 2003; Mottl & Wheat 1994). In these environments, abiotic reactions between rock and hydrothermal water significantly impact the geochemical cycling of elements. Indeed, through these reactions, the crust becomes a significant sink for sulfate and magnesium and source of manganese, iron, lithium, rubidium, cesium and ^{3}He to the ocean reservoir (Elderfield & Schultz 1996). Because of variations in spreading rate, crustal composition and fluid dynamics, individual vent structures and fluids can vary widely in physical and chemical composition. While the precise extent of their impact on heat and geochemical flux remains to be constrained, it is apparent that hydrothermal systems have a marked influence on the oceans' heat budget, currents and the chemical weathering of oceanic crust.

The unique geochemical characteristics of hydrothermal vents enable these environments to support thriving, dense and diverse populations of organisms. Here, chemoautotrophic microbes–those which fix carbon via the energy derived from the oxidation of reduced chemicals–form the base of the ecosystem. The mixing of reduced hydrothermal vent fluids and oxidized seawater creates geochemical energy gradients, which support the growth of diverse microbial populations (Schrenk *et al.* 2003; McCollom & Shock 1997). Culture-

independent approaches used to investigate hydrothermal vent microbial diversity have identified many novel lineages of uncultivated bacteria and archaea and show that diversity varies with geological setting, hydrothermal fluid composition, mineralogy, and chimney age (Takai *et al*. 2001; Schrenk *et al*. 2003; Suzuki *et al*. 2004; Opatkiewicz *et al*. 2009; Kormas *et al.* 2006; Brazelton *et al*. 2010; Hoek *et al*. 2003; Ehrhardt *et al*. 2007; Perner *et al.* 2007; Page *et al*. 2008; Anderson *et al*. 2012; Teske 2006; Huber *et al.* 2007; Sogin *et al*. 2006). *Epsilonproteobacteria* are commonly the dominant bacterial taxa, but other groups such as *Aquificales*, *Deltaproteobacteria*, *Gammaproteobacteria, Thermales*, *Thermotogales*, and *Thermodesulfurobacteriaceae* are also commonly identified from vents (Schrenk *et al*. 2003; Suzuki *et al*. 2004; Kormas *et al.* 2006; Nakagawa & Takai 2008; Jaeschke *et al*. 2012; Reysenbach *et al*. 2000; Wery *et al*. 2002; Takai *et al.* 2006b; Nakagawa *et al.* 2005b). Common archaeal lineages identified at vents tend to be thermophillic and associate to *Aciduliprofundales (DHVE2), Archaeoglobales*, *Desulfurococcales*, *Methanococcales* and *Thermococcales* (Page *et al.* 2008; Reysenbach & Longnecker 2000; Takai & Nakamura 2011; Huber *et al*. 2002; Jaeschke *et al*. 2012; Schrenk *et al.* 2003; Takai *et al.* 2001). Cultivated organisms from this environment suggest that a wide range of metabolic capabilities is available to support both autotrophic and heterotrophic microorganisms, including–but not limited to–the oxidation of hydrogen (Jeanthon *et al.* 2002; Takai *et al.* 2005b; Takai 2004; Nakagawa *et al.* 2004a), sulfide (Takai *et al.* 2006a, 2006b; Mori & Suzuki 2008; Inagaki 2003), Fe(II) (Edwards *et al.* 2003), Mn(II) (Templeton *et al.* 2005; Dick *et al.* 2006; Fernandes *et al.* 2005) and the reduction of nitrate (Nakagawa *et al*. 2005c), sulfate (Alazard *et al*. 2003; Huber *et al*. 1997; Jeanthon *et al*. 2002; Audiffrin *et al*. 2003), Fe(III) (Slobodkina *et al.* 2009; Sokolova

et al. 2007; Kashefi *et al.* 2002; Hirayama *et al.* 2007) and CO_2 (Takai *et al*. 2000b, 2002, 2004; L'Haridon *et al.* 2003).

The metabolic processes occurring in vent systems are of particular interest because they may be analogs of the first living systems to evolve on Earth (Martin *et al.* 2008). Community diversity and dynamics along complex and spatially compressed gradients of temperature and chemistry can also lead to ecological hypotheses about biochemical adaptations to extreme environments, when and where life may have evolved on a hot early Earth, the depth to which life may exist in the Earth's subsurface, and the potential for life in extraterrestrial environments. While we posit that hydrothermal vent organisms may have a strong impact on fluid chemistry, rock permeability and vent ecology, the details and extent of these impacts have not been well constrained. This review will focus on hydrothermal endolithic microbial metabolic modes and their potential implications in biogeochemical cycling.

1.2 Temporal and Spatial Microbial Colonization

The fundamental drivers of microbial succession, distribution and activity within hydrothermal vents are likely to be substrate availability and temperature. Endolithic microorganisms–those living within the interstitial spaces of minerals and mineral deposits–must be able to use available substrate efficiently and tolerate extreme environmental conditions. Over the decades-long lifetime of a typical hydrothermal vent, the precipitation, dissolution, and partitioning of different mineral components and the dynamic mixing of hydrothermal fluid and seawater create temporal and spatial variations in aqueous and mineral

substrate availability for energy utilization and biomass production. In the early stages of chimney formation, anhydrite (calcium sulfate; $CaSO_4$) precipitates from exiting hydrothermal fluids. As the anhydrite sheath thickens it insulates and isolates hydrothermal fluid from seawater, eventually allowing for the deposition of an inner zone of chalcopyrite ($CaFeS_2$) as fluids no longer become oxidized immediately by mixing with seawater. As chimneys mature, hydrothermal fluid continues to percolate horizontally through chimney walls until all pore spaces are filled with anhydrite or other (copper-iron) sulfates. As the outer anhydrite wall cools below 150°C, anhydrite dissolves back into seawater and, over time, amorphous silica begins to precipitate in pore spaces (Tivey 1995).

In response to chemical and physical changes during chimney senescence, the endolithic community undergoes a series of successive changes in taxonomic composition and abundance that take place on the order of hours (McCliment *et al.* 2006; Page *et al.* 2008) or days (Guezennec *et al*. 1998; Nercessian *et al.* 2003; Reysenbach *et al*. 2000) or years (Huber *et al*. 2002). The metabolic capacity of the community changes as a direct result of interactions among the microbes, their environment and cohabitants. Differences observed in archaeal 16S rRNA gene sequences suggest that the unique mineralogical and chemical composition (Tivey 1995) of young "proto-chimney" structures supports pioneering autotrophic archaeal communities distinct from those of mature chimneys (Page *et al.* 2008; McCliment *et al.* 2006). As the underlying chimney structure matures, microbial biomass accumulates and the phylogenetic diversity of the communities increases (Jackson *et al.* 2001, 2003). Once sufficient organic carbon has accumulated, communities apparently shift from predominately chemolithoautrophs to communities dominated by heterotrophic thermophiles, although

conclusive evidence is limited (Reysenbach & Longnecker 2000; Page *et al.* 2008). As the vent communities "stabilize", microbes may become less sensitive to particular environmental stresses facilitated by their increased ability to modify the microbial habitat (e.g. biofilm production) or by increases in the abundances of taxa that are either resilient or resistant to the stresses (Besemer *et al.* 2007; Schimel *et al.* 2007). Eventually, hydrothermal fluid flow within the structure ceases due to changes in the underlying geology, rendering the sulfide extinct. Without the input of hydrothermal fluids, thermal and chemical conditions within the chimney will tend to reflect ambient seawater, and the associated biota shifts to very different archaeal and bacterial communities (Brazelton *et al.* 2010; Sylvan *et al*. 2012; Toner *et al.* 2013).

Depending on the environmental setting and fluid composition, multiple chimney types are possible. For example, black smoker chimneys are typically columnar, and have redox gradients created by both the advection of heat and diffusion of fluids. This type of chimney is characterized by extremely high temperature fluid (>300°C) that is acidic, rich in metals (iron, copper, zinc) and sulfide, and contained within a central conduit (Tivey 1995). In contrast, white smokers emit fluids of intermediate temperatures (100-300°C) that precipitate silica, anhydrite and barite but have low concentrations of metals and sulfide. More diffuse chimneys, which lack a central conduit, are extremely porous and fragile and can support high temperature fluids (> 300°C). Flanges form as lateral outgrowths from sulfide mounds; these trap pools of buoyant high temperature fluids beneath them, often creating a visible mirror-like interface. Within flanges, the porosity and thermal conductivity of mineral assemblages affect the thermal gradients (Tivey 2000).

Variability in the extent of mixing between hydrothermal fluid and seawater across each type of chimney creates a diversity of potential endolithic microbial habitats poised at a range of redox potentials capable of supporting life through varied metabolisms. The fluids that are produced by hydrothermal activity vary as a function of the temperature of the magma chamber (which, for example, can cause phase separation and result in fluids with ionic compositions greater or less than saltwater), the petrological setting (e.g. the extent of terrestrial influence in the crust), and even fluid residence time. Thus, fluids within a chimney can range from near freshwater to brines, from pHs around 2 to circumneutral, temperatures from tens of degrees Celsius to over 450 °C, and a wide range of geochemical compositions (e.g. sulfide, dissolved metal, methane, carbon dioxide concentrations).

The first data to show the extreme spatial heterogeneity of microbial communities within vent habitats were reported in 1992 by Hedrick and colleagues (Hedrick *et al.* 1992) who analyzed lipids in vent environments. Since then, using a variety of 16SrDNA molecular and lipid geochemistry techniques, microbiologists have shown outer chimney walls to be colonized by mesophillic and slightly thermophillic autotroph and heterotroph phylotypes (Takai *et al.* 2001; Hoek *et al.* 2003; Schrenk *et al.* 2003; Nakagawa *et al*. 2005b; Kormas *et al*. 2006; Page *et al*. 2008). The warm interiors of chimneys support a higher prevalence of hyperthermophillic archaeal phylotypes (such as *Thermococcales, Archaeoglobales, Methanococcales, Thermoproteales Korarchaeota, Desulfurococcales;* Page *et al.* 2008; Schrenk *et al.* 2003; Jaeschke *et al.* 2012). The composition and structure of these endolithic communities are likely a direct result of physical, thermal and geochemical parameters of their habitats, but demonstrating direct correlations have proven difficult. Though our knowledge is very limited

within hydrothermal chimneys themselves, a recent comprehensive study revealed a direct correlation between geochemistry (specifically total organic carbon, iron, manganese and sulfate) and total prokaryotic community distribution within hydrothermal Mid-Atlantic Ridge sediment (Jørgensen *et al.* 2012). This study provides quantitative evidence that organic carbon is one of the fundamental factors shaping microbial communities and suggests that mineralogy is also a key determinant of the relative abundances of microbial taxa (Jørgensen *et al.* 2012).

1.3 Potential Metabolic Diversity of Endolithic Microbes

Within hydrothermal vents, the potential electron donors available for microbial redox reactions include H_2, H_2S, S, $S_2O_3^{2-}$, $S_4O_6^{2-}$, sulfide minerals, CH_4, Fe^{2+}, Mn (and other reduced metals), various mono-, di-, and hydroxy-carboxylic acids, alcohols, amino acids, and complex organic substrates; electron acceptors include O_2, Fe^{3+}, CO_2, CO, NO_3^-, NO_2^-, NO, N_2O, SO_4^{2-}, SO_3^{2-}, $S_2O_3^{2-}$, and S. The abundance and availability of these substrates are directly linked to the mixing of hydrothermal fluid and seawater, resulting in steep gradients in available redox couples and free energy within a chimney structure. Thermodynamic calculation of the Gibbs free energy change (ΔG_r) of redox reactions (McCollom & Shock 1997; Tivey 1995; Amend & Shock 2001) can predict the potential energy yields of the different metabolisms available in hydrothermal systems dependent on ecosystem conditions and fluid compositions. The transition between oxidizing and reducing conditions plays the prominent role in establishing which metabolic reactions are favorable. Geochemical models predict that at low temperatures, within the outer regions of the chimney wall, oxidative metabolisms (such as sulfide, sulfur, thiosulfate, methane, manganese (II) and iron oxidation) yield the most energy.

At higher temperatures, in the interior of the chimney, the reducing anaerobic conditions favor reductive processes (sulfur reduction, sulfate reduction and methanogenesis; McCollom & Shock 1997; Tivey 2000). While geochemical predictions of microbial metabolisms have yet to be completely verified based on microbiological community structure and activity, Table 1.1 depicts the metabolic modes potentially exploitable within hydrothermal vents and the isolates known to utilize them in culture.

1.3.1 Hydrogen Metabolism

Hydrogen concentrations within hydrothermal fluid in most systems can vary from 0.05-1 mmol kg^{-1} due to reactions of seawater with the mantle source rocks; thus, hydrogen is a key electron donor for many chemoautotrophic metabolisms (Takai *et al.* 2005a). Nickel-Iron (NiFe) membrane-bound hydrogenases are the key enzymes responsible for metabolizing hydrogen. Hydrogen is oxidized by the membrane-bound hydrogenase proton pump, and the electrons are transfered to various quinones and cytochromes (Bowien & Schlegel 1981). Chemoautotrophs with the ability to derive energy from hydrogen oxidation, including *Aquificales, Epsilonproteobacteria, Desulfurococcales, Methanococcales, Thermodesulfobacteriales and Defferibacterales,* have been isolated from various deep sea hydrothermal fields (Table 1.1).

Table 1.1: Potential Microbial Metabolisms within Hydrothermal vent Environments

Energy Metabolism	Overall Chemical Reaction	ΔG_r° (kJ mol^{-1})*	Cultured Isolates from Hydrothermal Systems
Hydrogen Metabolism			
Hydrogenotrophic O_2-reduction	$H_2 + 1/2O_2 \rightarrow H_2O$	-264, -249	Bacteria: *Caminibacter profundus* (Miroshnichenko *et al*. 2004), *Hydrogenivirga caldilitoris* (Nakagawa *et al*. 2004a), *Hydrogenimonas thermophila* (Takai 2004), *Sulfurimonas paralvinellae* (Takai *et al.* 2006b). Archaea: *Pyrolobus fumarii* (Blöchl *et al.* 1997)
Nitrogen Metabolism			
Nitrification (NO_2^- oxidazing O_2 reduction)	$NO_2^- + ½\ O_2 + 2OH^- + 2H^+ \rightarrow NO_3^- + 2H_2O$	-87.5, -78.4	Not detected
Nitrification (NH4-oxidazing O_2 reduction)	$NH_4^+ + 2O_2 \rightarrow NO_3^- + H_2O + H^+$	-315 (Strous *et al*. 1998)	Bacteria (Mevel *et al*. 1987)
Hydrogenotrophic denitrification	$H_2 + 2/5\ NO_3^- + 2/5H^+ \rightarrow 1/5\ N_2 + 6/5H_2O$	-637, -631	Bacteria: *Nitratifractor salsuginis Nitratiruptor tergarcus* (Nakagawa *et al*. 2005c).
Hydrogenotrophic ammonification	$H_2 + ¼\ NO_3^- + ½\ H^+ \rightarrow ¼\ NH_4^+ + ¾\ H2O$	-150 (Cord-ruwisch *et al.* 1988)	Bacteria: *Caminibacter hydrogeniphilus* (Alain, *et al.* 2002b),*Caminibacter mediatlanticus* (Voordeckers *et al*. 2005), *Caminibacter profundus* (Miroshnichenko *et al*. 2004), *Thioreductor micantisoli* (Nakagawa *et al*. 2005a). Archaea: *Pyrolobus fumarii* (Blöchl *et al*. 1997)
Anoxic ammonia-oxidation	$NH_4^+ + NO_2^- \rightarrow N_2 + 2H_2O$	-358 (van de Graaf et al. 1996)	Activity measurements (Byrne *et al.* 2009)
Sulfur Metabolism			
Hydrogenotrophic SO_4^{2-} -reduction	$H_2 + SO_4^{2-} + 2H+ \rightarrow ¼\ H_2S + H_2O$	-300, -335	Bacteria: *Desulfovibrio hydrothermalis* (Alazard *et al*. 2003), *Desulfonauticus submarines* (Audiffrin *et al.* 2003), *Thermodesulfobacterium hydrogeniphilum* (Jeanthon *et al.* 2002)
Hydrogenotrophic $S_2O_3^{2-}$ reduction	$S_2O_3^{2-} + 2H^+ + 4H_2 \rightarrow 2H_2S + 3H_2O$	-312, -352	Bacteria: D*esulfovibrio hydrothermalis* (Alazard *et a*l. 2003), *Desulfonauticus submarines* (Audiffrin *et al*. 2003), *Sulfurimonas paralvinellae* (Takai *et al*. 2006b). Archaea: *Archaeoglobus veneficus* (Huber *et al*. 1997), *Ferroglobus placidus* (Hafenbradl *et al*. 1996), *Pyrolobus fumarii* (Blöchl *et al*. 1997), *Stetteria hydrogenophila* (Peinemann-simon *et a*l. 1997)

*at P_{SAT} calculated at two temperatures (20°C, 200°C) from Amend & Shock 2001 unless otherwise cited

Table 1.1 Continued.

Energy Metabolism	Overall Chemical Reaction	ΔG_r° (kJ mol^{-1})*	Cultured Isolates from Hydrothermal Systems
Hydrogenotrophic S-reduction	$H_2 + S_0 \rightarrow H_2S$	-44.8, -51.0	Bacteria: *Caminibacter hydrogeniphilus* (Alain *et al.* 2002b), *Caminibacter mediatlanticus* (Voordeckers *et al.* 2005), *Caminibacter profundus* (Miroshnichenko *et al.* 2004), *Deferribacter desulfuricans* (Takai 2003), *Desulfonauticus submarines* (Audiffrin *et al*. 2003), *Lebetimonas acidiphila* (Takai *et al.* 2005*b*), *Nautilia profundicola* (Smith *et al*. 2008), *Sulfurimonas paralvinellae* (Takai *et al*. 2006b), *Thioreductor micantisoli* (Nakagawa et al. 2005a). Archaea: *Acidianus infernus, A. berleyi* (Sergerer et al. 1986), *Methanocaldococcus indicus* (L'Haridon *et al*. 2003), *Methanococcus infernos* (Jeanthon *et al*. 1998), *Methanococcus vulcanius* (Jeanthon *et al.* 1999), *Stetteria hydrogenophila* (Peinemann-simon *et al*. 1997)
Heterotrophic SO_4^{2-} reduction	$CH_3CHOOH + SO_4^{2-} \rightarrow H_2S + 2HCO_3^-$ $4HCO_2^- + SO_4^{2-} \rightarrow 2HCO_3^- + HS^-$ $2\ CH_3CHOHCOO^- + SO_4^{2-} \rightarrow 2\ CH_3CHOO^- + 2\ HCO_3^- + HS^- + H^+$ $2\ CH_3CHOHCOO^- + 3SO_4^{2-} \rightarrow 6HCO_3^- + 3HS^- + H^+$ See Rogers *et al.* 2006 for more examples	-47.6 -147 -160 -85	Bacteria: *Desulfovibrio hydrothermalis* (Alazard *et al.* 2003) Archaea: *Pyrococcus abyssi* (Erauso *et al*. 1993)
Heterotrophic S_0 reduction	$HCOOH + S_0 \rightarrow CO_2 + H_2S$ $CH_3COOH + 4S_0 + 2H_2O \rightarrow CO_2 + 4H_2S$ $C2H5COOH + 7S_0 + 4H_2O \rightarrow 3CO_2 + 7H_2S$ $CH_3CH(OH)COOH + 6S_0 + 3H_2O \rightarrow 3CO_2 + 6H_2S$ See Rogers *et al.* 2006 for more examples	(See Rogers *et al*. 2006)	Bacteria: *Marinitoga piezophila* (Alain *et al*. 2002a), *Nautilia profundicola* (Smith *et al*. 2008). Archaea (Belkin *et al*. 1985): *Thermococcus acidaminovorans* (Dirmeier *et al*. 1998), *Thermococcus alcaliphilus* (Braun *et al*. 1995), *Thermococcus barophilus* (Marteinsson *et al*. 1999), *Thermococcus barossii* (Duffaud *et al*. 1998), *Thermococcus onnurineus* (Bae *et al*. 2006), *Thermococcus profundus* (Kobayashi et al. 1994), *Thermococcus siculi* (Grote *et al*. 1999), *Pyrococcus abyssi* (Erauso *et al*. 1993), *Pyrococcus horikoshii* (González *et al*. 1998)
Thiotrophic (H2S-oxidizing) O_2-reduction	$H_2S + 2O_2 \rightarrow SO_4^{2-} + 2H^+$	-756, -659	Bacteria: *Thiobacillus hydrothermalis* (Durand *et al*. 1993), *Thiobacillus prosperus* (Huber & Stetter 1989), *Thiomicrospira crunogena* (Jannasch *et al*. 1985), *Sulfurimonas autotrophica* (Inagaki 2003).
Thiotrophic (S-oxidizing) O2-reduction	$S_0 + H_2O + 3/2O_2 \rightarrow SO_4^{2-} + 2H^+$	-537, -461	Bacteria: *Hydrogenivirga caldilitoris strain IBSK3* (Nakagawa *et al*. 2004a), *Thiobacillus hydrothermalis* (Durand *et al*. 1993), *Thiobacillus prosperus* (Huber & Stetter 1989), *Thiomicrospira crunogena* (Jannasch *et al*. 1985) , *Sulfurimonas autotrophica* (Inagaki 2003), *Sulfurovum lithotrophicum* (Inagaki *et al*. 2004),
Thiotrophic (S_2O^{3-} oxidizing) O2-reduction	$S_2O_3^{2-} + 2O_2 + H_2O \rightarrow 2SO_4^{2-} + 2H^+$	-739 (Kelly 1999)	Bacteria: *Thiobacillus hydrothermalis* (Durand *et al*. 1993), *Thiomicrospira crunogena* (Jannasch *et al*. 1985), *Sulfurimonas autotrophica* (Inagaki 2003), *Sulfurivirga caldicuralii* (Takai *et al*. 2006a), *Sulfurovum lithotrophicum*(Inagaki et al. 2004)
Thiotrophic denitrification	$S_2O_3^{2-} + 5/3NO_3^- \rightarrow 2SO_4^{2-} + 5/6\ N_2$	-751 (Kelly 1999)	Bacteria: *Sulfurovum lithotrophicum* (Inagaki *et al*. 2004)
S-disproportionation	$S_0 + H_2O \rightarrow 1/4SO_4^{2-} + 3/4H_2S + 1/2H^+$	120, 131	Not detected

Table 1.1 Continued.

Energy Metabolism	Overall Chemical Reaction	ΔG_r° (kJ mol^{-1})*	Cultured Isolates from Hydrothermal Systems
Metal Metabolism			
Hydrogenotrophic Fe(III)-reduction	$H_2 + 2Fe^{3+} \rightarrow 2Fe^{2+} + 2H^+$	-164, -201	Archaea: *Geoglobus ahangari* (Kashefi *et al*. 2002)
Fe(II)-oxidizing O_2-reduction	$Fe^{2+} + 1/4O_2 + H^+ \rightarrow Fe^{3+} + 1/2H_2O$	-65 (Edwards *et al*. 2005)	Bactiera: *Thiobacillus prosperus* (Huber & Stetter 1989)
Fe(II)-oxidizing denitrification	$Fe^{2+} + 1/5NO_3^- + 2/5H_2O + 1/5H^+ \rightarrow 1/10\ N_2 + Fe^{3+} + OH^-$	-100 (Edwards *et al*. 2005)	Archaea: *Ferroglobus placidus* (Hafenbradl *et al*. 1996)
Mn(II)-oxidizing O_2-reduction	$Mn^{2+} + 1/2O_2 + H_2O \rightarrow MnO_2(s) + 2H^+$	-50 (Edwards *et al*. 2005)	(Fernandes *et al*. 2005)
Heterotrophic Mn(IV) reduction	$CH_3COO^- + 4MnO_2 + 2HCO_3^- + 3H^+ \rightarrow 4MnCO_3 + 4H_2O$	-737 (Lovley & Phillips 1988)	Archaea: *Pyrococcus abyssi* (Erauso *et al.* 1993)
Arsenate Reduction	$½\ H_2AsO_4^- + ½\ H_2 \rightarrow ⅓As^0 + ½\ H_2O$ $⅓H_3AsO_3 + ½\ H_2 \rightarrow ⅓As^0 + H_2O$ $Acetate^- + 2HAsO_4^{2-} + 2H_2AsO_4^- + 5\ H^+ \rightarrow 4H_3AsO_3 + 2HCO$ $Lactate^- + 2HAsO_4^{2-} + 2H^+ \rightarrow 2H_2AsO_3^- + Acetate^- + HCO_3^-$	-115 (Newman & Ahmann 2009) -32 (Newman & Ahmann 2009) −172 (Stolz & Oremland 1999)	Bacteria: *Deferribacter desulfuricans* (Takai 2003)
Selenate Reduction	$½\ SeO_4^{2-} + ½\ H^+ + ½\ H_2 \rightarrow ½\ HSeO_3^- + ½\ H_20$ $Acetate^- + 4SeO_4^{2-} + H^+ \rightarrow 2CO_2 + 4SeO_3^{2-} + 2H_2O$ $Lactate^- + 2SeO_4^{2-} \rightarrow Acetate^- + 2SeO_3^{2-} + HCO_3^- + H^+$ $3\ Lactate^- + 2\ SeO_4^{2-} + H^+ \rightarrow 2\ Se(0) + 3\ acetate^- + 3\ HCO_3^- + 2\ H_2O$	−575 (Stolz & Oremland 1999) −343 (Stolz & Oremland 1999)	Not Detected
Selenite Reduction	$Lactate^- + SeO_3^{2-} + H^+ \rightarrow Se_0 + acetate^- + HCO_3^- + H_2O$ $Lactate^- + 2SeO_4^{2-} \rightarrow acetate^- + 2SeO_3^{2-} + CO_2 + H_2O$	-341, -354 -1046, -1146	Not Detected
Uranium Reduction	$Lactate^- + 3H_2O + 6UO_2^{+2} \rightarrow 6UO_2 + 3CO_2 + 12H^+$	-874, -1204	Not Detected

Table 1.1 Continued.

Energy Metabolism	Overall Chemical Reaction	ΔG_r° (kJ mol^{-1})*	Cultured Isolates from Hydrothermal Systems
C1 Metabolism			
Aerobic methanotrophy	$CH_4 + 2O_2 \rightarrow CO_2 + 2H_2O$	-859, -838	Bacteria
Anoxic methanotrophy with SO_4^{2-} -reduction	$CH_4 + SO_4^{2-} \rightarrow HCO_3^- + HS^- + H2O$	-40 (Dekas et al. 2009)	Archaea in association with bacteria
Anoxic methanotrophy with NO_3^- reduction	$5CH_4 + 8NO_3^- \rightarrow 5CO_2 + 4\ N_2 + 14\ H_2O$	-765 (Raghoebarsing et al. 2006)	Not detected
Hydrogenotrophic methanogenesis	$H_2 + ¼\ CO_2 \rightarrow ¼\ CH_4 + ½\ H_2O$	-195, 155	Archaea: *Methanocaldococcus indicus* (L'Haridon *et al*. 2003), *Methanococcus infernos* (Jeanthon *et al*. 1998), *Methanococcus jannaschi i*(Jones *et al*. 1983), *Methanococcus thermolithotrophicus* (Huber *et al*. 1982), *Methanococcus vulcanius* (Jeanthon *et al*. 1999), *Methanopyrus kandleri* (Kurr *et al*. 1991), *Methanothermococcus okinawensis* (Takai *et al*. 2002), *Methanotorris formicicus* (Takai *et al*. 2004b)
Organic Metabolism (See Rogers & Amend 2006 for comprehensive listing)			
Respiration	$C\ H_2O + O2 \rightarrow CO_2\ H_2O$	-500 (Edwards *et al*. 2005)	Many genera of bacteria and archaea
Fermentation	$C\ H_2O \rightarrow ⅓C_2H_6O + ⅓CO_2$	-50 (Edwards *et al*. 2005)	Many genera of bacteria and archaea
Amino Acids Reduction	Ala, Arg, Asp, Glu, Gly, His, Ile, Leu, Lys, Met, Phe, Ser, Thr, Tyr, Val	(Rogers & Amend 2006)	Bacteria: *Rhodothermus obamensis* (Sako *et al*. 1996) Archaea: *Thermococcus fumicolans* (Godfroy *et al*. 1996)
Aldose Reduction	Arabinose, Xylose, Galactose, Glucose, Mannose	(Rogers & Amend 2006)	Bacteria: Rhodothermus obamensis (Sako *et al*. 1996)
Carboxylic Acid Reduction	Formate, Acetate, Succinate, Lactate, Propionate, Pyruvate	(Rogers & Amend 2006)	Bacteria: Rhodothermus obamensis (Sako *et a*l. 1996)
Organic Sulfur Reduction	Methanethiol, Dimethylsulfide	(Rogers & Schulte 2012)	Not detected, predicted by thermodynamics (Rogers & Schulte 2012)

*at P_{SAT} calculated at two temperatures (20°C, 200°C) from Amend & Shock 2001 unless otherwise cited

1.3.2 Nitrogen Metabolism

Nitrogen-utilizing microbes at vents can contribute to nitrogen cycle via ammonification, nitrification and nitrogen reduction. Ammonia, produced by the thermal degradation of organic compounds in sediment, is abundant in hydrothermal fluids (up to several millimolar) and can serve as an electron donor for metabolism. Many species of nitrifying bacteria have complex internal membrane systems that house the key enzymes in nitrification. Ammonia monooxygenase oxidizes ammonia to hydroxylamine, hydroxylamine oxidoreductase converts hydroxylamine to nitrite, and nitrite oxidoreductase oxidizes nitrite to nitrate (Kowalchuk & Stephen 2001). The abundance and diversity of archaeal ammonia monooxygenase subunit A (*amoA*) suggest that novel ammonia-oxidizing archaea may exist in hydrothermal vent environments (Wang *et al.* 2009). Heterotrophic nitrite producers have been isolated and found to be distributed uniformly across hydrothermal ecosystems (Mevel *et al*. 1987). Recent amplification of 16SrRNA gene sequences related to known anammox (anaerobic ammonium oxidation) bacteria, analysis of ladderane lipids, and observed stable isotope values paired with rate measurements suggest that new deep branching anammox bacteria may be active within hydrothermal vents (Byrne *et al.* 2009). On the other end of the nitrogen cycle, archaea and bacteria that reduce seawater nitrate to ammonium (Alain *et al.* 2002b; Voordeckers *et al*. 2005; Miroshnichenko *et al*. 2004; Nakagawa *et al.* 2005a; Blöchl *et al.* 1997) or nitrogen (Nakagawa *et al*. 2005c) have been isolated and described (Table 1.1).

1.3.3 Sulfur Metabolism

Due to the high concentration of dissolved sulfide in hydrothermal fluid (3-12 mM kg^{-1}; Butterfield *et al*. 1994) and high concentrations of sulfate in seawater (28mM), sulfide oxidation and sulfate reduction are the most energy yielding metabolic processes in respective zones of hydrothermal chimneys. Many of the microorganisms that have been isolated from vents gain metabolic energy by oxidizing reduced sulfur compounds–such as sulfide (H_2S), inorganic sulfur (S_0), and thiosulfate ($S_2O_2^{3}$) (Takai *et al.* 2006a, 2006b; Mori & Suzuki 2008). The oxidation of sulfide and elemental sulfur is widely accepted as one of the principal chemosynthetic reactions leading to primary production in ridge ecosystems (Jannasch & Mottl 1985). At the highly reducing conditions present in submarine hydrothermal fluids, H_2S (aq) is the predominant form of dissolved sulfur. Energetically, sulfide is a much better electron donor than inorganic sulfur or thiosulfate. Biochemically, reduced sulfur compounds are converted to sulfite (SO_2^{3-}) and subsequently converted to sulfate (SO_2^{4-}) by the enzyme sulfite oxidase (Kelly *et al.* 1997). Other organisms, however, complete sulfide oxidation using a reversal of the APS reductase system used by sulfate-reducing bacteria.

Sulfate reduction is a relatively energetically poor process, but due to the high concentration of sulfate in seawater (28mM) it is known be utilized by many isolates (Alazard *et al*. 2003; Huber *et al*. 1997; Jeanthon *et al*. 2002; Audiffrin *et al.* 2003) cultivated from hydrothermal vents. Within these strictly anaerobic organisms, sulfate is transported into the cell and activated with ATP by ATP sulfurylase to APS (adenosine 5'-phosphosulfate). APS is then reduced to sulfite by adenosine 5'phosphosulfate reductase (aprA) and then finally reduced to sulfide by dissimilatory sulfite reductase (dsrAB). These genes have been extensively studied in sediments but have also been used as functional indicators for sulfate reduction in

vent environments (Nakagawa *et al*. 2004b; Meyer & Kuever 2007). Heterotrophic sulfate reducers require organic carbon compounds including acetate, lactate, formate and pyruvate as electron donors, while the autotrophs use hydrogen (H_2) as an electron donor (Rabus *et al.* 2006; Tarpgaard *et al*. 2011).

1.3.4 Metal Metabolisms

During hydrothermal alteration, hydrothermal fluids are enriched in reduced metals (i.e. Fe, Mn, As, Cu) leached from interactions of the fluid with crustal rock. Very little is known about energy yielding metal oxidizing or reducing metabolisms that may occur at vents. Biochemically, aerobic iron and manganese oxidation are energetically poor processes that require large amounts of metal to be oxidized to facilitate the formation of a proton motive force. However, cultivated organisms have been found that are capable of Fe(II) (Edwards *et al*. 2003) and Mn(II) (Templeton *et al.* 2005; Dick *et al.* 2006; Fernandes *et a*l. 2005) based metabolism. Thermodynamics predicts that organisms could use a number of other inorganic ions in anaerobic respiration such as manganese IV (Mn^{4+}) reduction to manganese II (Mn^{2+}), selenate (SeO_2^{-4}) reduction to selenite (SeO_2^{3-}), selenite reduction to inorganic selenium (Se_0), arsenate (AsO_3^{-4}) reduction to arsenite (AsO_3^{-3}), or uranium (UO_2^{+2}) reduction to uranium dioxide (UO_2) (Amend & Shock 2001). At least some of these metabolisms have been shown to occur in organisms isolated from hydrothermal vents. For example, *Deferribacter desulfuricans* has been shown to reduce arsenate (Takai 2003) and manganese oxidation has been observed in vent enrichments (Fernandes *et al.* 2005). As predicted microbes capable of many of these metabolisms have been identified (Lovley 1993), although not necessarily in vent environments.

1.3.5 C1 Metabolisms

Depending on the geology of the oceanic crust, the concentration of methane in the hydrothermal fluid ranges from 25-100µM kg^{-1}. Methane oxidizing free-living and symbiotic bacteria (Pimenov *et al*. 2000; Pond *et al*. 1998; Fujiwara *et al*. 2000; Holden *et al.* 1998; Distel *et al*. 1995; Angelis *et al*. 1991) and archaea (Brazelton *et al*. 2006; Merkel *et al*. 2013; Wankel *et al*. 2010; Biddle *et al.* 2012) have been identified from hydrothermal environment via electron microscopy observations, 16S identification and activity measurements. To date only one mesophilic methane oxidizer strain has been cultured from deep-sea hydrothermal samples (Jannasch 1995). Aerobic methanotrophs (bacteria) utilize methane monooxygenases (MMOs) to oxidize methane to acetate (CH_3OH) by the reduction of oxygen (Hanson & Hanson 1996). Anaerobic oxidation of methane (AOM) can occur via consortia of methane-oxidizing archaea (ANME) and sulfate or nitrate reducing bacteria (Dekas *et al*. 2009; Pernthaler *et al*. 2008; Brazelton *et al.* 2006). While, the exact mechanism of methane oxidation under anaerobic conditions is still a topic of debate, the most widely accepted theory is that the archaea use a reverse methanogenesis pathway to produce carbon dioxide and an intermediate which is then used by the sulfate reducing bacteria to gain energy (Valentine *et al*. 2000). However, a recent publication hypothesizes a new mechanisms for AOM wherein zero-valent sulfur compounds (S_0) are formed via a novel pathway for dissimilatory sulfate reduction performed by methanotrophic archaea alone (Milucka *et al.* 2012).

Many methanogenic archaea such as *Methanocaldococcus, Methanothermococcus* and *Methanotorris* have been isolated and identified from hydrothermal vents (L'Haridon *et al.* 2003; Jeanthon *et al.* 1998; Jones *et al*. 1983; Huber *et al.* 1982; Jeanthon *et al*. 1999; Kurr *et al.*

1991; Takai *et al.* 2002, 2004b). The biochemistry of methanogenesis is relatively complex, but the key enzyme is methyl coenzyme M reductase (*mcr*) that catalyzes the reduction of methyl coenzyme M to methane. Molecular based functional gene studies demonstrate remarkable diversity in *mcrA* sequences from hydrothermal vents and likely represent novel phylogenetic lineages (Nercessian *et al.* 2005). Methanogenesis is one of the only metabolic processes that can occur in the absence of electron acceptors other than carbon.

1.3.6 Other Metabolisms

While not very well represented in cultivated isolates, thermodynamics predicts that many other metabolisms are possible. The potential energy yield of specific metabolisms depends on the ecosystem conditions and fluid composition. Metabolic strategies identified in microbes cultured from other environments but not yet in vents can provide the backbones for geochemical models of energy yields within hydrothermal ecosystems. For example, a number of organisms may be capable of utilizing organic compounds to accept electrons from respiration. Examples may include fumarate reduction to succinate, trimethylamine N-oxide (TMAO) reduction to trimethylamine (TMA) or dimethyl sulfoxide (DMSO) reduction to dimethyl sulfide (DMS; Rogers & Schulte 2012). Providing evidence of these hypothetically favorable metabolic redox reactions or thoroughly documenting any of the known metabolic reactions actually occurring within vents requires a better integration of geochemistry, biology and energetic modeling as well as development of *in situ* experimentation.

1.4 In situ activity

Even with the isolation of actively metabolizing organisms in the laboratory, amplification of taxonomic genes closely related to a cultured metabolic group, and the amplification of functional genes for a metabolic process, limited evidence exists that reveal the taxonomic composition of active microbes and the metabolic pathways utilized in *situ*. Due to the short lifetime of extracellular RNA compared to DNA and the rapid turnover rate of intracellular RNA (Novitsky 1986), cDNA libraries are much better suited to interrogate the members of a hydrothermal microbial community that are active *in situ* (Baker *et al.* 2012; Lanzén *et al.* 2011; Lloyd *et al.* 2010; Dahle *et al*. 2013; Lesniewski *et al.* 2012; Zhang *et al.* 2012). The diversity of active hydrothermal communities, as assessed by 16S rRNA, is often less than predicted by 16S rDNA sequences (Lanzén *et al.* 2011; Zhang *et al.* 2012). Recent metatranscriptomic analysis of hydrothermal plumes points to methanotrophy, ammonia oxidation and sulfur oxidation as the main energetic pathways that fuel plume productivity (Baker *et al.* 2012; Lesniewski *et al.* 2012). Furthermore, metatranscriptomic analysis of hydrothermal chimney biofilm reveals that genes involved in respiration with sulfur species, hydrogen, formate, nitrate and oxygen, as well as key genes in the rTCA pathway, transposases, and genes involved in metal resistance, signalling, chemotaxis, biofilm formation and motility were expressed *in situ* (Dahle *et al.* 2013).

In addition to nucleic acid based approaches, community proteomics has the potential to provide high resolution information on the structure and metabolic capability of *in situ* hydrothermal communities. While transcriptomics has the advantage of revealing instantaneous changes in the community to environmental perturbations, proteomics is better suited to reflect the catalytic capacity of the *in situ* microbial community. While community

proteomics has yet to be applied within hydrothermal vents, it has the potential to provide unprecedented functional insight into endolithic microbial communities (Wilmes & Bond 2009).

1.5 Kinetics of biological processes

Thermodynamics is required to define which potential metabolisms may be utilized within a given environment, and RNA and proteomic studies are important for characterizing the active processes *in situ,* but it is the kinetics of these reactions that that determines the actual influence of vent communities on biogeochemical cycling. Data on metabolic rates within hydrothermal vents are extremely limited. In contrast to the numerous studies of metabolic rates in marine sediments (primarily sulfate reduction), however, studies in hydrothermal deposits are few (Olins *et al.* 2013; Frank *et al.* 2013a, 2013b; Bonch-Osmolovskaya *et al*. 2011; Wirsen & Molyneaux 1993), due in part to the challenges associated with sampling and studying the heterogeneous and consolidated sulfide deposits typical of hydrothermal vent chimneys. Sulfate reduction rates at vents can be measured in homogenized hydrothermal deposits incubated with $^{35}SO_4^{2-}$ anaerobically over a range of conditions and analyzed via chromium distillation (Frank *et al*. 2013a, 2013b). Rates of other energy metabolisms can be examined by incubating homogenized chimneys with radioactive substrates and measuring radioactive product accumulations. For example, rates of autotrophic and acetoclastic methanogenesis could be determined by incubating homogenized samples [^{14}C] sodium bicarbonate or acetate and measuring the accumulation of radioactive methane in the headspace of incubation (Crill & Martens 1986). Similarly, rates of overall chemoautotrophy in the system can be measured by looking at the incorporation of radiolabeled bicarbonate into

biomass (Olins *et al.* 2013; Wirsen & Molyneaux 1993). Additional radioisotopic tracer studies, using chimney material as inocula, are necessary to elucidate the metabolic activity of hydrothermal communities and to document the kinetics of targeted biological processes under varying conditions. These lab based incubations allow for the testing of specific hypotheses about substrate (e.g. hydrogen, nitrogen, sulfur, carbon) utilization based on energetic models and can eventually be developed to provide high spatial resolution of activity occurring within a hydrothermal chimney. Furthermore, utilization of *in situ* technology can facilitate the determination of the nature and extent of microbial influence on geochemical fluxes from hydrothermal vents (Wankel *et al.* 2010, 2011).

1.6 Current and Future Directions

To date, most hydrothermal vent microbial ecology studies have focused on the taxonomic diversity of the vent community rather than its functional or ecological dynamics. A majority of published works have utilized 16S clone library (Takai *et al*. 2001, 2006b; Schrenk *et al.* 2003; Suzuki *et al*. 2004; Opatkiewicz *et al.* 2009; Kormas *et al*. 2006; Hoek *et al*. 2003; Ehrhardt *et al.* 2007; Perner *et al.* 2007; Page *et a*l. 2008; Teske 2006; Nakagawa & Takai 2008; Jaeschke *et al.* 2012; Reysenbach *et al*. 2000; Wery *et al.* 2002; Nakagawa *et al*. 2005b) or tRFLP (tagged restriction fragment length polymorphism; Opatkiewicz *et al.* 2009) techniques. We now know, however, that the vast majority of a microbial habitat's diversity may be comprised of taxa present at abundances so low that they cannot be detected by these techniques (Sogin *et al.* 2006; Huber *et al*. 2007; Brazelton *et al*. 2010; Simon *et al*. 2009). Another major limitation to our knowledge is that many of these hydrothermal vent organisms cannot

currently be cultivated–cultivations inform us about the physiology, behavior, and functional capabilities of microbial organisms. Current research estimates that 99.9% of all microbes are uncultivated and unfortunately many of the microorganisms sequenced from hydrothermal vents lack even close relatives in culture, making them virtually unknown to us. Those organisms that are cultivated are often grown in pure culture under relatively static conditions and in isolation, so we therefore lack fundamental information about syntrophic interactions and the metabolic plasticity of these organisms that is presumably necessary for life across steep and dynamic redox gradients.

Most of the spatial studies are limited to description of microbial distribution within single structures rather than pairing microbial analyses with assessments of *in situ* conditions. Many spatial surveys use sulfide mineralogy as proxy for temperature (Kormas *et al.* 2006; Jaeschke *et al.* 2012; Schrenk *et al*. 2003), which is important for understanding mineral microbe interactions, but this method only takes into consideration the temperature during mineral formation and does not necessary correspond to the average temperature or fluctuations in that lamination at time of sampling. *In situ* growth chambers such as a vent cap (Nercessian *et al*. 2003; Reysenbach & Longnecker 2000), or thermocouple arrays (Page *et al*. 2008) allow for co-registered measurement temperature and de novo microbial growth. While incredibly informative, these *in situ* deployment studies often lack chemistry measurements (using temperature as a proxy for chemistry) and only investigate microbes associated with new chimney formation.

Though we know a bit about the succession of communities at both the beginning (formation) and end (extinction) of a chimney's lifetime, we know little to nothing about the

community response to changes on smaller time scales. In many systems, like water column and microbial mats, there is much evidence supporting diel cycle changes to community composition relative to changing redox gradients during the day-night cycle (Dillon *et al.* 2009; Fourçans *et al.* 2008). In the hydrothermal environment devoid of light fluctuations, tidal fluctuations may strongly influence the structuring of redox gradients within the wall of a chimney. Unpublished temperature data of fluid across chimney walls within mature actively venting sulfides shows a clear tidal signature such that the temperatures of fluids across the chimney oscillate with respect to the tides (D. Kelley pers. communication). Tidal influence on microbial community composition in environments like estuaries is directly related to the tidally associated changes in available metabolic substrate (like dissolved organic carbon; Chauhan et al. 2009). Tidally associated changes in temperature and chemistry are parameters never before considered at hydrothermal vents.

Most of the information we have to date about which metabolic processes occur within vents is relatively speculative based on thermodynamic predictions, cultured isolates or DNA studies. Most geochemical models are limited by the lack of precise chemical measurements across the mixing gradient and because of this necessarily make assumptions about the type of mixing occurring within vents. We know that these environments likely support globally important microbially mediated processes such as the oxidation and/or reduction of sulfur, iron, nitrogen, and carbon because we have isolated organisms and functional genes that suggest this to be true. Only a few studies have actually isolated RNA (Baker *et al*. 2012; Lanzén *et al*. 2011; Lloyd *et al*. 2010; Dahle *et al.* 2013; Lesniewski *et al.* 2012; Zhang *et al*. 2012) or proteins, or performed rate experiments on hydrothermal chimney samples (Bonch-

Osmolovskaya *et al*. 2011; Olins *et al*. 2013; Frank *et al*. 2013a, 2013b; Wirsen & Molyneaux 1993) to provide concrete documentation and descriptions of specific metabolic reactions that are actually occurring within vents. While much progress has been made in the decades since the discovery of hydrothermal vents, we still have limited understanding of the spatial distribution of endolithic organisms at biologically relevant scales, microbial community succession, specific biogeochemical redox reactions (and their interactions) that occur within these ecosystems, kinetics of biological processes, taxonomy and physiology of the organisms responsible, complex syntrophic interactions amongst community members, metabolic plasticity within the organism, and the extent to which they influence the marine or global cycling of these compounds and elements.

Despite the current limitations, future research needs to investigate how environmental variables, such as temperature and redox chemistry, influence the endolithic microbial community structure (in terms of diversity, density, distribution, function and rates of activity) within the vents itself. This field would benefit greatly from research aimed to better resolve the distribution of microbial taxa across the redox gradients of a hydrothermal chimney. Furthermore, future work should focus on generating functional metagenomic data, which would be invaluable to develop and test ecological hypothesis about metabolic plasticity, novel metabolic pathways and biochemical adaptations to extreme conditions. Moving forward, it is essential that ecologists consider their data in the context of *in situ* geochemical data and there should be a push to develop the tools necessary to measure geochemistry at biologically appropriate scales. Most importantly, data needs to be generated on the actual rates of microbial metabolisms. Even though there may be genetic evidence for a particular metabolism

within a vent, are microbes actively utilizing that pathway? And if so, are these metabolisms happening at a scale that is relevant to the global sulfur cycle?

1.7 Conclusions

As discussed in this review, studies have laid the foundation for our understanding of the extent of diversity in relation to varying hydrothermal settings, but few studies exists regarding the detailed spatial or temporal relationships among vent geochemistry, temperature, mineralogy, and the composition, abundance, distribution, and metabolic characteristics of the endolithic microbial communities. Even fewer data have been generated on the metabolic rates occurring within hydrothermal systems, and in particular hydrothermal sulfide chimneys themselves. Understanding the extent of the influence that hydrothermal microbes have on biogeochemical cycles requires understanding the relationship between geochemistry and biology and allying taxonomic identity to function and rates. The field needs additional *in situ* chemistry measurements, diffuse fluid flux estimates, growth yields, metabolic fluxes and many more real time observations.

The work presented within this dissertation is aimed at addressing how the environment (temperature and chemistry) influences the microbial ecology (diversity, density and distribution), functional capacity and metabolic activity of hydrothermal communities to bridge some of the gaps between geochemistry and biology. The overarching goal of this dissertation is to better understand microbially mediated sulfur cycling at hydrothermal vents by allying phylogenetic identity to metabolic potential (i.e. genomic descriptions) and rates of sulfur metabolism within hydrothermal chimneys at thermal and chemical conditions representative

of mature, diffusely venting chimneys. Here I address how environmental variables, such as temperature and redox chemistry influence the endolithic microbial community in terms of their ecology (diversity, density and distribution), functional capacity (metagenomics) and metabolic activity (rate measurements).

The work I describe in chapter two of this dissertation features the use of an *in situ* sulfide colonization device to sample directly the endolithic communities within the pre-established gradients of an actively venting mature chimney with co-registered temperature, mineralogy and microbiology. This allows us to take replicate samples within a chamber to look at the statistically relevant effects of temperature and fluid chemistry on community structure. This work provides the first well-constrained set of data on the spatial relationship between microbial communities and the physical/chemical conditions *in situ* including temperature, fluid chemistry and mineralogy. Studying the spatial distribution of endolithic organisms in the context of the biogeochemical environment enhances our understanding of biogeochemical cycling and our ability to predict the metabolisms used by uncultured microbes.

In chapter three I will provide evidence for sulfate reduction activity at vents and evaluate the effect of temperature on the rates of sulfate reduction within hydrothermal vent chimneys in the context of bacterial and archaeal diversity, total biomass, the abundance of functional genes related to sulfate reduction, and *in situ* geochemistry. The data shown here are among the first to constrain the potential for heterotrophic sulfate reduction at vents (in particular those with higher organic carbon loads), as well as the relationship between sulfate reduction rates, temperature, microbial biomass and community density and composition. Moreover, they underscore the potential role of heterotrophic sulfate reduction in

hydrothermal systems, and constrain their potential influence on both sulfur and carbon cycling,

Finally in chapter four, I highlight the influence key chemical variables have on the rates of microbial sulfate activity. This research presents an opportunity to better understand the key variables that influence the rates of microbial sulfate reduction in hydrothermal environments and provides a framework for modeling sulfate reduction in mid-ocean ridge systems. Direct metabolic rate measurements, in particular of sulfate reduction, will in conjunction with the incubator data facilitate defining key environmental and energetic parameters for microbial community colonization in hydrothermal sulfide. Better understanding of the metabolic and taxonomic relationship of these endolithic communities in the geochemical context of hydrothermal vents will help to constrain the microbial impact on global biogeochemical cycling.

CHAPTER TWO:

Breaks in the physiochemical environment correlate with sharp biological boundaries within the active hydrothermal vent chimney Roane.

Kiana L. Frank[1], Matt Schrenk[2], Marv Lilley[3], Geoff Wheat[4], Deborah S. Kelley[3], Peter R. Girguis[5]

1. Department of Molecular and Cellular Biology , Harvard University, Cambridge, MA, USA
2. Department of Biology, East Carolina University, Greenville, NC, USA
3. School of Oceanography, University of Washington, Seattle, WA, USA
4. GURU, NURP/University of Alaska, Moss Landing, CA, USA
5. Department of Organismic and Evolutionary Biology, Harvard University, Cambridge, MA, USA

Corresponding supplemental material is appended in Appendix A.

2.1 Abstract

The unique physico-chemical gradients that are characteristic of hydrothermal vents provide diverse niches for prokaryotic communities. To date, our knowledge of environmental factors that shape bacterial and archaeal community composition and metabolic activities across these gradients within the active sulfide structures has been limited by a lack of co-registered data. Specifically, no studies have spatially paired *in situ* measurements of temperature data with analysis of prokaryotic taxonomic and metabolic genetic markers. To address these deficiencies, we characterized *de novo* endolithic prokaryotic communities with spatially co-registered temperature within the hydrothermal vent chimney Roane using a novel sulfide microbial incubator. During a three-month deployment, the *in situ* temperatures measured within the sulfide microbial incubator suggest a reducing environment in the middle and inner chambers, with average temperatures above 100 °C, and a more dynamic zone in the outer chamber, with temperatures ranging from ~10 °C to 70 °C. Taxonomic assessments of bacterial diversity via 16S rRNA genes from the outer, middle, and inner chambers of the incubator revealed a correlation between community distribution and the physiochemical environment. Communities from the outer chamber were dominated by epsilon-proteobacteria, whereas the middle and outer chambers were dominated by gamma-proteobacteria. We posit, based on analyses of taxonomic and metagenomic data that the observed differences in community composition may be due in part to physiological tolerances of specific microbial taxa, as well as the metabolic capacity of each community. This hypothesis stems from our observations that genes for electron-donating reactions, sulfide oxidation pathways, were enriched in the outer chamber. In contrast, we observed an enrichment of

genes for electron accepting reactions in the middle chamber, suggesting that this chamber is dominated by anaerobic metabolisms. Together, these observations provide strong evidence that hydrothermal vents harbor a diverse but predictable assemblage of physiochemical niches, which may have influenced the structure of endolithic prokaryotic communities.

2.2 Introduction

Deep-sea hydrothermal vent fields host dynamic endolithic habitats for bacteria and archaea. In these environments, hot hydrothermal fluids (>400 °C) rich in metals, carbon dioxide, and hydrogen sulfide mix with cold oxygenated seawater (2 °C) to precipitate large and complex sulfide mineral structures, referred to as chimneys. The continuous mixing of chemically reduced, vent-derived fluids and oxidized seawater within the permeable mineral matrix provides diverse niches for prokaryotic growth, allowing them to capitalize on a variety of thermodynamically favorable metabolisms (McCollom & Shock 1997; Schrenk *et al.* 2003). Previous studies have identified many novel lineages of uncultivated bacteria and archaea at deep-sea hydrothermal vents and have thus far revealed that diversity varies with geological setting, chimney age, mineralogy, and hydrothermal fluid composition (Takai *et al.* 2001; Schrenk *et al*. 2003; Suzuki *et al.* 2004; Huber *et al*. 2006; Kormas *et al.* 2006; Ehrhardt *et al*. 2007; Perner *et al*. 2007; Page *et al*. 2008; Zhou *et al*. 2009). Since the discovery of deep-sea vents, the mineralogy of hydrothermal structures has been studied in great detail (Tivey & Delaney 1986; Tivey *et al*. 1999; Kristall *et al*. 2006), and significant progress has been made in constraining the composition and variability of end-member hydrothermal fluids exiting directly from chimney orifices (Butterfield *et al*. 1994; Lilley *et al*. 2003; Von Damm *et al*. 1995, 1997).

However, accessing the *in situ* thermal and chemical conditions within a mature and active chimney has proven difficult. Consequently, the study of environmental constraints on microbial community composition and metabolic activity within active sulfide structures has been limited.

Despite these limitations, a few microbiological observations have demonstrated differences in prokaryotic populations within individual chimney structures (Harmsen *et al*. 1997; Schrenk *et al*. 2003; Kormas *et al*. 2006; Takai *et al*. 2001; Page *et al*. 2008). Using a variety of 16S rRNA molecular and lipid geochemistry techniques, paired with mineralogical analysis to infer temperature and chemistry, these studies have shown that outer chimney walls are typically colonized by mesophilic and slightly thermophilic autotroph and heterotroph phylotypes (Takai *et al*. 2001; Hoek *et al.* 2003; Schrenk *et al*. 2003; Nakagawa *et al*. 2005b; Kormas *et al*. 2006; Page *et al.* 2008). Furthermore, they observed a higher prevalence of hyperthermophilic archaeal phylotypes (such as *Thermococcales, Archaeoglobales, Methanococcales, Thermoproteales, Korarchaeota, Desulfurococcales;* Page *et al*. 2008; Schrenk *et al*. 2003; Jaeschke *et al*. 2012) in the interior of the chimney structure. Unfortunately, defining the distribution of metabolic strategies utilized by these endolithic bacteria and archaea by 16S rRNA gene analysis is limited. Moreover, spatial surveys of targeted functional genes have not yet been reported. Recent metagenomic analyses of epilithic and endolithic communities on the outer wall of a chimney revealed genes for sulfur oxidation, putatively coupled to nitrate reduction and inorganic carbon fixation through the Calvin Benson Bassham cycle (Xie *et al*. 2011). Although this study is incredibly informative as the first metagenome of an endolithic vent community, it describes the metabolic potential of communities associated

with the outer chimney only, and it does so in the absence of any geochemical context. The functional potential of communities thriving in the inner portions of the chimney remains unknown.

To date, bioenergetic models are the best tools for predicting the spatial distribution of biogeochemical processes within a vent (McCollom & Shock 1997; Tivey 2000). These models evaluate the energy yields for potential metabolic reactions while accounting for variations in host rock composition, fluid chemistry, and flow regime. Models hypothesize that the oxidation of sulfide, methane, iron, and manganese are favorable in the outer walls of the chimney (where oxidants like oxygen and nitrate are available; Johnson *et al*. 1986). Methanogenesis and reduction of sulfate or S_0 are favored at higher temperatures within the interior of the chimney (McCollom & Shock 1997; Tivey 2000). Energetic models further suggest that hydrothermal chimneys provide habitats for mesophilic (but not thermophilic) aerobes and thermophilic (but not mesophilic) anaerobes.

Our understanding of hydrothermal vent microbial diversity, ecology and physiology has significantly advanced over the last three decades. Nevertheless, much remains to be learned about the relationship between environmental conditions and microbial ecology and physiology at vents, where it is likely that the gradients in physical and chemical conditions-as well as their temporal dynamics-act on microbial community structure, function and evolution. A first step towards better understanding these relationships is to concurrently examine the physical and geochemical conditions and the endolithic microbial communities from actively venting sulfide chimneys.

In this study, we evaluate *de novo* endolithic microbial growth within a novel *in situ* titanium sulfide microbial incubator deployed within the walls of the active hydrothermal vent chimney Roane, which is located in the Mothra Hydrothermal vent field on the Endeavour Segment of the Juan de Fuca Ridge. The titanium incubator included a high-density thermistor array, surrounding an assemblage of sterile, environmentally relevant substrates for microbial colonization. This enabled collection of co-registered data on the thermal conditions and prokaryotic community composition within the sulfide chimneys. Furthermore, the incubator design allowed spatially segregated sampling within different chimney regions to assess the statistically relevant effects of temperature and fluid chemistry on microbial density, diversity, spatial distribution or heterogeneity, and functional capacity.

We hypothesize that thermodynamics drive community assembly along the thermal and chemical gradients within a sulfide chimney. The metabolic differences among taxa would allow specific taxa to dominate in areas where specific resources are available. Furthermore, differences in physiological tolerances (such as temperature, pH, and oxygen sensitivity) would allow better-adapted taxa to dominate within specific regions. The distribution of metabolic activity will likely exhibit a modality that reflects the periodicity of geochemical conditions due to features such as tidal pumping, the nature of ecological interactions, and the heterogeneity inherent to mineral precipitates. The data presented here provide the first comprehensive assessment of taxonomic and functional diversity within a mature actively-venting chimney in the context of *in situ* geochemistry.

2.3 Materials and Methods

2.3.1 Geologic Setting

The hydrothermal vent chimney Roane is located in the Faulty Towers Complex of the Mothra hydrothermal field on the Endeavour Segment of the Juan de Fuca Ridge (Figure 2.1). Mothra is the most extensive of the five major hydrothermal fields at Endeavour, extending ~600 m along-axis and hosting five distinct venting complexes (Kristall *et al.* 2006; Glickson *et al*. 2007). This diffusely-venting edifice is one of fourteen active and inactive chimneys that form a cockscomb array which defines the Faulty Tower Complex (Figure 2.1c; Glickson *et al*. 2007).

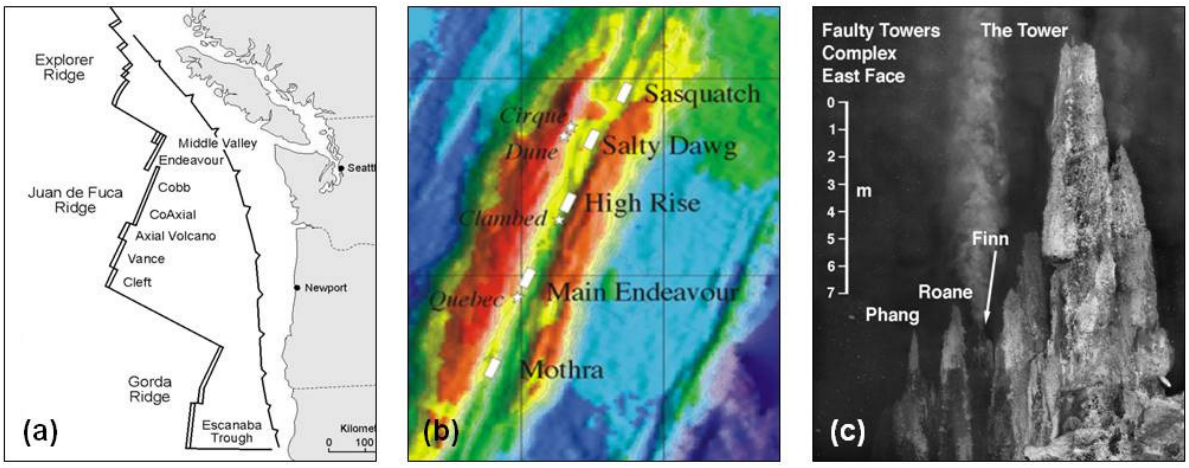

Figure 2.1: (a) Location of Endeavour Segment on the Juan de Fuca Ridge. (b) Bathymetric map of the intermediate rate spreading ridge in the Endeavour Segment showing the five high-temperature vent fields (boxes) and distal diffuse flow sites (stars). (c) Photomosaic of the southeast face of the Faulty Towers Complex showing the Roane structure and adjacent. Edifices. Mosaic by M. Elend, University of Washington. Figure modified from Kristall *et al.* 2006

In 1998, a portion of Roane was recovered as part of the Edifice Rex Sulfide Recovery Project. Mineralogical studies indicate that Roane lacks an open central conduit, and instead hosts a discontinuous network of narrow flow channels and a highly permeable sponge-like matrix of amorphous silica, sulfide, sulfate, and clay minerals. The outermost portion of the wall is highly porous and allows significant mixing between seawater and hydrothermal fluids (Kristall *et al*. 2006). Yearlong measurements in instrumented drill holes, as well as temperature surveys of Roane, demonstrated that fluids within the interior reach temperatures of 210-278 °C (Kelley *et al.* unpublished). The composition of Roane's end-member fluids is characteristic of other Endeavor Segment fluids, with a relatively low pH (4.7-4.8) and high concentrations of both methane (1.77 mmol/kg) and ammonia (>450 µmol/kg) (Schrenk *et al.* 2003). These fluids also have higher chlorinity than seawater and are sulfide-dominated.

2.3.2 Sulfide Microbial Incubator Design

The sulfide microbial incubator is designed for deployment within horizontal drill holes inside the walls of active black smoker chimneys to obtain co-registered temporal-spatial information on environmental conditions and *in situ* composition of microbial communities over various time scales. It is composed of concentric titanium inner and outer barrels, 53 cm in length and 5 cm diameter on the inner barrel (Figure 2.2). Holes drilled into the concentric barrels can be positioned in and out of alignment, which minimizes contamination from larger particulate debris while the incubator is being delivered through the water column (to eliminate particulate matter as a source of organic matter for microbial growth). Prior to deployment, the barrels were rotated into the closed position (holes out of alignment). Once

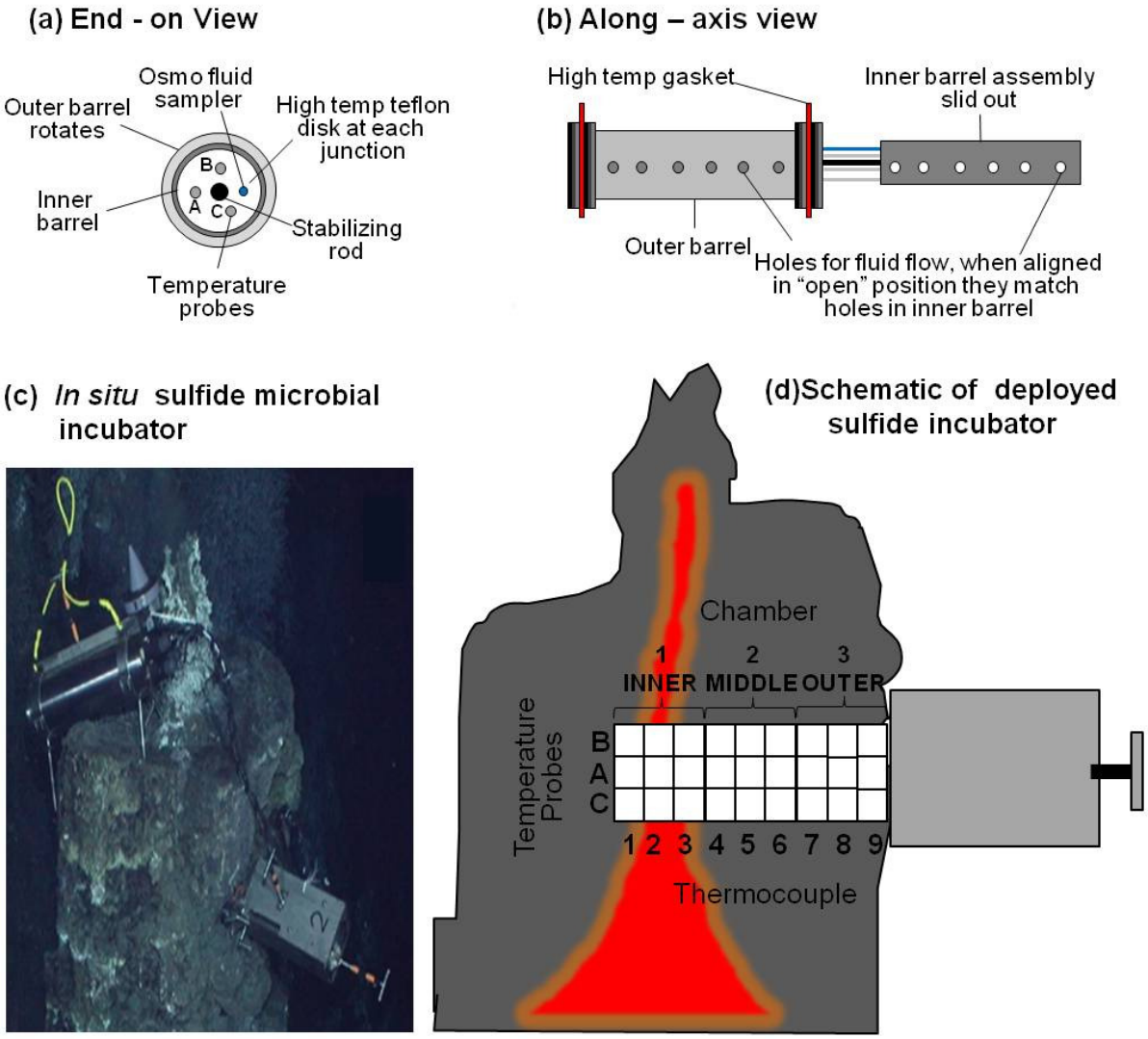

Figure 2.2: *In situ* experimental design of sulfide microbial incubator. Except for an array of Teflon disks, the entire 46-53 cm long sulfide microbial incubator is made of titanium and filled with sterilized glass wool. Temperatures from 0- 500°C with a resolution of 2°C are recorded with 27 temperature probes that are housed within three discrete incubation chambers. The inner barrel contains three discrete chambers separated by tight-fitting, impermeable high-temperature Teflon disks that prevent the along-axis flow of fluids. (a) End-on view and (b) along axis schematic of the titanium sulfide microbial incubator. (c) Photograph of the sulfide microbial incubator *in situ.* (c) Illustration of the sulfide microbial incubator in Roane (in cross-section) and sample nomenclature (chamber (3, 2, 1), longitudinal position within the chimney wall (9=innermost, 1=outermost) and thermistor probe from (A, B or C).

the incubator was successfully placed inside the drill hole, the outer barrel was rotated such that the holes in the outer barreled aligned with those in the inner barrel (Figure 2.2b).

The inner barrel contains three discrete chambers separated by tight-fitting, high-temperature Teflon baffles that prevent the along-axis flow of fluids. Within the inner barrel, three 0.3 cm diameter ceramic-filled titanium tubes run along the length of the assembly. Each sheath contains nine Type E thermocouples equidistantly distributed along the length of the tube. Each chamber houses nine temperature probes. In addition, there are three reference temperature probes located on the outside of the assembly and exposed to ambient seawater. When viewed end-on, the three thermistor probe sheaths (labeled A, B, C) are positioned at 12, 6, and 9 o'clock positions (Figure 2.2a), providing temperature measurements along and across axis (Figure 2.2b). The temperature probes are capable of measuring from 0-500 °C with a resolution of 2 °C.

Prior to deployment, each chamber was filled with a number of sterile substrates for molecular and microscopic analyses. For molecular analyses, sterilized glass wool was placed into titanium mesh (0.5 mm mesh size) to serve as nucleation points for sulfide precipitation. Samples were named according to their longitudinal position within the chimney wall (9=innermost, 1=outermost) and by the probe from which they were suspended (A, B or C: Figure 2.2d).

2.3.3 Incubator Installation and Sample Recovery

On June 20, 2003, the ROV *Jason* was used to drill a 53.5 x 7.62 cm hole into the active black smoker Roane ~0.75 m below the flat-topped summit of the edifice. The incubator was

deployed on May 24, 2004 at 04:38:00 with the submersible *Alvin* on dive A4013 (Figure 2.2c). The data logger was recovered on July 13, 2004 at 18:14:00 with ROV *Tiburon* on dive T724, yielding 50.567 continuous days of records. Temperature measurements were recorded every 8 min, resulting in 180 per day. During recovery, the barrel assembly was placed into a PVC "holster," which consisted of a PVC cylinder capped with a slotted rubber membrane through which the incubator barrel could be inserted. The bottom of the holster was also capped with a PVC plug. After the barrel was inserted, the holster was filled with 0.2-µm filter-sterilized artificial seawater, pH 6.5 and replete with sodium sulfide to achieve a final concentration of 100 µM. These measures were taken to minimize perturbations to the extant microbial community prior to recovery. After the assembly was brought to the surface, all substrates including the glass wool, titanium mesh, and authigenic mineral precipitates were flash-frozen in liquid nitrogen and stored at -80 °C until processing.

2.3.4 DNA isolation and Whole-Genome Amplification

Authigenic Roane mineral precipitates directly associated with each of the 27 temperature probes were ground in a mortar with liquid nitrogen during processing to facilitate homogenous crushing and minimize nucleic acid degradation. Total nucleic acids were then extracted using MoBio™ Ultra Clean Mega Prep Kit (MoBio Inc., Carlsbad, CA) following manufacturer's protocol, with the addition of a 1 min incubation at 80 °C to facilitate cell lysis. The resulting nucleic acids were further purified by cesium chloride density ultracentrifugation as needed, then stored at -80 °C prior to amplification. DNA samples for sequencing were amplified via whole genome amplification (REPLI-g Ultrafast Mini Kit, Qiagen, Valencia, CA) and

purified (QIAamp DNA Mini Kit, Qiagen) to acquire enough material for 16S rRNA gene amplicon sequencing and metagenomic sequencing.

2.3.5 Enumeration of Bacterial and Archaeal 16S rRNA Genes via Quantitative PCR

Quantitative PCR (qPCR) was used to determine the total abundance of bacterial and archaeal 16S rRNA genes in each sample using assays targeting each domain (Table S2.1). Reactions containing 2 µl of diluted DNA template were performed in triplicate for each sample with the Stratagene MX3005p qPCR System (Agilent Technologies, Santa Clara, CA) using the PerfeCTa SYBR Green FastMix with low ROX (Quanta Biosciences, Gaithersburg, MD). Samples were quantified using standard curves for bacterial and archaeal 16S rRNA genes that spanned eight orders of magnitude, and no-template controls were used to confirm the absence of contamination. Bacterial and archaeal standard curves were constructed using linearized plasmid (StrataClone vector, Agilent Technologies Inc., Santa Clara, CA) containing the 16S rRNA genes of *Arcobacter nitrofigulis* (ATCC 33309) and *Methanosarcina acidovorans,* respectively. These linearized plasmids were serially diluted to range from 10^8 to 10^1 copies in each reaction. The temperature program for all assays was 94 °C for 10 min, followed by 35 cycles of 94 °C for 1 min and the appropriate annealing temperature for 1 min.

2.3.6 Bacterial 16S rRNA Gene Pyrotag Sequencing and Analyses

Bacterial 16S rRNA genes were amplified and sequenced using 454 pyrotag methods similar to those described previously (Dowd *et al*. 2008). All samples were sequenced at the Research and Testing Laboratory (Lubbock, TX) using a Roche 454 FLX instrument (454 Life

Sciences, Branford, CT) with Titanium™ reagents using (Primers in Supplementary Table A2.1). The resulting bacterial 16S rRNA sequences were analyzed via Mothur (Schloss *et al*. 2009). Sequencing error was reduced by running the Mothur implementation of the AmpliconNoise algorithm (shhh.seqs). The 16S rRNA gene sequence data was aligned to the SILVA-compatible alignment database reference alignment (Schloss *et al*. 2009). Sequences were screened and selected to start at the same position, then those sequences within 2 bp of a more abundant sequence were merged in a pre-clustering step, in which a difference of 1 bp per 100 bp of sequence length was allowed. Chimeric sequences were identified and removed using the command chimera.uchime, which uses the abundant sequences in the sample set as a reference database. Sequences were classified using the Mothur version of the Bayesian classifier against the RDP database (Cole *et al*. 2005; Maidak *et al*. 1997). Sequences affiliated with organelles such as chloroplasts and mitochondria were removed. Operational taxonomic units (OTUs) were built by generating a distance matrix with pairwise distance lengths smaller than 0.15. The data were then clustered and each OTU was classified. Rarefaction curves were used to examine the number of OTUs as a function of sampling depth. Alpha diversity was assessed by generating values from the Chao1 richness estimators and the inverse Simpson diversity index. Beta diversity was assessed via the Yue & Claton measure of dissimilarity (Yue & Clayton 2005) and used to perform various analyses, such as parsimony (dependent only on the presence absence of a taxa), UniFrac (dependent on phylogenetic relationships between taxa), and weighted UniFrac (dependent on taxa abundance and phylogenetic relationships) to evaluate the difference in the microbial communities among chambers. Despite multiple sequencing attempts, archaeal 16S runs routinely failed or resulted in amplification and

sequencing of only bacterial phylotypes, limiting information on the archaeal contribution to metagenomic 16S data.

2.3.7 Metagenomic Sequencing and Analyses

Metagenomic sequencing of samples 3A2, 3B1 (outer section), 2A5, and 2C4 (middle section) was performed using pyrosequencing on a Roche GS FLX (Duke IGSP Sequencing Core Facility, Durham, NC). Samples were trimmed with Mothur to exclude reads of length less than 200 and average quality scores less than 25. These data sets were analyzed using MG-RAST (Meyer *et al*. 2008) for known metabolic function against the non-redundant database M5NR, which is an integration of many sequence databases into one single, searchable database which allows similarity searches into many name spaces (e.g., NCBI's nr database, KEGGs database, SEED subsystems, and COG database) using a maximum e-value of 10^{-5}. Samples annotated by M5NR were parsed manually to reassemble metabolic pathways. The base-10 logarithm of the odds ratio was calculated by $(G_{Mid}/T_{Mid})/(G_{Out}/T_{Out})$, where G is the number of reads for a given gene or category, T is the total number of reads in a given metagenome, MID refers to a samples from the middle chamber (i.e. 2A5), and OUT refers to a sample from the outer chamber (i.e. 3A2 or 3B1). Unfortunately, over 50% of annotated 16S genes and approximately 75% of protein features for sample 2C4 aligned to *Escherichia coli*. Due to obvious contamination, data from this sample are not considered hereafter.

2.3.7.1 Accession Numbers

The taxonomic and metagenomic data from the middle and outer chimney will be publically available in the MG-RAST system under the following project identifiers: 4479838.3

(3A2), 4479647.3 (3B1), 4479839.3 (2A5), and 4479794.3 (2C4), as well as in the NCBI SRA under SRX 15673 through 15691 upon publication.

2.4 Results

2.4.1 Temperature Analyses

During the 51-day experiment, the sensors logged 9,104 discrete temperatures (Figure 2.3). Each chamber yielded different thermal responses to fluid flow, with distinct gradients measured in each chamber. All chambers recorded small daily perturbations (~2 °C) in temperature that were tidally influenced. The highest temperatures were recorded in the thermocouples near the top of the chamber (the B string), which is likely due to an artifact of the chamber design, wherein warmer, more buoyant fluids pool at the top of the chamber. Within the outer chamber, temperatures were highly variable (perturbations up to 27 °C) and had an average temperature range across the three thermistor strings of 10 °C to 70 °C. The highest temperature recorded was 132 °C. The middle chamber temperatures reached steady state conditions much faster than those in the outer chamber. The average temperatures within the middle chimney ranged from 150 °C to 190 °C, and the highest temperature recorded was 201 °C. The temperatures within the inner chamber immediately increased to near steady state conditions, with the largest temperature perturbation of 2 °C. The highest temperature measured in the inner chamber was 208 °C. Temperatures on all sensors were tightly coupled, varying by ~10 °C from the top of the chamber to the bottom.

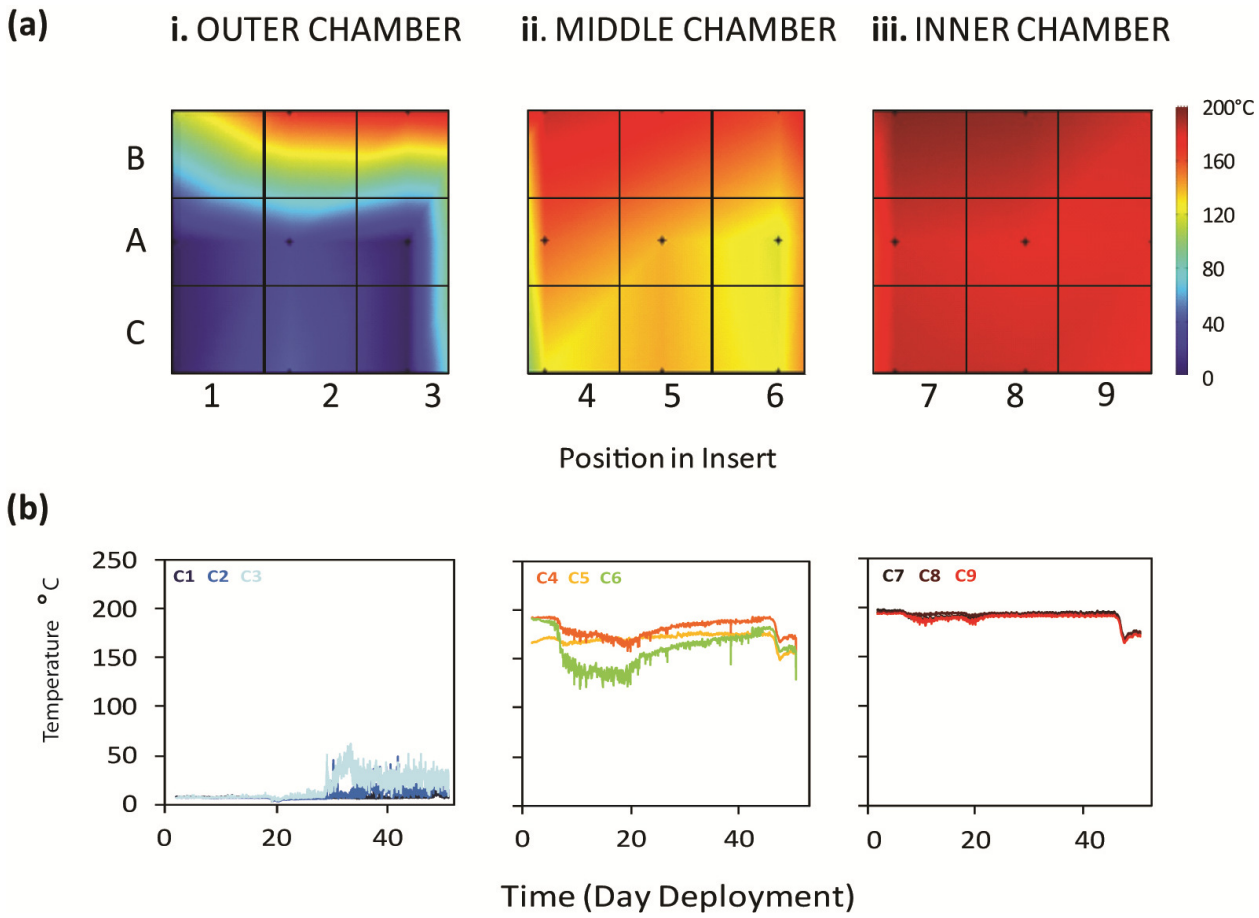

Figure 2.3: (a) Temperature distribution across axis at day 24. (b) Temperature record of the thermistor C probe during 51 day incubation. Temperatures on all sensors were tightly coupled, varying by ~10°C from the top of the chamber to the bottom. Within the outer chamber (i), temperatures were highly variable with an average temperature range of 10°C to 70°C. The middle chamber (ii) and inner chamber (iii) temperatures reached steady state conditions much faster than those in the outer chamber with average temperature ranges of 150-190°C and 195-205°C. Temperatures on all sensors were tightly coupled, varying by ~10°C from the top of the chamber to the bottom.

2.4.2 Bacteria and archaea Density Across Structure

Bacteria and archaea communities (as estimated by 16S rRNA gene copies g^{-1} mineral) from samples within each chamber (except for inner chamber sample 1C9) were dominated by

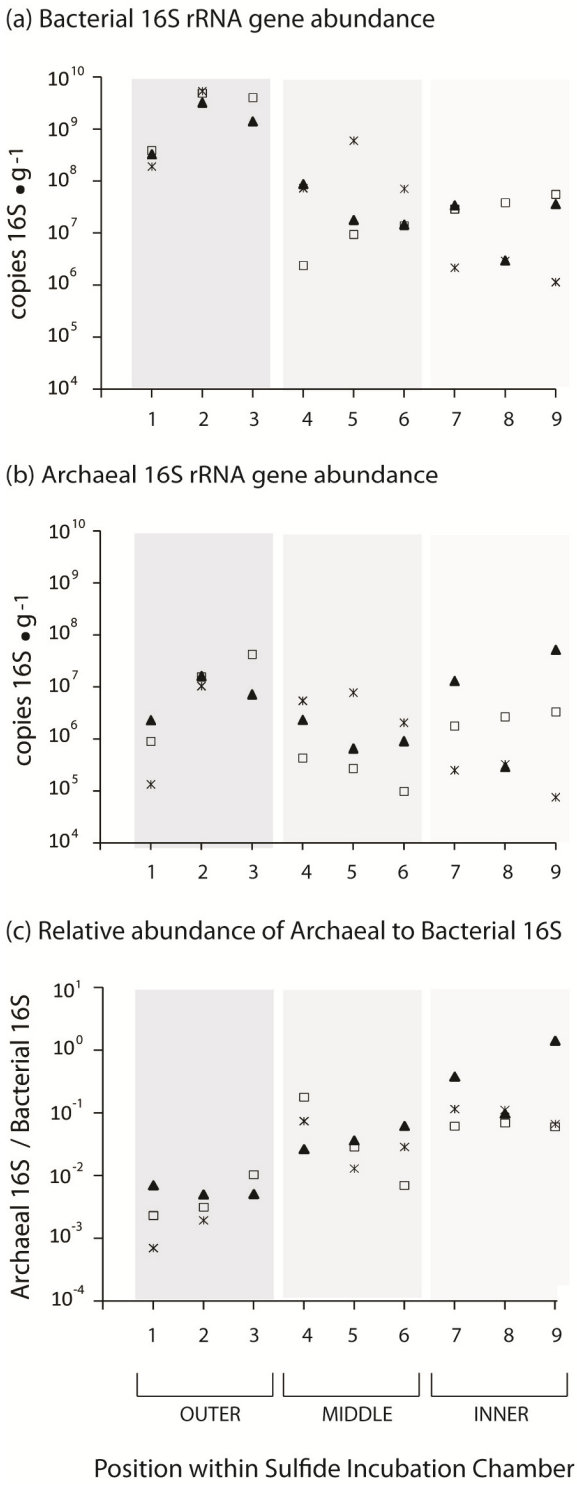

Figure 2.4: Abundance of (a) bacterial 16S rRNA genes and (b) archaeal 16S rRNA genes per gram sulfide and (c) the ratio of archaeal to bacterial 16S copy number across the length of the titanium incubator. After a three month incubation of the sulfide microbial incubator in Roane, samples of authigenic hydrothermal sulfide material were sampled from each of 27 thermocouples housed in the three discrete chambers and DNA was extracted using described protocols. Bacterial and archaeal 16S rRNA genes were enumerated by qPCR using published primer sets and normalized to grams of extracted sulfide.

bacteria (Figure 2.4a, 2.4b). Bacterial abundance was at least ten times greater in the outer chamber than either the middle or inner chambers (Figure 2.4a). Assuming an average of 4.19 copies of 16S rRNA gene per bacterium (Klappenbach *et al*. 2001), the highest bacterial abundances were observed in sample 3A2 (4.5×10^7 cells/gram sulfide), 3B2 (4.1×10^7 cells/gram sulfide), and 3C2 (2.7×10^7 cells/gram sulfide mineral). There was no distinct trend in archaeal abundance among chambers (Figure 2.4b). Assuming 1.71 copies of 16S rRNA gene per archaeon (Lee *et al*. 2009; Klappenbach *et al*. 2001), the highest archaeal abundances were observed in samples 1C9 (1.8×10^5 cells/gram sulfide mineral) and 1B3 (1.5×10^5 cells/gram sulfide mineral). The total number of cells estimated in each chamber ranged from 10^6 - 10^7 cells/g mineral in the outer chamber, 10^4 - 10^5 cells/g mineral in the middle chamber, and 10^3 - 10^5 cells/g mineral in the inner chamber. The ratio of archaea to bacteria increased from the outermost samples (position 1, Figure 2.4c) to the inner most samples (position 9, Figure 2.4c). The variation in microbial abundance within each chamber (position 1, 2, 3 and thermocouple strings A, B, C) is likely representative of the mesoscale heterogeneity of the environment (temperature, chemistry, and mineralogical precipitation) within the incubation chambers.

2.4.3 Prokaryotic Diversity and Community Composition

Rarefaction analyses and alpha diversity metrics revealed measureable differences in the diversity of prokaryotic communities from the three chambers of the sulfide microbial incubator. Based on rarefaction assessments, communities isolated from the outer chamber host a more diverse assemblage of bacteria, while the middle and inner chamber host communities of comparable diversity (Figure 2.5). Rarefaction results were corroborated by

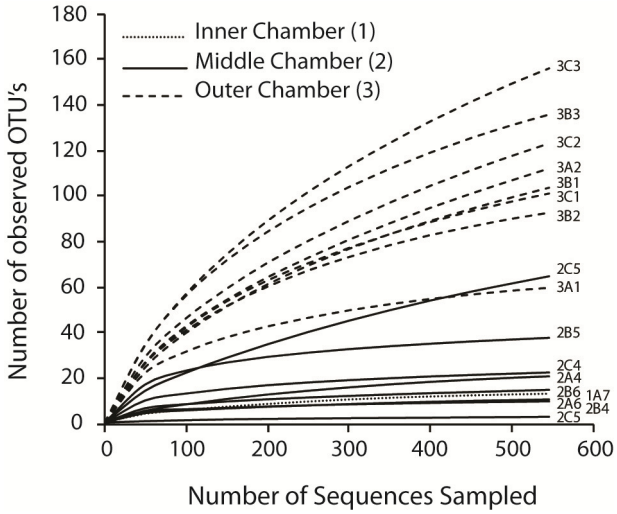

Figure 2.5: Rarefaction analysis of bacterial sequences from three chambers at the 97% OTU clustering level. All 16S rRNA libraries were randomly sampled down to the smallest sample size n = 545. Samples isolated from the outer chamber (dashed line) are more diverse than samples isolated from the middle chamber (solid line) or inner chamber (dotted line).

nonparametric-based estimates of total richness and diversity (Table 2.1). The bacterial community in the sample from the outer chamber 3C3 had the highest diversity as shown by rarefaction analysis, Chao1 species richness estimators, and the Shannon index (Figure 2.5, Table 2.1). The number of OTUs shared between any two samples is shown in Table 2.2. Because nonparametric tests often underestimate microbial diversity, these results illuminate the relative differences between outer, middle, and inner chambers, rather than provide accurate predictions of true species richness.

The communities also differed in their taxonomic composition. The NMDS plot depicts the relative difference among communities in two dimensions (Yue & Clayton 2005), showing that communities isolated from the same chamber cluster together, and thus, are more similar

Table 2.1: 16S rRNA gene sequence characteristics and alpha diversity.

	Sample	Trimmed Reads	Sampled Reads	OTU (97%)	coverage	npshannon	simpson	chao
In	1A7	2125	545	13	0.994495	0.924452	0.586083	14
Middle	2A4	2439	545	21	0.985321	0.957276	0.664611	27
	2A5	11050	545	65	0.933945	2.532822	0.251046	113
	2A6	914	545	38	0.985321	2.818606	0.1051	45
	2B4	2205	545	10	0.99633	1.345688	0.358972	11
	2B5	639	545	11	0.994495	0.990969	0.55282	12
	2B6	1269	545	15	0.990826	1.584174	0.302435	20
	2C4	545	545	23	0.988991	2.017447	0.225459	31
	2C5	1837	545	3	0.998165	0.074277	0.97815	3
Outer	3A1	1058	545	60	0.974312	3.379717	0.058628	66
	3A2	12433	545	112	0.891743	3.874123	0.061879	198
	3B1	1527	545	104	0.910092	3.739745	0.0636	166
	3B2	1909	545	93	0.944954	3.823365	0.049575	113
	3B3	809	545	136	0.900917	4.513446	0.022639	184
	3C1	774	545	101	0.926606	3.722476	0.089564	134
	3C2	1638	545	123	0.884404	4.172054	0.033797	204
	3C3	1962	545	156	0.856881	4.608287	0.022909	253

(Figure 2.6). Statistical tests underscore this observed pattern, since the communities in the samples from the outer chamber were significantly different from those isolated from the middle chamber ($p < 0.001$ for parsimony, unweighted UniFrac, and weighted UniFrac). The examination of OTUs at 97% sequence similarity revealed differences in community membership among the three chambers (Figure 2.7) that are likely driving the observed patterns of clustering.

Table 2.2: Shared OTUs at 97% similarity levels among subsamples of the outer, middle, and inner chamber.

Comparison		Shared OTUs	Comparison		Shared OTUs	Comparison		Shared OTUs	Comparison		Shared OTUs
1A7	2A4	4	2B6	2C5	3	2A5	3B2	30	3B1	3C1	54
1A7	2A5	5	2C4	2C5	2	2A6	3B2	2	3B2	3C1	35
2A4	2A5	14	1A7	3A1	6.5	2B4	3B2	0	3B3	3C1	63
1A7	2A6	4	2A4	3A1	11	2B5	3B2	0	1A7	3C2	6
2A4	2A6	5	2A5	3A1	22	2B6	3B2	1	2A4	3C2	16
2A5	2A6	7	2A6	3A1	4	2C4	3B2	3	2A5	3C2	32
1A7	2B4	3	2B4	3A1	5	2C5	3B2	0	2A6	3C2	14
2A4	2B4	4	2B5	3A1	2	3A1	3B2	19	2B4	3C2	2
2A5	2B4	4	2B6	3A1	7	3A2	3B2	49	2B5	3C2	4
2A6	2B4	3	2C4	3A1	7	3B1	3B2	63	2B6	3C2	10
1A7	2B5	3	2C5	3A1	2	1A7	3B3	0	2C4	3C2	5.5
2A4	2B5	4	1A7	3A2	1	2A4	3B3	8	2C5	3C2	1
2A5	2B5	6.5	2A4	3A2	12	2A5	3B3	12	3A1	3C2	48
2A6	2B5	4	2A5	3A2	34	2A6	3B3	6	3A2	3C2	65
2B4	2B5	3	2A6	3A2	4	2B4	3B3	1	3B1	3C2	54
1A7	2B6	5	2B4	3A2	2	2B5	3B3	1	3B2	3C2	31
2A4	2B6	5	2B5	3A2	1	2B6	3B3	2	3B3	3C2	45
2A5	2B6	9.5	2B6	3A2	5	2C4	3B3	3	3C1	3C2	94
2A6	2B6	5	2C4	3A2	6.5	2C5	3B3	0	1A7	3C3	0
2B4	2B6	6	2C5	3A2	1	3A1	3B3	25	2A4	3C3	12
2B5	2B6	4	3A1	3A2	40	3A2	3B3	45	2A5	3C3	16
1A7	2C4	7.3	1A7	3B1	2	3B1	3B3	101	2A6	3C3	4
2A4	2C4	8.5	2A4	3B1	14	3B2	3B3	52	2B4	3C3	1
2A5	2C4	11	2A5	3B1	17	1A7	3C1	2	2B5	3C3	2
2A6	2C4	5	2A6	3B1	6	2A4	3C1	12	2B6	3C3	2
2B4	2C4	2	2B4	3B1	3	2A5	3C1	16	2C4	3C3	3
2B5	2C4	4	2B5	3B1	3	2A6	3C1	5	2C5	3C3	0
2B6	2C4	5	2B6	3B1	6	2B4	3C1	2	3A1	3C3	23
1A7	2C5	3	2C4	3B1	3	2B5	3C1	2	3A2	3C3	47
2A4	2C5	2	2C5	3B1	23	2B6	3C1	3	3B1	3C3	80
2A5	2C5	2	3A1	3B1	23	2C4	3C1	4	3B2	3C3	38
2A6	2C5	2	3A2	3B1	46	2C5	3C1	1	3B3	3C3	54
2B4	2C5	3	1A7	3B2	0	3A1	3C1	37	3C1	3C3	51
2B5	2C5	2	2A4	3B2	12	3A2	3C1	57	3C2	3C3	86

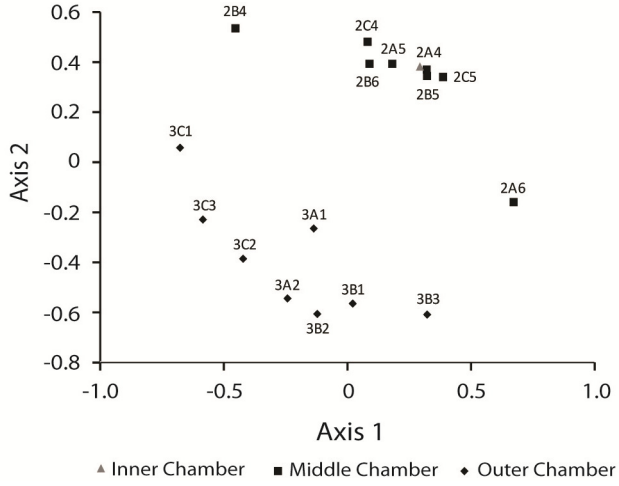

Figure 2.6: Non-metric dimensional scaling plot (NMDS) of the Yue & Clayton measure of dissimilarity (thetayc) between the structures of communities isolated from the outer (diamond), middle (square) and inner (triangle) chambers at 97% sequence similarity groups. Communities from the outer and middle chambers prove to be statistically significantly different with p-values of less than 0.001 by parsimony, UniFrac and unweighted UniFrac.

2.4.3.1 Outer Chamber

Communities from the outer chamber were dominated by epsilon-proteobacteria, which accounted for 55% of all sequences amplified from these samples (Figure 2.7). Within the epsilon-proteobacteria, sequences related to the genera *Sulfurovum* and *Sulfuromonas* were highly represented (22% and 11% of all sequences from the outer chamber, respectively). In particular, sample 3A2 had the highest percentage of each of these genera, with 42% of its

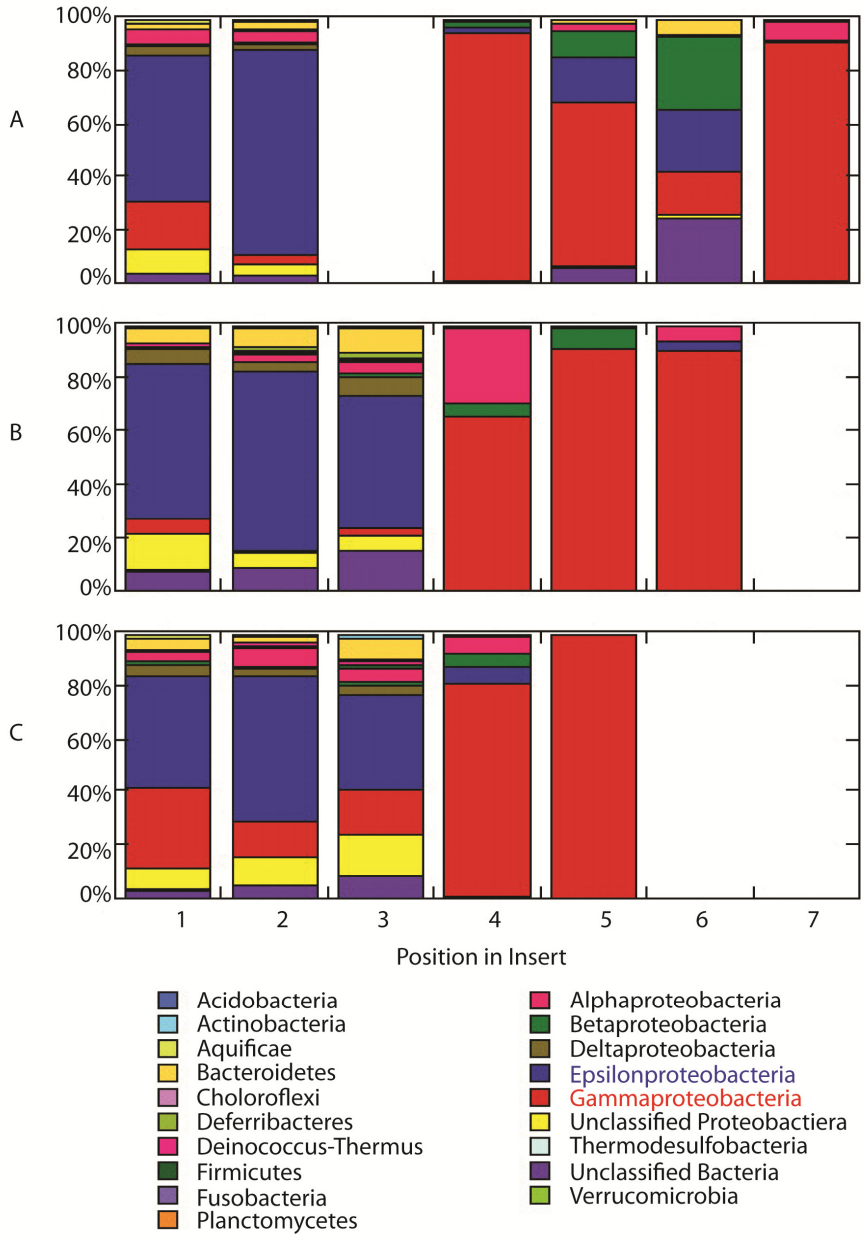

Figure 2.7: Bacterial taxonomic distribution of communities isolated from the outer (1-3), middle (4-6) and inner (7) chamber of the sulfide microbial incubator revealed striking differences in microbial community composition. The outer chamber sequences were dominated by epsilon-proteobacteria (blue) whereas the middle and inner chamber sequences were dominated by gamma-proteobacteria (red). Bacteria V1-V3 region and archaeal V3-V4 regions of the 16S were sequenced by 454, analyzed with Mothur, and all libraries were randomly resampled down to the smallest sample size, n = 545.

sequences allied to *Sulfurovum* and 15% allied to *Sulfuromonas*. Additionally, sequences related to the epsilon-proteobacterial genera *Hydrogenimonas, Camnibacter, Nautila, Nitrafractor, and Nitratiruptor* (all chemoautotrophic, microaerophilic mesophiles; Takai, 2008) were also abundant. Sequences related to the gamma-proteobacterial genus *Thiomicrospira* were also present in the outer samples and represented 28% of the sequences from sample 3C1. Additionally, sequences with high similarity to *Hydrogenivigra*; *Thermovibrio* (Aquificae); *Anaerolineales* (Chloroflexi); *Caldithrix* (Deferribacteres); *Oceanithermus*; *Vulcanithermus* (Deinococcus-Thermus); *Ralstonia*; *Acidovorax* (beta-proteobacteria); *Desulfobulbus, Desulfocapsa*, and *Desulfuromonas* (delta-proteobacteria); and *Thermodesulfobacteria* were found only in samples from the outer chamber at varying abundances. Only five OTUs (four allied to epsilon-proteobacteria *Sulfurovum* and one to delta-proteobacteria *Desulfocapsia*) were shared by all samples from the outer chamber.

2.4.3.2 Middle Chamber

At 97% similarity, 72% of all sequences isolated from the middle chamber were related to gamma-proteobacteria, with the most abundant OTUs for the genera *Erwinia, Escherichia* and *Shigella* (Figure 2.7). While we initially considered these sequences as contaminants given their affiliation to known gut-associated taxa, identification was only possible to genus level of classification. Via Blast-n (Altschul *et al*. 1997), the majority of the sequences comprising these OTUs best matched to partial 16S rRNA gene sequences recovered from seawater from the Sargasso Sea (Venter *et al*. 2004), off the coast of Hawaii (Kembel *et al*. 2011) and hydrothermal vents (Nunoura & Takai 2009; Sylvan *et al*. 2012). Seven OTUs were shared by 4 or more samples isolated from the middle chamber (*Delftia*, and 6 γ-proteobacteria OTUs including

Thiomicrospira). Numerous sequences from the A and B thermal couple strings (up to 25% in sample 3A3) were related to *Delftia* a beta-proteobacteria. *Brevundiamonas* (alpha-proteobacteria*), Cupravidus* and *Methylophilus* (beta-proteobacteria) were found only in samples from the middle chamber at varying abundances. Many of the OTUs related to the epsilon-proteobacteria that dominated the outer chamber were present in the middle chamber samples but at much lower percentages.

2.4.3.3 Inner chamber

Due to difficulty in generating appropriate quantities of DNA for sequencing via whole genome amplification, only one sample from the inner chamber yielded enough material to generate pyrosequencing data. From this one sample, thirteen OTUs were classified. The majority of these sequences were phylogenetically allied to *Erwinia* (73%) or *Escherichia* (14%) (Figure 2.7). However, 7% of all sequences were related to *Methylobacterium* an alpha-proteobacteria. The remaining sequences were either unclassified or had representatives related to *Flavobacteria, Streptococcus*, or were only able to be classified to the level of beta- and gamma- proteobacteria. As these are not common among hydrothermal vents, and due to the increased risk of contamination when amplifying from substrates with few or no native microbes, we are assuming these are likely contaminants and do not consider them in further analyses.

2.4.4 Comparative Metagenomic Analysis

The functional capacity of the microbial community within the outer and middle chambers were assessed by comparisons of pyrosequencing-derived metagenomic sequences from two discrete samples within each chamber (Outer: 3A2, 3B1, Middle: 2A5, 2C4) to

multiple annotated protein databases using MG*Rast*'s non-redundant database, M5NR. A summary of sequence statistics is shown in Table 2.3. These metagenomic data corroborate our pyrotag data wherein the most abundant 16S rRNA gene sequences identified from the outer chamber samples were epsilon-proteobacteria compared with gamma-proteobacteria from the middle chamber sample. Unlike pyrotag sequencing, metagenomics analysis provided insight into the composition of the archaeal community within both chambers. Sequences related to methanogenic archaea *Methanomicrobia, Methanobacteria, Methanococci, Methanopyri* were detected in both chambers and dominated the 16S rRNA gene sequences from the outer chamber. Sequences related to *Thermoprotei* and *Thermococci* were more abundant in the middle chamber metagenome though they were detected in both. Sequences classified to *Archaeoglobi* and *Halobacteria* were also identified in both chambers at varying abundances.

2.4.4.1 Metabolic Diversity

2.4.4.1.1 Carbon fixation

Four autotrophic carbon fixation pathways were reconstructed from the metagenomic data (Figure 2.8); the Calvin Benson Bassham (CBB) cycle, reverse tricarboxylic acid cycle (rTCA), the 3-hydroxypropionate (3-HP) cycle and the reductive Wood-Ljungdahl pathway (WL). The key enzyme of the CBB cycle (RubisCO) was differentially enriched in the middle chamber sample 2A5 (Log_{10}(Odds Ratio) with respect to the outer samples is 0.36). All but three genes in the CBB cycle were identified in all three metagenomes (Figure 2.8a). The gene for fumarate reductase, a key enzyme in the rTCA cycle, was slightly enriched in the outer samples (Log_{10}(Odds Ratio) = -0.046). Homologs to genes encoding two enzymes also essential for rTCA,

Table 2.3: Summary of metagenomic sequences from outer and middle Chimney

Process	Item	3A2	3B1	2A5	2C4
Upload	Total Base Pairs	403,592,281	381,066,965	238,914,816	232,077,712
	Sequences Count	785,269	411,199	461,480	263,426
	Mean Sequence Length	513 ± 93	926 ± 435	517 ± 107	880 ± 393
	Mean GC %	43 ± 8 %	42 ± 8 %	46 ± 7 %	46 ± 10 %
	Artificial Duplicate Reads: Sequence Count	33,541	25,841	20,918	19,243
Post QC	Total Base Pair Count	300,363,672	156,781,484	135,966,816	88,560,570
	Sequences Count	561,955	128,638	262,430	81,983
	Mean Sequence Length	534 ± 48	1,218 ± 332	518 ± 66	1,080 ± 402
	Mean GC %	43 ± 8 %	43 ± 8 %	47 ± 8 %	50 ± 7 %
Processed	Predicted Protein Features	578,986	156,021	255,574	82,979
	Predicted rRNA Features	49,163	11,997	64,075	30,372
Alignment	Identified Protein Features	398,934	88,583	161,160	62,234
	Identified rRNA Features	689	208	1,755	386
Annotation	Identified Functional Categories	375,267	80,679	144,778	52,854
	GenBank	428,894	114,518	215308	157625
	IMG	426,020	112,313	182046	140827
	KEGG	395,251	89,849	165890	77856
	PATRIC	431,452	109,678	179405	127590
	RefSeq	440,964	112,690	207133	140396
	SEED	385,928	88,539	165422	83758
	SwissProt	81,717	24,266	33465	29188
	TrEMBL	431,115	110,861	200031	140379
	eggNOG	387,703	84,331	156170	57813
	COG	331,235	69,218	107836	24702
	KO	241,634	49,892	78753	11529
	NOG	37,923	8,603	19701	12814
	Subsystems	586,718	126,637	176354	55962
	Greengenes	113	74	87	14
	LSU	529	132	292	141
	RDP	139	69	90	16
	SSU	166	78	1474	247

2-oxyglutrate synthetase and ATP-citrate lyase, were not detected in any of the three metagenomes (Figure 2.8b). Genes for majority of the enzymes involved in the 3-HP cycle and the WL cycle were not identified in metagenomes (Figure 2.8c and 2.8d).

Figure 2.8: Enrichment of genes involved in Carbon Fixation

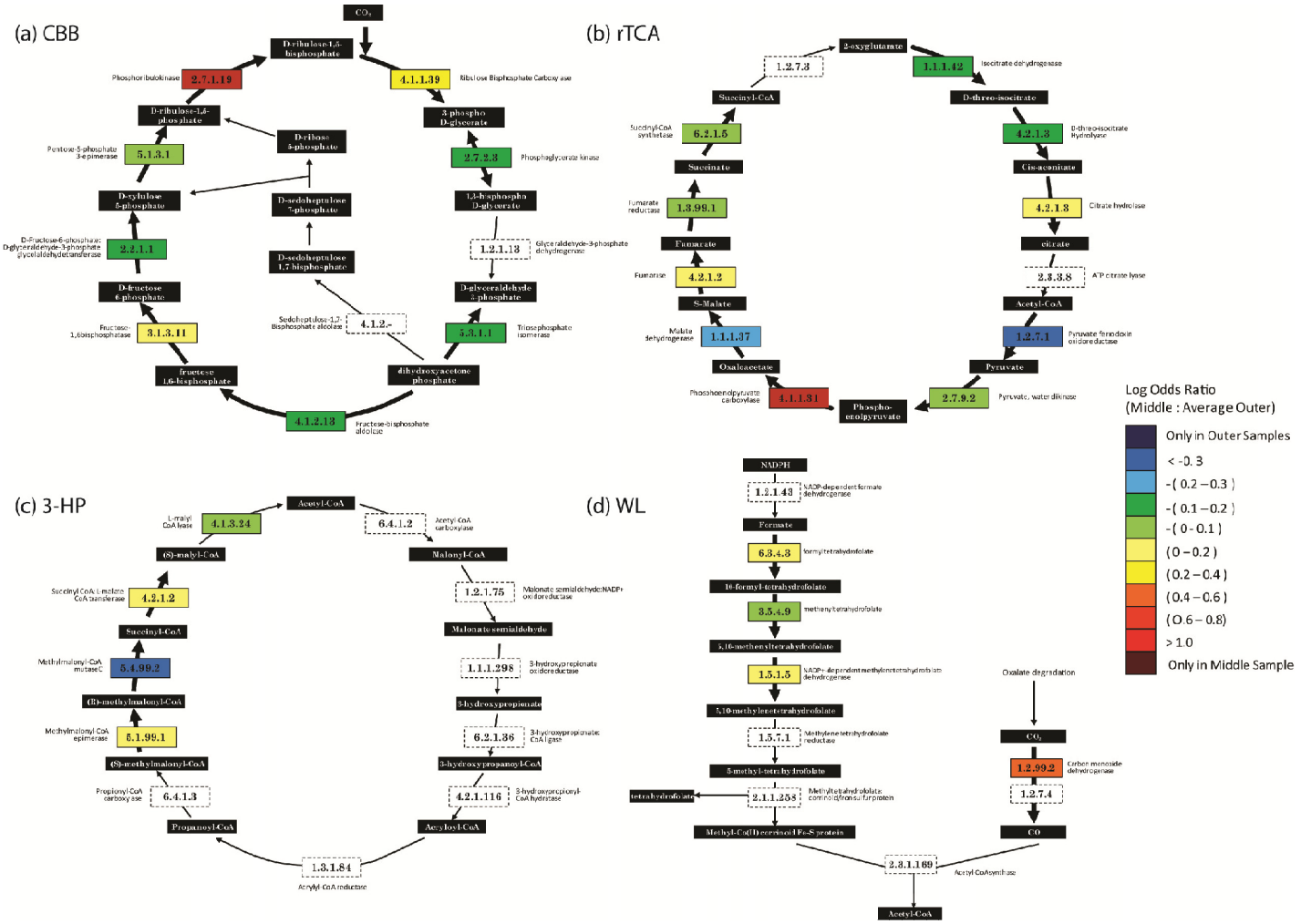

Figure 2.8: Enrichment of genes involved in Carbon Fixation via (a) Calvin Benson Bassham (CBB) cycle, (b) reverse tricarboxylic acid cycle (rTCA), (c) the 3-hydroxypropionate (3-HP) cycle and the Wood-Ljungdahl pathway (d). Box color indicates the base-10 logarithm of the odds ratio between 2A5 and the average percent of hits from the two outer chamber samples. Warm colors indicate genes are more enriched in sample 2A5 (log(odds ratio) > 0), whereas cool colors (log(odds ratios)<0) indicate genes enriched in the outer sample. Gene annotations are represented by functional M5NR ontology as annotated in MG-RAST.

2.4.4.1.2 C-1 Metabolisms

The concentration of methane in hydrothermal fluid around a neighboring chimney in the Mothra Faulty Tower complex (Tower chimney) is high and ranges from 881-899 µM in focused flow and 9 – 176 µM in diffuse flow (Wankel *et al*. 2011). The gene for the enzyme methyl coenzyme M reductase, an essential enzyme for methanogenesis, is differentially enriched in the middle chamber sample with respect to the outer chamber samples (Log_{10}(Odds Ratio) = -0.82). Genes for methane monooxygenases (MMOs), key enzymes for the oxidation of methane, were not identified in any of the metagenomes.

2.4.4.1.3 Hydrogen Oxidation

The concentration of hydrogen in hydrothermal fluid around the Faulty Tower complex to support autotrophic metabolisms ranges from 64-68 µM in focused flow and 0.3 – 14 µM in diffuse flow (Wankel *et al*. 2011). Genes encoding Ni/Fe hydrogenases indicative of hydrogen oxidation were enriched in the outer chamber sample with respect to the middle chamber sample. Of all the metabolisms reconstructed hydrogen oxidation had the greatest enrichment in the outer chamber samples (Log_{10}(Odds Ratio) = -0.59).

2.4.4.1.4 Nitrogen Metabolism

Genes for nitrogen fixation, ammonification and denitrification and were enriched in the outer chamber samples with respect to the middle chamber sample 2A5 (Figure 2.9). Genes essential for ammonia oxidation and nitrite oxidation were not detected. The nitrate reductase gene responsible for the conversion of nitrate to nitrite was enriched in the middle sample (Log_{10}(Odds Ratio) = -0.16). Genes for only one type of nitrate reductase was identified across all genomes where as genes for two types of nitrite reductases were detected.

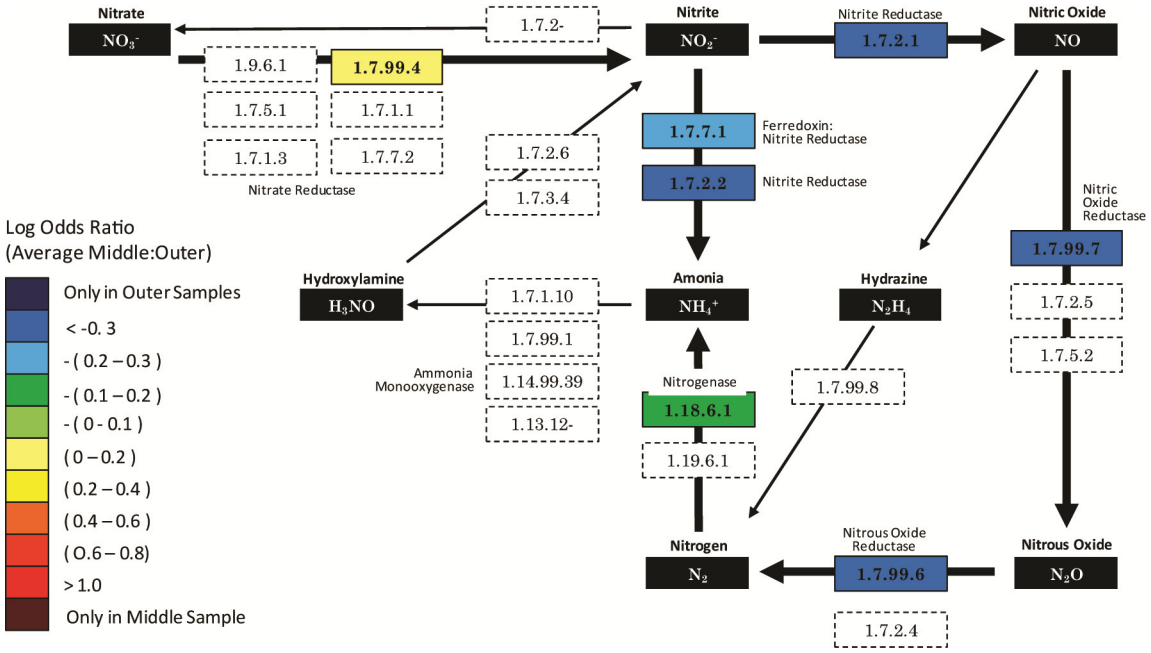

Figure 2.9: Enrichment of genes involved in dissimilatory nitrogen metabolisms. Box color indicates the base-10 logarithm of the odds ratio between 2A5 and the average percent of hits from the two outer chamber samples. Warm colors indicate genes are more enriched in sample 2A5 (log(odds ratio) > 0), whereas cool colors (log(odds ratios)<0) indicate genes enriched in the outer sample. Gene annotation is represented by functional M5NR ontology as annotated in MG-RAST.

2.4.4.1.5 Sulfur Metabolism

Due to the high concentration of dissolved sulfide in hydrothermal fluid (3-12 mM kg^{-1}; Butterfield *et al.* 1994) and high concentrations of sulfate in seawater (28mM), sulfide oxidation and sulfate reduction are the most thermodynamically favorable metabolic processes in respective zones of hydrothermal chimneys. Genes encoding key enzymes involved the sulfur-compound oxidation (Sox)-dependent pathway were found to be differentially enriched in the outer chamber samples with respect to the middle chamber samples. The genes identified from this pathway included soxA, soxB, soxD, soxX, soxY and soxZ (Figure 2.10). Gene homologs for *soxC* were not detected. Genes for sulfite oxidase and sulfite dehydrogenase, which are involved in the sulfite:cytochrome c oxidoreductase pathway, were found to be differentially enriched in the middle sample. Genes encoding flavocytochrome c/sulfide dehydrogenase (FccAB) were both identified but putative sulfide quinone oxidoreductase and cytochrome C oxidoreductases were not. Genes encoding canonical sulfate reduction enzymes, dissimilatory sulfate reductase, adenosine-5'-phosphosulfate reductase and ATP sulfurylase were also enriched in the outer chamber (Figure 2.10).

2.4.4.2 Other functions

Several other differences in gene content were also observed (Figure 2.11a). The metagenomic data discussed further focuses on subcategories that have been shown in previous studies to be enriched in hydrothermal systems (Xie *et al.* 2011). Genes enriched in the outer samples were related to quorum sensing, electron donating reactions and heat shock stress. On the other hand, sample 2A5 was enriched in genes for electron accepting reactions,

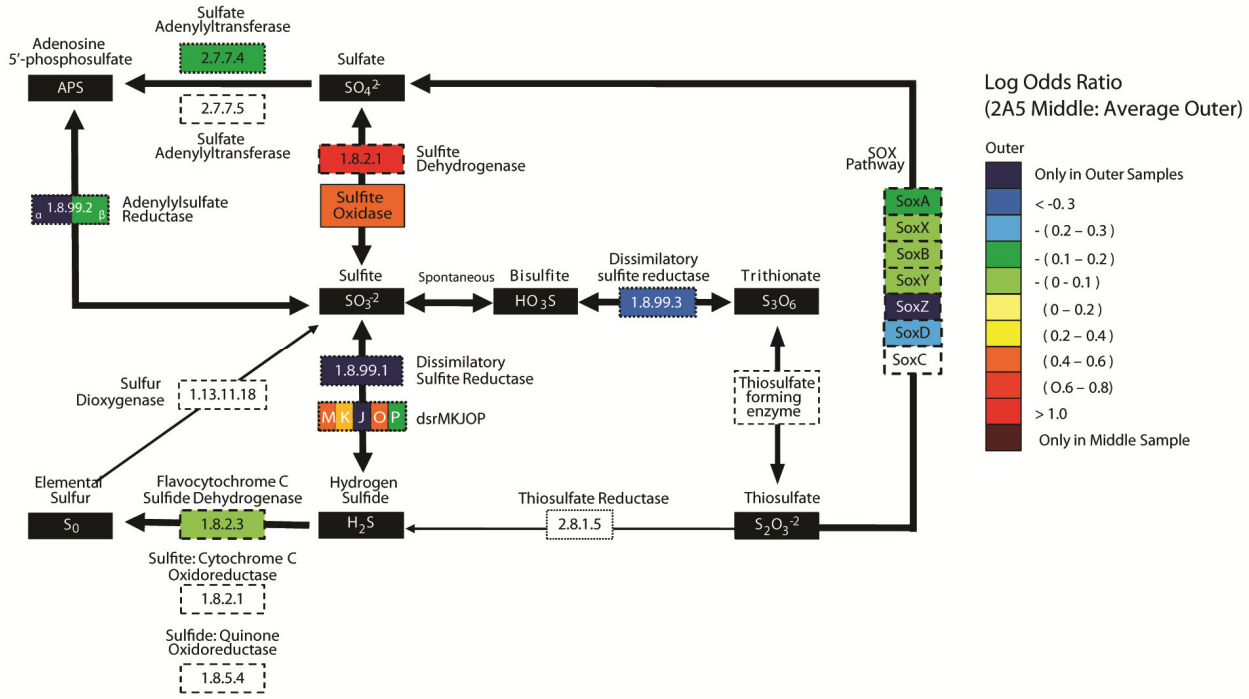

Figure 2.10: Enrichment of genes involved in dissimilatory sulfur metabolisms. Box color indicates the base-10 logarithm of the odds ratio between 2A5 and the average percent of hits from the two outer chamber samples. Warm colors indicate genes are more enriched in sample 2A5 (log(odds ratio) > 0), whereas cool colors (log(odds ratios) < 0) indicate genes enriched in the outer sample. Gene annotation is represented by functional M5NR ontology as annotated in MG-RAST.

detoxification and osmotic stress. Genes for archaeal lipids, acid stress, dormancy and sporulation were enriched differently between samples 3A2 and 3B1, with 3A2 having a greater gene abundance than 2A5 and 3B1 having a lower gene abundance. Variation of sequences observed within the subsamples of the outer chamber further reflects the heterogeneity of the environment possible within a sulfide chimney.

a) Enrichment of SEED Subsystem Categories

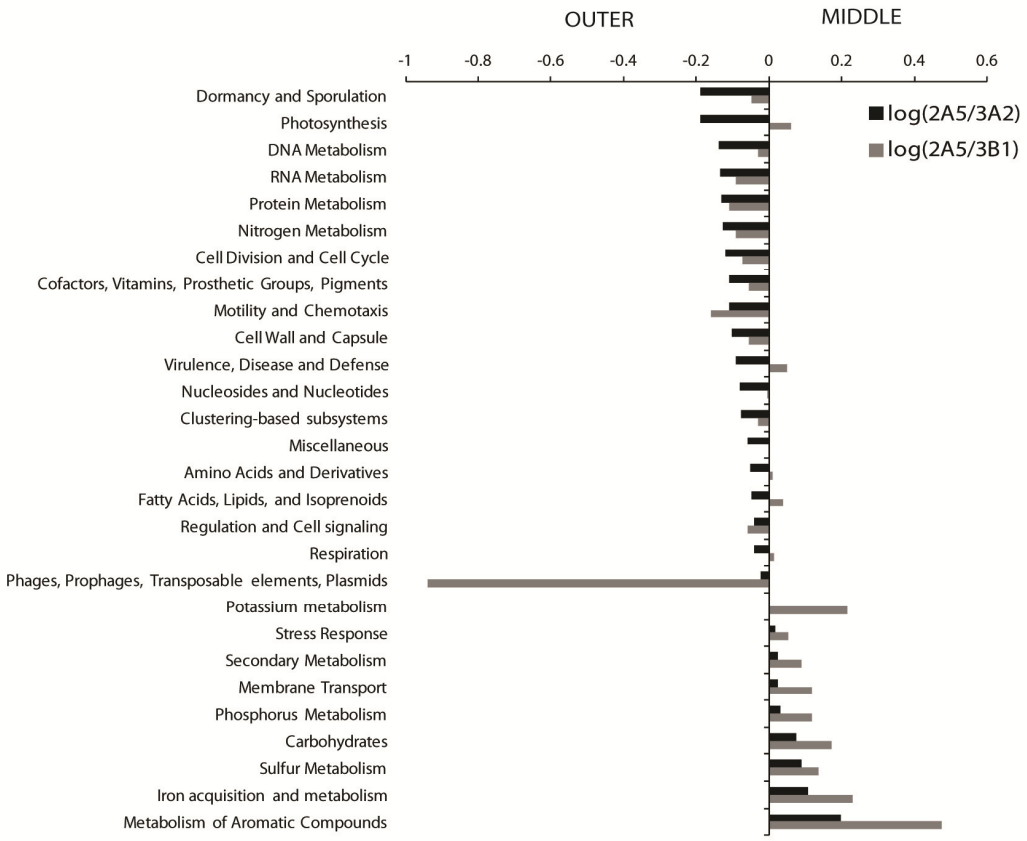

b) Enrichment of genes for particular pathways

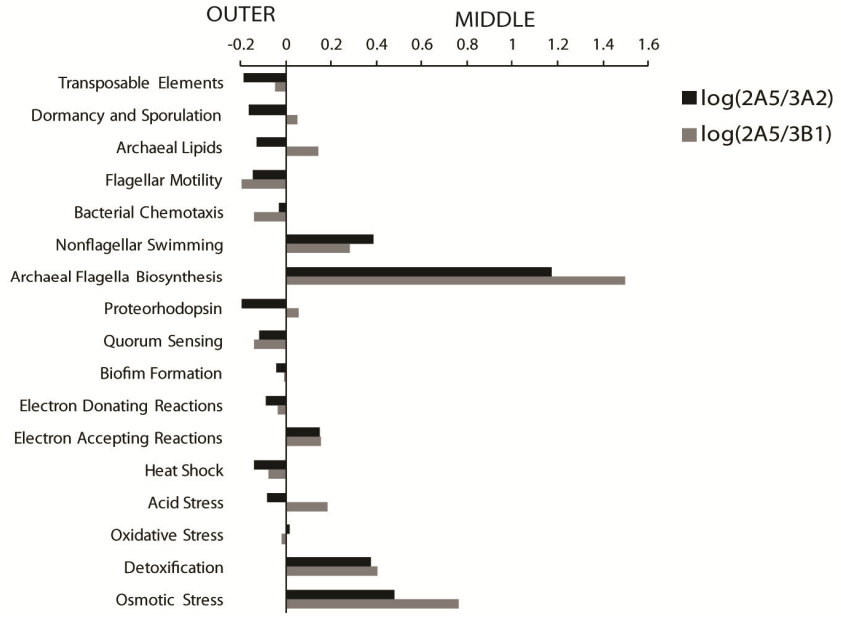

Figure 2.11: Differences in the enrichment of M5NR subsystem categories between metagenomes

Figure 2.11 (continued): Differences in the enrichment of M5NR subsystem categories between metagenomes from the outer and middle chamber. Bars indicate the base-10 logarithm of the odds ratio $((G_{Mid}/T_{Mid})/(G_{Out}/T_{Out})$, where G is the number of reads to a given gene or category and T is the total number of reads in a given metagenome. Positive log (odds ratios) indicate that genes are more enriched in sample 2A5, whereas negative log(odds ratios) indicated genes or categories that are enriched in one of the outer samples. Black and Gray bars indicate relative levels of enrichment in comparison between outer samples 3A2 or 3B1 with middle sample 2A5, respectively, on a linear scale. Genes categories represent (a) level 2 or (b) select level 3 categories of the M5NR Subsystems ontology as annotated in MG-RAST.

Genes for motility and chemotaxis accounted for less than 1.5% of the annotated proteins with known function in each sample. Genes for flagellar motility (e.g. Flagellar biosynthesis proteins FlhA/B/F/R, Flg/B/C/F/G/N/H/I/A/D/L/E/K, FliC/L/O/P/Q/R/S/T/F/D/E/K; Flagellar motor rotation proteins MotA, MotB; Flagellar motor switch proteins FliM, FliN; Flagellum-specific ATP synthase FliI; signal transduction) and bacterial chemotaxis (e.g. chemotaxis protein CheC/D/V/X; Methyl-accepting chemotaxis protein I/ III/IV; ABC transporter) are differentially enriched in both 3A2 and 3B1 with respect to 2A5. However, archaeal flagella biosynthesis genes (FlaC/H/I/J) and genes for nonflagellar swimming are enriched in 2A5 with respect to the two outer samples (Figure 2.11b).

Genes for DNA metabolism account for roughly 4% of annotated proteins via SEED Subsystems categorization. Genes for DNA base repair in UvrABC, RecFOR, UvrD, MutL-S pathways were enriched in the outer samples, whereas genes for DNA repair via DinG, UmuCD and Non-homologus endjoining proteins were enriched in the middle 2A5 sample.

2.5 Discussion

This study characterized *de novo* endolithic prokaryotic communities with spatially co-registered temperature within the hydrothermal vent chimney Roane using a novel sulfide microbial incubator. The *in situ* temperatures measured within the sulfide incubation device revealed that Roane hosted at least three distinct thermal regimes across the width of the chimney. The middle and inner chambers host relatively high temperatures above 150°C, which results from an increased proportion of hot hydrothermal fluid, suggests a reducing environment. The outer chamber is much cooler with temperatures ranging between 10°C and 70°C, and suggests less chemically reducing conditions. These distinct breaks in the physiochemical environment between each chamber correlate with sharp biological boundaries for community density, composition and metabolic potential.

16S rRNA gene surveys of Roane's bacterial and archaeal communities reveal significant differences in density, diversity and taxonomic composition across the outer and inner regions of Roane. The taxonomic classifications were consistent with previous 16S rRNA work at vents (Brazelton *et al*. 2010; Huber *et al*. 2006; Kormas *et al*. 2006) and reveal patterns of distribution comparable to previously published observations (Schrenk *et al*. 2003; Kormas *et al*. 2006; Page *et al*. 2008). For example, like Kormas *et al.* (2006) the outer chamber samples were dominated by epsilon-proteobacterial sequences most closely related to the genus *Sulfurovum*. The middle and outer chambers were dominated by sequences most closely related to gamma-proteobacteria. The majority of the sequences analyzed in the outer chamber (i.e., most of the epsilon-proteobacteria and gamma-proteobacteria) corresponded to mesophilic organisms, whereas, a greater percentage of sequences related to thermotolerant

archaea (i.e. *Thermoprotei, Thermococci* and *Archaeoglobi*) were observed in the middle chambers. The mesoscale heterogeneity of community within each chamber is likely due to temporally dynamic nature of the environment and may represent small-scale differences with respect to mineralogy, temperature and chemistry.

Via 16S rRNA gene qPCR, there were also more cells (10^6 - 10^7 cells/g mineral) observed in the outer chamber than the middle (10^4 - 10^5 cells/g mineral) and inner chambers (10^3 - 10^5 cells/g mineral) which is consistent in magnitude to previous microscopy-based cell counts of sulfide-associated microbes (Schrenk *et al*. 2003). Furthermore, this qPCR data is corroborated by an enrichment of genes for archaeal lipid and flagella biosynthesis in the middle chamber sample 2A5. These findings support previous studies that find increased archaeal abundance towards the interior of the chimney (Schrenk *et al*. 2003; Kormas *et al.* 2006; Page *et al*. 2008). The patterns of prokaryotic composition that we observed may also be due in part to differences in the physiological tolerances of specific microbial taxa.

Notably, the greater bacterial diversity observed in the outer chamber samples as compared to the middle and inner chamber samples may be reflective of the pronounced thermal oscillations observed within the outer chamber. Low temperature measurements (i.e. ~10 °C) are consistent with influxes of seawater supplying oxidants like oxygen and sulfate, whereas higher temperature measurements (70 °C) would be indicative of greater end-member mixing - supplying reduced substrate and creating anoxic pockets for anaerobic metabolisms to function. Here, the endolithic microbial community from the outer chamber likely encounters daily or near-daily fluctuations in temperature and data suggests that the environment has the

potential to support both aerobic and anaerobic organisms. The middle chamber on the other hand is a much more stable environment though with a much greater temperature (120 °C).

Autotrophic metabolisms were detected in both chambers and presumably linked to inorganic carbon fixation via the CBB cycle. The CBB pathway is responsible for the majority of global primary productivity and is thought to be the dominant carbon fixation pathway utilized by vent microorganisms (Elsaied *et al.* 2007; Elsaied & Naganuma 2001; Ferrera *et al.* 2007; Olins *et al.* 2013). The key enzyme of this pathway, Ribulose-1,5-bisphosphate carboxylase/oxygenase (RuBisCO) was shown to be enriched in the middle chamber sample, though most of the other CBB genes were enriched in the outer chamber. Because RuBisCO has been shown to be highly oxygen tolerant and only stable in temperatures up to 75 °C (Berg 2011), the enrichment of RuBisCO genes in the middle chamber may not reflect the actual expression of the gene *in situ*, though we cannot exclude the possibility of thermotolerant forms of RuBisCO in this system.

Evidence for autotrophic carbon fixation via the rTCA cycle is scant in these samples. Hydrothermal epsilon-proteobacteria and Aquifacae have been shown to express enzymes for the rTCA cycle (Perner *et al*. 2007; Takai *et al*. 2005a; Hügler *et al*. 2007; Hu *et al*. 2005), suggesting that rTCA is a potentially important carbon fixation pathway at hydrothermal vents. However, the fumarate reductase gene (a key enzyme in the rTCA cycle) was slightly enriched in the outer samples, though homologs to genes encoding 2-oxyglutrate synthetase and ATP-citrate lyase (two other enzymes also essential for rTCA) were not detected in any of the three metagenomes. The most enriched genes in the rTCA pathways such as malate dehydrogenase

and pyruvate:ferrodoxin oxidoreductase are utilized in other pathways (i.e. Embden–Meyerhof pathway of sugar degradation) and may not be indicative of the rTCA cycle.

Carbon fixation by the WL pathway is utilized by archaeal methanogens and strictly anaerobic organisms and is thought to be the most thermal tolerant carbon fixation pathways (Berg 2011). Because knowledge of this process is still limited, the gene for methyl coenzyme M reductase (*mcr*) is commonly used as a proxy to identify this pathway (Luton *et al.* 2002). Genes involved in methanogenesis (including *mcr*) were enriched in the middle chamber along with 16S rRNA gene sequences allied to archaeal methanogens *Methanopyri* (Nakagawa & Takai 2008). While majority of the unique genes for the WL pathway were not identified in metagenomes, including the key enzyme CO dehydrogenase/acetyl-CoA synthetase (Ljungdahl 1986; Ragsdale & Pierce 2008; Zarzycki *et al*. 2009), our data do not exclude the possibility of WL as a carbon fixation pathway.

The key enzymes for 3-HP pathway, acetyl-CoA/propionyl-CoA carboxylase, malonyl-CoA reductase and propionyl-CoA synthase were not detected in any of the metagenome data sets which is consistent with previous vent observations (Xie *et al*. 2011). Most chemoautotrophs (like *Crenarchaeota symbiosum* or *Chloroflexus aurantiacus;* Herter *et al*. 2002; Strauss & Fuchs 1993) that utilize the 3-HP or 3-HP/4-HB cycle for carbon fixation are not prevalent at deep-sea vents. This further supports previous hypothesize that the 3-HP cycle of the 3-HP/4-hydroxybutyrate is not likely an important carbon fixation pathway within deep-sea hydrothermal vents (Nakagawa & Takai 2008; Xie *et al*. 2011; Minic & Thongbam 2011).

Metagenomic analysis further revealed an enrichment of genes for electron donating reactions in the outer chamber. Consistent with this 16S rRNA sequences allied to cultured

representatives with known aerobic metabolisms dominated sequences from the outer chamber samples. Genes encoding Ni/Fe hydrogenases indicative of hydrogen oxidation were enriched in the outer chamber sample with respect to the middle chamber sample. Sequences related to chemoautotrophs with capacity to utilize hydrogen as an electron donor and oxygen (*Hydrogenimonas, Hydrogenivigra*; Takai 2004a; Nakagawa *et al*. 2004a), nitrate *(Caminibacter, Nautila, Nitrafractor* and *Nitratiruptor*; Alain *et al*. 2002b; Miroshnichenko 2004; Voordeckers *et al.* 2005; Smith *et al.* 2008; Nakagawa *et al.* 2005c), or sulfur *(Thermovibrio, Thermodesulfobacteria;* Vetriani 2004; Huber *et al.* 2002; Jeanthon *et al*. 2002) as an electron acceptor were present in outer chamber samples.

Genes for nitrogen fixation, ammonification and denitrification were also enriched in the outer chamber samples with respect to the middle chamber sample. Evidence for nitrification and denitrification has been detected in hydrothermal environments (Mehta & Baross 2006) and nitrogen fixation has been identified as an important processes contributing to the nitrogen cycle at deep sea vents. In pure culture, members of the genus *Caminibacter, Nautila, Nitrafractor* and *Nitratiruptor* (present in the outer chamber) have been shown to reduce seawater nitrate to ammonium (Alain *et al.* 2002b; Voordeckers *et al.* 2005; Miroshnichenko 2004; Nakagawa *et al.* 2005c; Blöchl *et al.* 1997) or nitrogen (Nakagawa *et al*. 2005c). Even though end-member fluids of Roane are known to have high concentrations of ammonia (>450µmol/kg), the amoA gene encoding a key enzyme in ammonium oxidation was not identified in any of the metagenomes. The nitrate reductase gene (nar) responsible for the conversion of nitrate to nitrite was enriched in the middle sample suggesting that nitrate may

be an important electron acceptor at higher temperatures, perhaps coupled to sulfide or hydrogen oxidation.

Sulfide oxidation is likely the most dominant metabolic mode in the outer chamber as it is predicted to be one of the most thermodynamically favored processes (McCollom & Shock 1997). The taxonomic dataset from the outer chamber samples are all dominated by sequences related to common vent associated sulfide oxidizing organisms *Sulfurovum and Sulfuromonas* (Inagaki *et al.* 2004). Sequences related to chemoautotrophic sulfur oxidizing *γ-proteobacteria Thiomicrospira* were also abundant. Furthermore, consistent with taxonomic data, genes encoding key enzymes involved in (Sox)-dependent sulfur oxidation pathway, along with genes for flavocytochrome c/sulfide dehydrogenase (FccAB), were enriched in the outer chamber. The presence of FccAB may be indicative of differential bacterial niche utilization in response to sulfide concentration gradients as FccAB is hypothesized to be adapted for function at low sulfide concentrations (Mussmann *et al*. 2007).

From the three metagenomes (3A2, 3B1, 2A5), gene fragments annotated as partial dissimilatory sulfite reductase subunit A were aligned with *dsrA* clusters from sulfate reducing organisms (data not shown). The fact that the majority of the dissimilatory sulfite reductases cluster with those from sulfate reducers confirms the presence of sulfate reduction rather than a functional reverse dissimilatory sulfate reductase pathway for sulfur oxidization (Hipp et al. 1997). Furthermore, sequences allied to common hydrothermal vent sulfate reducing organisms *Desulfobulbus, Desulfocapsa* and *Desulfurommonas* (delta-proteobacteria*)* and *Thermodesulfobacteria* were detected in 16S rRNA samples from the outer chamber. While the activity of sulfate reducers can only be conjectured (as this is a DNA based study), the outer

chamber does host optimal thermal conditions (around 50°C) that have been observed to support sulfate reduction activity in pyrite dominant vents (Frank *et al*. 2013b). Additionally, the presence of sequences related to *Thermodesulfobacteria* may be indicative of potential thermophilic sulfate reduction (Frank *et al.* 2013a).

Metagenomic data suggested that the communities may be tolerant of different stresses. Genes for heat shock were enriched in the outer chamber along with genes for dormancy and sporulation, whereas genes for detoxification and osmotic stress were enriched in the middle chamber. Metagenomic data also showed an elevated potential for bacterial motility and chemotaxis in the outer chamber, suggesting that this community had a higher capacity to sense and respond to environmental cues such as oxygen concentration or thermal stress. Furthermore, different mechanisms for DNA base repair were enriched in each chamber. The outer chamber samples were also enriched in genes for biofilm formation and quorum sensing. Biofilm morphologies may help to protect organisms from the dynamic nature of the environment and contributed to the high microbial diversity observed in the outer chamber (James *et al*. 1995; Wolfaardt *et al*. 1994; MacLeod *et al*. 1990; Costerton *et al*. 1994, 1995; Donlan & Costerton 2002). The middle chamber sample was also enriched in genes for nonflagellar swimming and archaeal flagella biosynthesis.

The dynamic thermal and chemical regimes within a sulfide –and accordingly within the incubator- reveal the complexity of life in the endolithos, and provide a framework for more informed assessment of how the community structure is influenced by temperature. The data herein reveal that the distribution, abundance and physiological capacity of endolithic vent communities are governed by the chemical and physical characteristics of the environment.

Particularly, thermal fluctuations in the outer chamber suggest temporal variation in the chemical regime thereby facilitating a wider niche space conducive to greater functional and phylogenetic diversity. The distinct differences in community composition that we observed may be due in part to physiological tolerances of specific microbial taxa, as well as metabolic capacity of each community. In this study the utilization of a novel *in-situ* sulfide microbial incubator containing arrays of temperature probes allowed for direct access to the endolithic community within a mature, actively venting sulfide and provided co-registered environmental and microbiological information necessary to quantify the physiological diversity of microorganisms within different thermal-chemical environments. With the development and application of new molecular tools and appropriate sampling devices like the sulfide microbial incubator, a more in depth analysis of the communities that thrive endolithically at vents can be established. By investigating community diversity at these scales along complex and extreme gradients of temperature and chemistry we can impose constraints on the microbial colonization and metabolic activity at vents to estimate the microbial impact on global biogeochemical cycling.

2.6 Acknowledgements

We are grateful for the expert assistance of the *R/V Atlantis* and *R/V Western Flyer* crews and the pilots and team of the *DSV Alvin*, *ROV Jason* and *ROV Tiburon* for enabling the drilling of hydrothermal deposits and the deployment and recovery of the sulfide incubation device. We also thank John Baross (University of Washington), Eric Cordes (Temple University), James Holden (University of Massachusetts), Jon Sanders (Harvard), Heather Olins (Harvard),

Roxanne Beinart (Harvard) and Andrew Jones (Yale) for providing assistance with various technical aspects of the experiments, analysis and manuscript review. Financial support for this research was provided by the National Science Foundation (NSF OCE-0838107 and NSF OCE-0426109 to D.S. Kelley), and the National Aeronautic and Space Administration (NASA-ASTEP NNX09AB78G to C. Scholin).

CHAPTER THREE:

Characterizing the distribution and rates of microbial sulfate reduction at Middle Valley hydrothermal vents

Kiana L. Frank[1], Daniel R. Rogers[2], Heather C. Olins[2], Charles Vidoudez[2] and Peter R. Girguis[2]

1 = Department of Molecular and Cellular Biology, Harvard University, 16 Divinity Ave., Cambridge, MA
2 = Department of Organismic and Evolutionary Biology, Harvard University, 16 Divinity Ave., Cambridge, MA

This chapter is presented with slight formatting modifications as it appeared in *The ISME Journal* (2013) 7, 1391–1401; doi:10.1038/ismej.2013.17. Corresponding supplemental information is appended in Appendix B.

3.1 Abstract

Few studies have directly measured sulfate reduction at hydrothermal vents, and relatively little is known about how environmental or ecological factors influence rates of sulfate reduction in vent environments. A better understanding of microbially mediated sulfate reduction in hydrothermal vent ecosystems may be achieved by integrating ecological and geochemical data with metabolic rate measurements. Here we present rates of microbially mediated sulfate reduction from three distinct hydrothermal vents in the Middle Valley vent field along the Juan de Fuca Ridge, as well as assessments of bacterial and archaeal diversity, estimates of total biomass and the abundance of functional genes related to sulfate reduction, and *in situ* geochemistry. Maximum rates of sulfate reduction occurred at 90°C in all three deposits. Pyrosequencing and functional gene abundance data reveal differences in both biomass and community composition among sites, including differences in the abundance of known sulfate reducing bacteria. The abundance of sequences for *Thermodesulfovibro*-like organisms and higher sulfate reduction rates at elevated temperatures, suggests that *Thermodesulfovibro*-like organisms may play a role in sulfate reduction in warmer environments. The rates of sulfate reduction presented here suggest that - within anaerobic niches of hydrothermal deposits - heterotrophic sulfate reduction may be quite common and might contribute substantially to secondary productivity, underscoring the potential role of this process in both sulfur and carbon cycling at vents.

3.2 Introduction

Deep sea hydrothermal vent ecosystems are complex dynamic habitats characterized by steep gradients in temperature and geochemistry (Jannasch & Mottl, 1985). In these habitats, as hot hydrothermal fluid mixes with cold seawater, the precipitation of minerals creates large and complex hydrothermal chimney deposits. Within these permeable mineral structures, the continued mixing of chemically reduced, vent-derived fluids and oxidized seawater provides favorable conditions that support the growth of endolithic microbial communities (Schrenk *et al.* 2003)

Sulfide oxidation is considered to be one of the most important microbial chemosynthetic pathways at ridge ecosystems, as evidenced by the ubiquity of sulfide oxidizing *Epsilon-* and *Gammaproteobacteria* at ridge environments (Nakagawa *et al*. 2004b, 2005b; Huber *et al*. 2007; Nakagawa & Takai, 2008; Campbell *et al.* 2006). To date, significantly less attention has been paid to the distribution and magnitude of sulfate reduction at vents, though sulfate reducing bacteria and archaea have frequently been isolated from deep sea hydrothermal environments (Houghton *et al*. 2007; Audiffrin *et al*. 2003; Alazard *et al*. 2003; Jannasch *et al*. 1988; Blöchl *et al*. 1997). Moreover, analyses of functional genes that express key proteins required for sulfate reduction suggest there is a high diversity of sulfate reducing organisms at vents, higher than predicted via 16S rRNA gene analyses alone (Nakagawa *et al*. 2004b; Nercessian *et al*. 2005).

From a biogeochemical and bioenergetic perspective, both sulfide oxidation and sulfate reduction would be favored at hydrothermal vents, though to varying degrees as a function of environmental chemistry. Sulfide oxidation is most favorable when coupled to oxygen or nitrate

as an electron acceptor (Amend & Shock 2001). Around vents, sulfide is typically in µM to mM concentrations (Butterfield, *et al*. 1994; Butterfield *et al*. 1994), while oxygen and nitrate are around 110 and 40 µM respectively (Johnson *et al*. 1986). In contrast, sulfate reduction is highly favored in anoxic niches at vents, as it is in other marine anaerobic environments (Muyzer & Stams, 2008). Here, as in most marine systems, sulfate is abundant at 28 mM (Dittmar, 1884), two to three orders of magnitude higher than oxygen. At vents, sulfate reduction would occur in regimes where seawater-derived sulfate is still present but oxygen is absent, e.g. within hydrothermal vent deposits. Sulfate reducing microorganisms commonly use hydrogen and/or dissolved organic matter as electron donors, both of which are found within hydrothermal fluids (Lang *et al*. 2006; Cruse & Seewald, 2006). Sulfate reduction –as a function of its extent and magnitude- could readily influence the cycling of sulfur and sulfur isotopes, as well as carbon, within hydrothermal environments.

To date, studies have quantified rates of sulfate reduction in hydrothermal-influenced sediments (Weber & Jørgensen, 2002; Jørgensen *et al*. 1992; Elsgaard *et al.* 1994a, 1994b, 1995; Kallmeyer & Boetius, 2004) and isolated vent microorganisms (Hoek *et al*. 2003). In contrast to the numerous studies of sulfate reduction in marine sediments (Canfield 1989), studies of sulfate reduction in hydrothermal deposits are few (Bonch-Osmolovskaya *et al*. 2011), due in part to the challenges associated with sampling and studying the heterogeneous and consolidated sulfide deposits typical of hydrothermal vent chimneys.

Here we present rates of microbially mediated sulfate reduction from three distinct, hydrothermal mineral deposits from active hydrothermal “chimneys” found in the Middle Valley field along the Juan de Fuca Ridge, as well as assessments of bacterial and archaeal

diversity, estimates of total biomass and the abundance of functional genes related to sulfate reduction, and *in situ* geochemistry. These analyses further our understanding of sulfate reduction (including rates, diversity and distribution of known sulfate-reducing microbes) in vent ecosystems. Moreover, they underscore the potential role of heterotrophic sulfate reduction in hydrothermal systems, and constrain their potential influence on both sulfur and carbon cycling,

3.3 Methods

3.3.1 *Geologic Setting and Sampling of hydrothermal deposits*

Middle Valley (48°27'N, 128°59' W) is an intermediate spreading, axial rift valley, located along the Endeavor Segment of the Juan de Fuca Ridge in the Northwest Pacific ocean. Layers of continental-derived sediments characteristically cover Middle Valley, though the hydrothermal vents remain prominent above the sediments. Hydrothermal deposits were collected from 3 active hydrothermal spires during dive 4625 with the *HOV Alvin* (*R/V Atlantis* expedition AT15-67, July 2010) and brought to the surface in a sealed, temperature-insulated polyethylene box. Samples were recovered from actively venting sulfide deposits at Needles (48.45778, -128.709, 2412.212 m, T_{max} = 123 °C), Dead Dog (48.45603,-128.71, 2405.268 m, T_{max} = 261 °C), and Chowder Hill (48.455543, -128.709, 2398.257 m, T_{max} = 261 °C) vents. Once on board ship, samples were directly transferred to sterile anaerobic seawater and handled/processed using appropriate sterile microbiological techniques. Subsamples were immediately transferred to gastight jars (Freund Container Inc.), filled with sterile anaerobic seawater containing 2 mM sodium sulfide at pH 6, and stored at 4 °C. Upon return to the

laboratory, all samples were maintained in anaerobic seawater (0.2 μm filter-sterilized prior to use) supplemented with 2mM ΣH_2S (defined as the sum of H_2S, HS^- and S^{2-}) and adjusted to pH 6. The vent-like media was replenished every 8 to 12 weeks, and all samples were kept in the dark and 4 °C prior to incubation.

3.3.2 *Vent fluid volatile geochemistry via in situ mass spectrometry*

In situ concentration of dissolved volatiles (H_2S, H_2, CO_2, O_2, and others.) were measured at each site with an *in situ* mass spectrometer (ISMS) as previously described (Wankel *et al*. 2011). Briefly, dissolved volatiles were quantified *in situ* by sampling vent effluent for up to 10 minutes, until partial pressures reached steady state (data was monitored in real time within the submersible). Concentrations were determined from empirically derived calibrations and validated by comparison with discrete samples collected using titanium gastight samplers.

3.3.3 *Measuring sulfate reduction rates*

Hydrothermal deposits were homogenized in a commercial blender (Xtreme™ blender, Waring Inc.) under a nitrogen atmosphere. Anaerobic homogenization was designed to minimize fine-scale geochemical and microbial heterogeneity and facilitate more accurate experimental replication. Hydrothermal homogenate (made up of both mineral deposit and interstitial fluid)) was aliquoted volumetrically (7.5 mL, approximately 29 g wet weight and 20 g dry weight) into Balch tubes in an anaerobic chamber. The tubes were supplemented with 15 mL of sterile artificial vent fluid media designed to mimic the geochemical composition of fluids within the pores of a sulfide deposit (pH 6, 14 mM SO_4^{2-}, 2.3 mM $NaHCO_3$, 1 mM H_2S, and 10

μM each of pyruvate, citrate, formate, acetate, lactate). Organic acid concentrations are comparable to those measured *in situ* along the Juan de Fuca ridge (Lang *et al*. 2006). Sufficient $^{35}SO_4^{2-}$ was added to achieve 555 kBq (15 μCi) of activity. Due to technical difficulties with post processing methodology, shipboard incubations using fresh material were not successful. The data presented here were generated using samples that had been maintained in sulfidic vent-like effluent (as described above) for one year. Samples were incubated anaerobically for 7 days at 4, 30, 40, 50, 60, 80 and 90 °C. Controls for sulfate reduction consisted of samples amended with 28 mM molybdate, a competitive inhibitor of sulfate reduction (Saleh *et al.* 1964; Newport & Nedwell, 1988). Six biological replicates were run for each treatment, and three biological replicates for each control. Upon completion, reactions were quenched with the injection of 5 mL 25% zinc acetate (which is ~20-fold more Zinc than the maximum sulfide concentration), and all samples were frozen at -20 °C to enable further analysis.

To determine sulfate reduction rates, samples were thawed and the supernatant was removed and filtered through a 0.2 μm syringe filter. The crushed deposits that remained in the tube were washed three times with deionized water to remove any remaining sulfate. One gram (wet weight) of crushed deposit was analyzed via chromium distillation (see Supplemental Methods) and sulfate reduction rates (SRR) were calculated as in (Fossing & Jørgensen, 1989)using the following calculation.

$$SRR = \frac{nSO_4^{2-} \cdot a \cdot 1.06}{(a+A) \cdot t} \quad \text{Eq.1}$$

Where nSO_4^{2-} is the quantity (in moles) of sulfate added to each incubation (14 mM * 15 mL = 210 μmol), *a* is the activity (dpm) of the trapped sulfide, 1.06 is the fractionation factor between the sulfide and sulfate pools, *A* is the activity of the sulfate pool at the completion of

the incubation and t is the incubation time (days). The rates are presented in units of nmol S g^{-1} day^{-1}.

3.3.4 *DNA Extraction*

Immediately prior to conducting the rate experiments, a subsample of the homogenized hydrothermal deposit was removed and frozen at -80 °C for molecular analysis. This approach ensures that the resulting sequences best represent those communities responsible for the observed activity. DNA was extracted from this crushed deposit sample with a protocol modified from (Santelli *et al*. 2008). Subsamples were washed with 0.1 N HCl, followed by two rinses with a sterile solution containing 10 mM Tris (pH 8.0) and 50 mM EDTA. A known mass of material was added to PowerSoil beadbeating tubes (MoBio Laboratories, Carlsbad CA), incubated at 70 °C for 10 minutes, and then amended with 200 ng of poly-A. Subsamples were subjected to beadbeating, followed by three cycles of freeze-thaw steps to further lyse cells. Nucleic acids were extracted using hot phenol (60 °C for 3 min.), followed by two chloroform:isoamyl separations and precipitated with ethanol. DNA was resuspended in TE (pH 8.0) and quantified using the Qubit™ fluorometer (Life Technologies, Grand Island, NY).

3.3.5 *Enumeration of gene abundance via quantitative PCR*

Quantitative PCR (qPCR) was used to determine the abundance of bacterial and archaeal 16S rRNA genes. To provide additional constraints on the abundance of sulfate reducing microbes, qPCR was also used to enumerate A) the adenosine 5‘-phosphosulfate reductase (*aprA*) gene using primers that target both sulfate reducing bacteria and

archaea(Christophersen *et al*. 2011); B) bacterial dissimilatory sulfite reductase (*dsrA*) using primers that target bacteria (Kondo *et al.* 2004); and C) *Deltaproteobacteria* via primers that target their 16S rRNA genes (Stults *et al*. 2001). Quantification was performed in triplicate with the Stratagene MX3005p qPCR System (Agilent Technologies) using the Perfecta SYBR FastMix with low ROX (20 µL reactions, Quanta Biosciences, Gaitherburg, MD), specific primers and annealing temperatures (Table 1) and 10 ng of template gDNA. The temperature program for all assays was 94 °C for 10 minutes, 35 cycles of 94 °C for 1 minute, the annealing temperature for 1 minute (Table 1), extension at 72 °C for 30 seconds and fluorescence read after 10 seconds at 80 °C. Following amplification, dissociation curves were determined across a temperature range of 55 °C to 95 °C. Ct values for each well were calculated using the manufacturer's software. Plasmids containing bacterial and archaeal 16S rRNA and functional gene inserts (amplified from *Arcobacter nitrofigulis* (ATCC 33309), *Methanosarcina acidovorans* and *Desulfovibrio vulgaris* Hildenborough (ATCC 29579/ NCIMB 8303/ AE017285) respectively) were used as standards for calibration (see Supplemental Methods for more detail).

3.3.6 *Sequencing and Phylogenetic Analysis via 454 pyrosequencing*

DNA samples were sequenced using 454 pyrotag methods similar to those described previously (Dowd *et al*. 2008). All samples were sequenced at the Research and Testing Laboratory (Lubbock, TX) using a 454FLX instrument (Roche Inc.) with Titanium™ reagents. The resulting bacterial and archaeal 16S rRNA (bacterial V1-V3 and archaeal V3-V4 of the 16S rRNA genes; primers are shown in Table 3.1) as well as *drsB* sequences were analyzed via Mothur (Schloss *et al*. 2009). Sequences were trimmed, quality checked, aligned to the SILVA-

Table 3.1: Primers used for the enumeration of 16S rRNA and sulfate reduction functional genes.

Target gene	Forward Primer	Conc [nM]	T (°C)*	Reverse Priemr	Conc [nM]	T (°C) *	Reference
Bacterial 16S	**Bact1369F-** CGGTGAATACGTTCYCGG	1000	59	**Prok1541R-** AAGGAGGTGATCC RGCCGCA	1000	59	(Suzuki *et al.* 2001)
Bacterial 16S[1]	**Gray28F** - GAGTTTGATCNTGGCTCAG	500	54	**Gray519R**- GTNTTACNGCGGCKGCTG	500	54	(modified from *Frias-lopez et al*., 2002; modified from Manefield *et al*., 2002)
Archaeal 16S	**Arch1-1369F-** CGGTGAATACGTCCCTGC **Arch2- 1369F**- CGGTGAATATGCCCCTGC	500 (1:1 Mix)	59	**Prok1541R**- AAGGAGGTGATCC RGCCGCA	1000	59	(Suzuki *et al.* 2001)
Archaeal 16S[1]	**Arch349F**- GYGCASCAGKCGMGAAW	500	54	**Arch806R**- GGACTACVSGGGTATCTAAT	500	54	(Takai & Horikoshi, 2000)
δ-proteobacteria[2]	**Delta361GF**- AAGCCTGACGCASCAA	600	55	**Delta685R**- ATCTACGGATTTCACTCCTACA	600	55	(Stults *et al*. 2001)
Disimmilatory[3] **sulfite reductase**	**DSR1-F+**- ATCGGNCARGCNTTYCCNTT	400	58	**DSR-R**- GTGGMRCCGTGCAKRTTGG	600	58	(Kondo *et al*. 2004)
Disimmilatory[1] **sulfite reductase**	**DSR2060F** CAACATCGTYCATACMCAGGG	500	50	**DSR4R-** GTGTAGCAGTTACCGCA	500	50	(Oakley *et al*. 2011; Wagner *et al.* 1998)
Adenosine 5'-phosphosulfate reductase	**aps3F** TGGCAGATCATGWTYAAYGG	400	55	**aps2R-** GCGCCGTAACCRTCYTTRAA	400	55	(Christophersen *et al.* 2011)

*Annealing temperature

1. Primers used for 454-pytrotag sequencing, all other primers used for qPCR.

2. Primers Delta361F and Delta685R allowed for quantification of iron- and sulfate- reducing genera within the δ-Proteobacteria including *Geobacter*, *Pelobacter* (including fermentative species), *Desulfovibrio*, *Desulfomicrobium*, *Desulfuromusa*, and *Desulfuromonas* (including dissimilatory S reducers) (Stults et al. 2001).

3. Though these primers amplify bacterial *dsrA* gene sequences, they may not detect some gram-positive species and cannot detect select thermophilic bacterial and archaeal sulfate reducing lineages (Kondo et al. 2004).

4. Targets both bacterial and archaeal *aprA* gene (Christophersen et al. 2011).

compatible alignment database reference alignment (*dsrB* gene datasets were aligned to a *dsrB* gene database generated from the Ribosomal Database Project (RDP)), analyzed for chimeras, classified against the Greengenes99 database and clustered in to OTUs (see Supplemental Methods for more detail). Rarefaction curves were used to examine the number of OTUs as a function of sampling depth. Alpha diversity was assessed by generating values from the Chao1 richness estimators and the inverse Simpson diversity index.

3.3.6.1 *Sequence Accession numbers*

The 16S rRNA and *dsrB* gene sequences reported in this study have been submitted to Sequence Read Archive under the accession numbers SRX154520 through SRX154528.

3.4 Results

3.4.1 Physical and geochemical characteristics of the study sites

The hydrothermal deposits sampled from Middle Valley were all relatively friable and were composed predominantly of anhydrite ($CaSO_4$, M. Tivey, pers. comm). Chowder Hill and Dead Dog had the highest observed venting fluid temperatures (measured *in situ* at 261 °C), followed by Needles (123 °C). *In situ* measurements of dissolved hydrogen sulfide (H_2S) revealed significant differences in hydrothermal fluid composition among hydrothermal deposits. Unfortunately the inline pH probe with the ISMS malfunctioned during the dive. Using previously reported pH values (Butterfield *et al*. 1994), Chowder Hill would have the highest *in situ* measurement of total sulfide (3.9 mM), followed by Dead Dog (2.2 mM), and Needles (0.59 mM) (Table 3.2). These concentrations are within the same magnitude of previously reported H_2S in focused vent fluids at Middle Valley (Butterfield *et al*. 1994). Chowder Hill did exhibit the

highest *in situ* concentration of hydrogen (1.86 mM) followed by Dead Dog (1.66 mM) and Needles (~1.42 mM). These values are also consistent with previous studies (Cruse & Seewald 2006), as well as gastight samples collected and analyzed shipboard (M. Lilley, pers. comm).

Table 3.2: In situ $\sum H_2S$ measurements compensated for a range of hydrothermally relevant pH's

pH	Chowder Hill H_2S (mM)	Dead Dog H_2S (mM)	Needles H_2S (mM)
not pH compensated⋆	3.91	2.10	0.660
3.5	3.9	2.1	0.55
4.0	3.9	2.1	0.55
4.5	3.9	2.1	0.55
5.0	3.9*	2.1	0.56
5.5	4.0	2.2*	0.56*
6.0	4.2	2.3	0.59
6.5	4.8	2.6	0.68
7.0	6.8	3.7	0.96
7.5	13	7.1	1.9
8.0	33	18	4.7
8.2	50.	27	7.1

Values represent the median values of the 10 highest sampling points

⋆ The first row of values refers only to $[H_2S]$ and not $\sum H_2S$.

* Total sulfide calculation at the most environmentally relevant pH (Butterfield *et al*. 1994)

3.4.2 Sulfate Reduction Rates

Among all samples, sulfate reduction was observed at temperatures between 4 °C to 90 °C (Figure 1). Maximal rates of sulfate reduction were observed between 88-90°C (2670 nmol g^{-1} day^{-1} at Needles, 1090 nmol g^{-1} day^{-1} at Chowder Hill, and 142 nmol g^{-1} day^{-1} at Dead Dog; Figure 1). Notably, the highest sulfate reduction rates were observed from Needles samples, which were ~20-fold higher than those observed at Dead Dog, and ~2-fold greater than at

Chowder Hill. Many of the rates exhibit large deviations due to the high variability among the biological replicates, most likely due to persistent mineralogical and microbiological heterogeneity across incubations, even after homogenization. Sulfate reduction was also observed in molybdate amended experiments, though we suspect that molybdate was scavenged by minerals that attenuated the effect of the inhibitor as has been previously observed in metal-rich environments (Bostick *et al*. 2003; Xu *et al*. 2006).

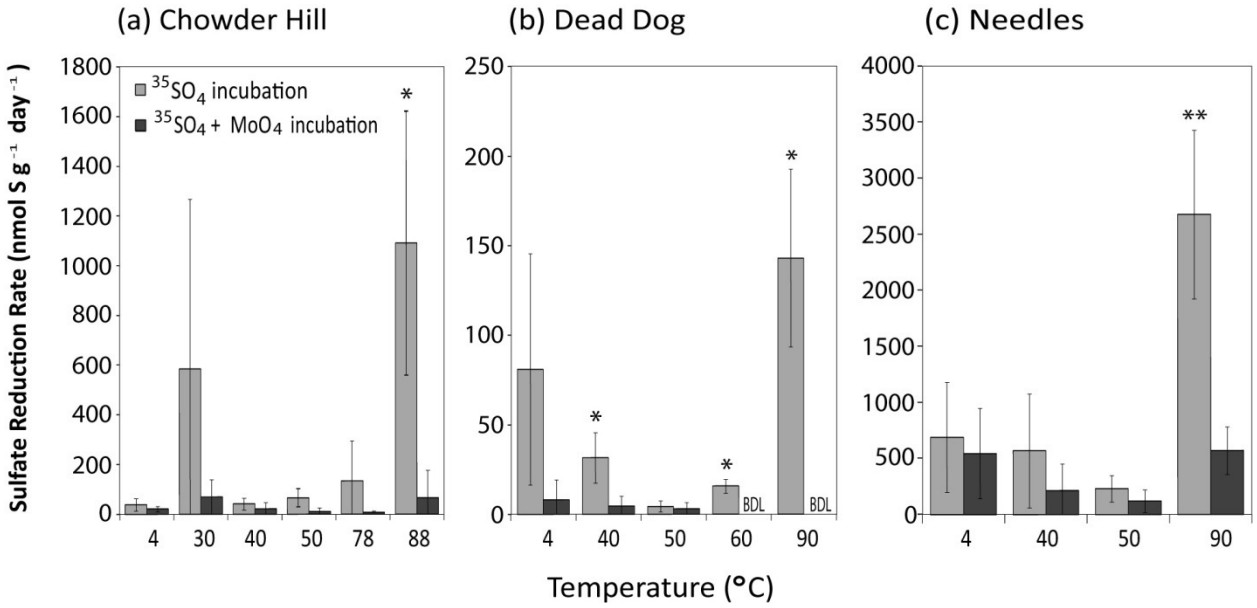

Figure 3.1: Temperature dependent sulfate reduction in hydrothermal deposits recovered from Middle Valley. Slurried samples were incubated for 7 days with (■) or without (■) the addition of 28 mM molybdate (a competitive inhibitor for sulfate reduction). Error bars represent 1 standard deviation from the average. Statistical significance from the controls (Wilcox-Mann-Whitney) are shown as (*) $p < 0.1$, (**) $p < 0.05$. Scintillation measurements of 0 cpm for radioactive sulfide ($Zn^{35}S$) were considered below the detection limit (BDL).

3.4.3 Quantification of Taxonomic and Functional Genes

Microbial density (as estimated by 16S rRNA gene copies g^{-1} mineral) was greatest at Needles and lowest at Dead Dog. Microbial communities at each site were dominated by archaea (Figure 3.2A), with Needles showing the highest ratio of archaea to bacteria (227:1 as compared to 14:1 at Dead Dog or 17.5:1 at Chowder Hill). Assuming an average of 4.19 copies of 16S rRNA gene per bacterium and 1.71 copies of 16S rRNA gene per archaeon genome (Lee *et al*. 2009; Klappenbach *et al*. 2001), Needles hosts a microbial community of 4.12 x 10^8 cells g^{-1} sample, 3 orders of magnitude higher than Chowder Hill (8.96 x 10^5 cells g^{-1} sample) and Dead Dog (5.65 x 10^5 cells g^{-1} sample).

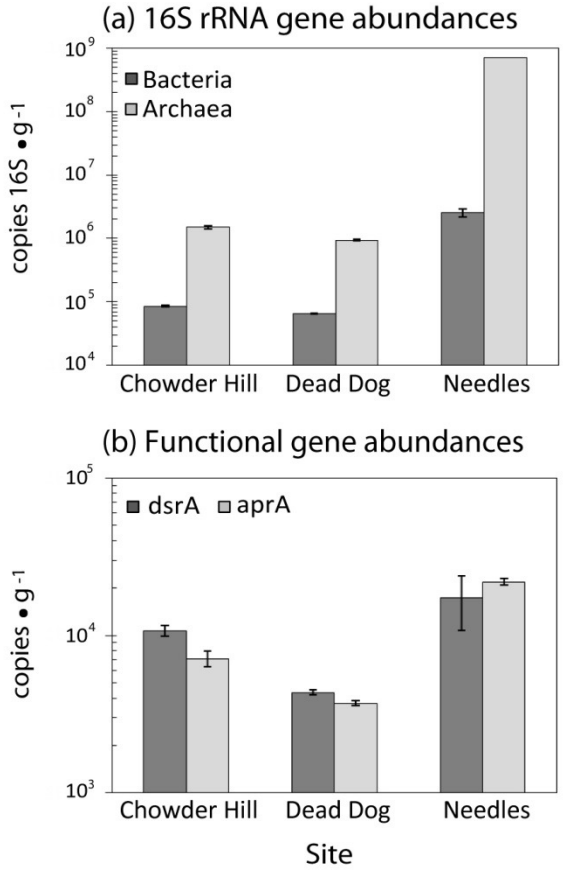

Figure 3.2: Abundance of (a) 16S rRNA genes and (b) functional gene markers for sulfate reduction across three massive sulfide deposits. Samples of hydrothermal sulfide material were collected from each of the three vent sites, frozen upon return to the surface and DNA was extracted using described protocols. Bacterial and archaeal 16S rRNA, *dsrA* and *aprA* genes were enumerated by qPCR using published primer sets and normalized to grams of extracted sulfide. Error bars represent 1 standard deviation.

16S rRNA gene primers specifically targeting ribotypes allied to *Desulfovibrio, Desulfomicrobium, Desulfuromusa*, and *Desulfuromonas* were used to enumerate *Deltaproteobacteria* known to mediate sulfate reduction in many marine systems (Stults *et al.* 2001). However, given the difficulty in amplifying 16S rRNA genes from deep-sea thermophiles with typical primer sets - due to mismatches with limited sequence representation in GenBank - it is probable that these assays similarly underestimate abundances in these environments (Teske & Sorensen, 2008). *Deltaproteobacterial* abundance at Needles was approximately 4.48 x 10^5 copies g^{-1} sample (approximately 26% of the entire bacterial population), though none were detected at Chowder Hill or Dead Dog (data not shown). The abundance of both functional genes for sulfate reduction, *dsrA* and *aprA*, was greatest at Needles and lowest at Dead Dog (a pattern similar to that seen in the 16S rRNA gene abundance estimates; Figure 3.2B). If we assume an average of 1 *dsrA* gene copy per genome (Klein *et al*. 2001; Kondo *et al*. 2004), the proportion of sulfate reducing bacteria in the bacterial populations is only 2.7% in Needles as compared with 28% in Dead Dog and 53% at Chowder Hill.

3.4.4 Microbial Diversity

454 pyrotag sequencing, rarefaction analyses, and diversity metrics all revealed measureable differences in microbial community composition among the three hydrothermal deposits (Figure 3.3, Figure 3.4, Table 3.3). Via these assessments, Needles hosts the least diverse assemblage of bacteria and archaea, while Chowder Hill and Dead Dog host

Table 3.3: 16S rRNA sequence tag and alpha diversity characteristics among sites

Sample	Trimmed reads	Sampled Reads	OTU (97%)	coverage	npshannon	simpson	chao
Chowder Hill-Bacteria	3997	3544	340	0.948	3.30	0.168	647.23
Dead Dog-Bacteria	3544	3544	341	0.957	3.69	0.141	572.12
Needles-Bacteria	3983	3544	278	0.966	3.19	0.203	458.02
Chowder Hill-Archaea	783	308	76	0.877	3.59	0.095	134.58
Dead Dog-Archaea	308	308	58	0.903	3.34	0.071	97.55
Needles-Archaea	2587	308	35	0.938	2.24	0.233	63.5

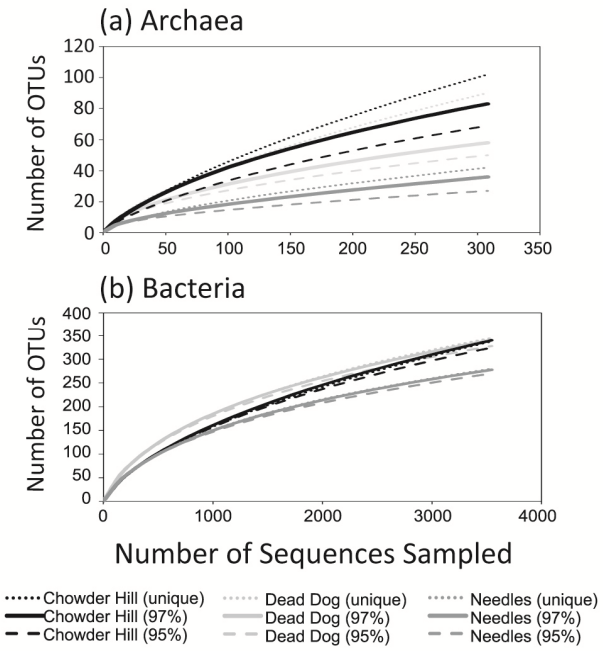

Figure 3.3: Rarefaction analysis of archaeal (a) and bacterial (b) sequences from each site at OTU clustering at the 95%, 97% and unique level. All 16S rRNA libraries were randomly sampled down to the smallest sample size, (a) n = 308 (Dead Dog), (b) n = 3544 (Dead Dog). For both bacteria and archaea, Needles had the least diverse populations.

communities of comparable diversity. Examination of OTUs at 97%, 95% and 92% sequence similarity further reveal differences in microbial community membership among the three sites. Among archaea at the 97% level, only two archaeal OTUs (1% of all archaeal OTUs classified) are shared among the hydrothermal deposits. The sequences classified to these OTUs represent 69%, 48% and 18% of all the library sequences from Needles, Dead Dog and Chowder Hill respectively. One of these OTUs is allied to the ammonium oxidizing archaeal Candidatus

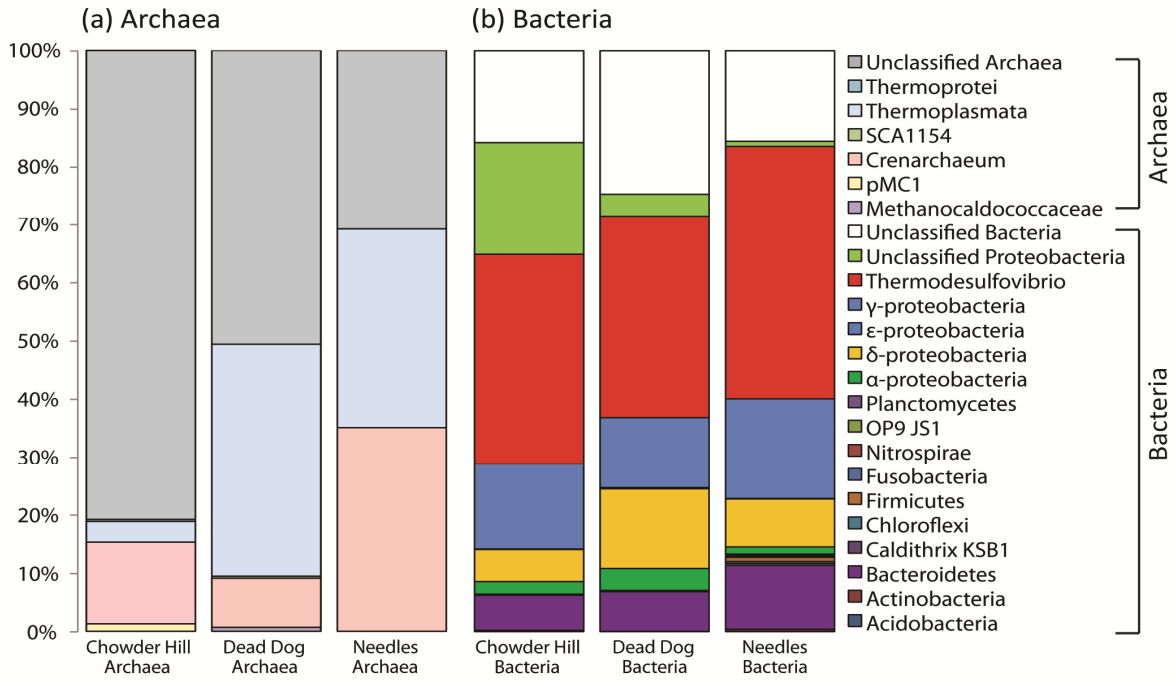

Figure 3.4: Archaeal (a) and Bacterial (b) taxonomic distribution among the different hydrothermal deposits revealed differences in microbial community composition. Bacteria V1-V3 region and archaeal V3-V4 regions of the 16S were sequenced by 454, analyzed with Mothur, and all libraries were randomly resampled down to the smallest sample size, (a) n = 308 (Dead Dog), (b) n = 3544 (Dead Dog).

Cenarchaeum in the phylum *Thaumarchaeota*, and accounts for 35% of Needles and less than 5.0% of Dead Dog or Chowder Hill library sequences. The other OTU is allied to a thermophilic sulfur respiring archaeon within the class *Thermoplasmata*. Nearly 40% of the archaeal sequences from Dead Dog were allied to this archaeon. Methanogens allied to *Methanocaldococus* comprised about 1.0% of the total archaeal sequences from Dead Dog, and were not represented in the libraries from Chowder Hill or Needles. Most of the archaeal diversity at Chowder Hill (80% of sequences) and Dead Dog (50% of sequences) was unclassified. No sequences allied to true sulfate reducing archaeal lineages such as

Archaeoglobus fugilis or Aciduliprofundus boonei were recovered. However, the potential diversity of thermophilic sulfate reducing archaea in these samples is likely much greater than suggested here. This may be explained in part by biases in primer binding, sequencing, or even DNA extractions. For example the archaeal sequencing primers used in this study only target about 34% of the *Archaeoglous*-like sequences contained in the RDP database (as assayed by Probe Match; Cole *et al*. 2005). Furthermore, the primers may miss members of the dominant *Thermoplasmatales* as *in silico* analysis only returns 48% (1715/3558 sequences) of the RDP reported sequences. In total, these archaeal sequencing primers (349F-806R) miss 42% of the total archaeal sequences (67713/117373 sequences) in the RDP database. Similar bias has been reported in other studies in the deep sea and deep subsurface biotopes (e.g. Dhillion *et al*., 2003, 2005, Teske *et al*. 2007).

Among bacteria at the 97% similarity level, 54 of the bacterial OTUs classified (7.0%) were shared among all hydrothermal deposits, and account for 84%, 80%, 71% of the sequences from Chowder Hill, Needles and Dead Dog respectively (Figure 3.4). One of these OTUs accounted for 44%, 36% and 25% of the sequences from Chowder Hill, Dead Dog and Needles respectively. Aligning representative sequences from this OTU via Blast-n (Altschul *et al.* 1997) reveals a best match to *Thermodesulfovibrio*, an anaerobic, thermophilic, sulfate-reducing bacterium, from the phylum *Nitrospira* (81% identity). Given its abundance, we postulate that it likely contributes substantially to the high thermophilic sulfate reduction rates. Furthermore, the *dsrB* gene library was dominated by sequences phylogenetically allied to *Thermodesulfovibrio* (Supplementary Table B3.1). Other dominant groups of bacteria include members of the *Gammaproteobacteria, Bacteroidetes, Deltaproteobacteria* and *α*-

proteobacteria. Via Blast-n, most of the unclassified sequences matched to partial 16S rRNA gene sequences from hydrothermal vent fluid communities (Nunoura *et al*. 2010; Sylvan *et al*. 2012). Sequences classified as *Deltaproteobacteria* comprised 5.5%, 8.2%, or 14%, of the total population of Chowder Hill, Needles, or Dead Dog respectively. While Dead Dog may have had the highest proportion of its amplicons classified as *Deltaproteobacteria*, sequences related to known sulfate reducers within the *Deltaproteobacteria (Desulfobacteraceae, Desulfobulbus rhabdoformis, Desulfovibrio)* were only found at Needles and comprised 1.1% of the 16S rRNA gene library. The majority of the sequences classified as *Deltaproteobacteria* in each of the three sites were from one unclassified *Deltaproteobacterial* OTU consisting of 4.4, 5.3, and 13% of the sequences from Chowder Hill, Needles and Dead Dog respectively.

3.5 Discussion

Sulfate reduction rates measured in deposits recovered from the Middle Valley vent field reveal the potential for active sulfate reduction within hydrothermal deposits. The magnitude of all measured rates (from 15.7 nmol g^{-1} day^{-1} at Dead Dog at 60°C to 2670 nmol g^{-1} day^{-1} at Needles at 90 °C) are comparable in magnitude to those previously observed in hydrothermally influenced sediments (eg. Guaymas basin or Lake Tanganyika (Weber & Jørgensen, 2002; Kallmeyer & Boetius, 2004; Elsgaard *et al*. 1994a, 1994b), even though the availability of organic carbon is markedly higher in these hydrothermal vent sediments, with Guaymas having up to 200-times greater concentrations of organic carbon (Lang *et al*. 2006; Cruse & Seewald, 2006; Chen *et al*. 1993). However, they are measurably higher than those typically observed in non hydrothermal deep sea sediments (0.1-10 nmol g^{-1} day^{-1}, converted

here for comparison assuming an average sediment density of 2 g cm^{-3}; Elsgaard *et al*. 1994a; Weber & Jørgensen, 2002; Joye *et al*. 2004). To date, the only other measurement of sulfate reduction from sulfide deposits along the East Pacific Rise exhibited rates comparable to those reported here, (Bonch-Osmolovskaya *et al*. 2011), but it should be noted that their samples were incubated under pure H_2 atmosphere, and likely represented autotrophic sulfate reduction.

Notably, the maximum rates of sulfate reduction in Middle Valley sulfides occurred at 90°C in all three deposits. This is in contrast to measurements of sulfate reduction in hydrothermal sediments, where the greatest rates are often observed between 40-70 °C, and more modest rates of sulfate reduction have been reported between 80-91 °C (Weber & Jørgensen, 2002; Elsgaard *et al*. 1994a, 1994b). The relatively low or insignificant sulfate reduction rates between 4-80 °C suggest Middle Valley deposits harbor a high proportion of hyperthermophilic sulfate-reducing microbes.

The significant differences in the rates we observed among deposits (Kruskal-Wallis, $p<0.0001$) are likely due to differences in biomass and the composition of microbial communities. These differences in density and composition are, in turn, a reflection of the availability of relevant substrates, and the physic-chemical conditions at each site. Indeed, microbial biomass (as estimated by 16S rRNA genes) directly correlates to rates of activity and is likely one of the strongest factors affecting the observed rates of sulfate reduction (Pearson correlation coefficient $r=0.879$, $p<0.0005$). Needles had both the highest observed rates as well as the highest cell density (Figure 3.2 and 3.3). Of all the deposits sampled, Needles had the lowest venting fluid temperature (123 °C) resulting in the largest zone of microbial habitability.

Consistent with this, Needles also had the greatest abundance of *dsrA* and *aprA* genes per gram, suggesting a larger potential sulfate reducing community. Here, *Deltaproteobacteria* allied to *Desulfovibrio, Desulfobulbus, Desulfobacteria*, and *Desulfuromonas* account for 25.7% of the bacterial community. These clades of *Deltaproteobacteria* were not observed at Chowder Hill or Dead Dog by either qPCR enumeration or pyrosequencing. Cultured representatives from some of these *Deltaproteobacterial* clades (*Desulfovibrio vulgaris* and *Desulfovibrio desulfuricans)* have been shown to reduce sulfate at high rates (ranging from 10-1340 nmol min^{-1} mg^{-1} protein) with varying electron donors (Fitz & Cypionka, 1991; Cypionka & Konstanz, 1989).

Thermodesulfovibrio-like organisms dominated the bacterial communities within each hydrothermal deposit (35-44%; Fig. 3.4). *Thermodesulfovibrio* sp. are considered obligately anaerobic, thermophilic bacteria that can reduce sulfate and other sulfur compounds (Garrity & Holt, 2001). In pure cultures, members of this genus are able to link growth with hydrogen and a limited range of organic carbon molecules (formate, pyruvate and lactate), maintaining optimal growth between 55-70 °C (Sekiguchi *et al*., 2008). Needles has a greater proportion of sequences (from pyrosequencing) related to *Thermodesulfovibrio-like* species than the other two deposits. The combination of sequences related to a thermophilic sulfate reducing bacteria and higher rates of sulfate reduction at elevated temperatures (90°C) suggests that *Thermodesulfovibrio*-like organisms may play a substantial role in sulfate reduction in warmer environments. However, constraining the relative proportion of sulfate reduction by *Thermodesulfovibrio*-like organisms in these mixed communities was beyond the scope of this study.

It is unclear why Chowder Hill and Dead Dog exhibit large differences in rates of sulfate reduction despite other similarities in geochemistry and biomass. One plausible explanation might be that different types of biological interactions (e.g. syntrophy or competition) occur due to differences in the composition and distribution of microbial communities within the mineral matrix of each deposit. Slight differences in community composition, like Dead Dog having a higher representation of sequences related to sulfur respiring (*Thermoplasmata)* and methanogenic (*Methanocaldococus-like*) archaea than Chowder Hill, may reflect differences in biological interactions, which have implications for rates of sulfate reduction in each deposit. Also, substrate competition for H_2 or consumption of locally produced DOC (Oremland & Polcin, 1982; Lovley & Phillips, 1987) may be more prevalent in one deposit over another. Future experiments should aim to better resolve how specific interaction between populations, for example, syntrophy or competition for a common substrate, may influence sulfate reduction.

3.5.1 The potential role of heterotrophic sulfate reduction in productivity and biogeochemistry

Heterotrophic sulfate reduction is likely a prominent metabolic mode within Middle Valley sulfides and sediments, and the sulfate reduction rate data herein (which solely measure hetrotrophic sulfate reduction) support that supposition. Sedimented vent fields typically contain allochthonous organic carbon that could readily support heterotrophy. Indeed, at Middle Valley, bottom waters contain 3.5 mg DOC/L (about 7 fold higher than the overlying surface seawater), while porewater concentrations range from 0.1 – 84.0 mg DOC/L at sediment depths to 200 mbsf (Ran & Simoneit, 1994). Based on data from culture studies of

Desulfovibrio strains, including the H^+/H_2 ratio of 1.0 for *Desulfovibrio vulgarius* Marburg (Fitz & Cypionka, 1991), a $P/2e^-$ ratio of 1/3 for *Desulfovibrio gigas* (this is the number of ATPs produced for every 2 electrons transferred to an electron acceptor (Barton et al. 2003), and the assumption that 10% of ATP production supports growth (20 mmol ATP per gram biomass), our estimates suggest that - at our maximum empirically measured rates - heterotrophic sulfate reduction could support 140 g biomass yr^{-1} (~1.5×10^{14} cells) at Chowder Hill (volume = 109,900 cm^3), 16 g biomass yr^{-1} (~1.7×10^{13} cells) at Needles (volume = 5495 cm^3), and 2.1 g biomass yr^{-1} (~2.2×10^{12} cells) at Dead Dog (volume=12560 cm^3). These values are modest in comparison to global estimates of chemoautotrophic biomass production on the global ridge system (10^{10}–10^{13} g of biomass yr^{-1}; McCollom & Shock 1997; Bach & Edwards 2003), yet may be significant in the context of local secondary productivity. Moreover, with respect to the sulfur cycle, the sulfide produced by these heterotrophic sulfate reducers could represent up to 3% of the H_2S flux from Middle Valley deposits (given previously published vent fluid flow rates from the Main Endeavor field; Wankel *et al*. 2011), which can influence, for example, sulfur isotope biogeochemistry. Additional rate measurements that represent the diversity of physico-chemical conditions found within deposits or ridge systems are necessary to better constrain the contribution of heterotrophic sulfate reducers to global vent biomass and geochemistry.

Hydrothermal vents are dynamic environments where carbon and sulfur cycling are intimately linked. Both autotrophic and heterotrophic sulfate reducing microbes have been isolated from vents, and the data shown here are among the first to constrain the potential for heterotorophic sulfate reduction at vents (in particular those with higher organic carbon loads), as well as the relationship between sulfate reduction rates, temperature, microbial biomass

and community density and composition. These data, as well as the vent field estimates of sulfate reduction, underscore the relevance of sulfate reduction in hydrothermal ecosystems and further indicate the need for continued studies of sulfur cycling along ridge systems.

3.6 Acknowledgments

We are grateful for the expert assistance of the *R/V Atlantis* crews and the pilots and team of the *DSV Alvin* for enabling the collections of hydrothermal deposits used in our experiments. We also thank Steve Sansone, Dr. Joseph Ring, Ms. Julie Hanlon, Dr. Kathleen Scott, Dr. Vladimir Samarkin, Dr. David Johnston, and Dr. Jan Amend for providing assistance with various technical aspects of the experiments. We are also very thankful for the constructive feedback from the reviewers. Financial support for this research was provided by the National Science Foundation (NSF OCE-0838107 and NSF OCE-1061934 to P.R. Girguis), and the National Aeronautic and Space Administration (NASA-ASTEP NNX09AB78G to C. Scholin and P. R. Girguis and NASA-ASTEP NNX07AV51G to A. Knoll and P. R.Girguis).

CHAPTER FOUR:

Key factors influencing rates of heterotrophic sulfate reduction in hydrothermal massive sulfide deposits

Kiana L. Frank[1], Daniel R. Rogers[2], Karyn L. Rogers[3], David T. Johnston[4], and Peter R. Girguis[2]

1 = Department of Molecular and Cellular Biology, Harvard University, 16 Divinity Ave. Cambridge, MA
2 = Department of Organismic and Evolutionary Biology, Harvard University, 16 Divinity Ave., Cambridge, MA
3 = Department of Earth and Environmental Sciences, Rensselaer Polytechnic Institute, 100 8th St., Troy, NY
4 = Department of Earth and Planetary Sciences, Harvard University, 20 Oxford Street, Cambridge, MA

Corresponding supplemental material is appended in Appendix C.

4.1 Abstract

The diverse community of bacteria and archaea that live within hydrothermal chimneys are continuously subject to dynamic thermal and geochemical gradients. To date, the magnitude of sulfate reduction (SR) rates and factors controlling reaction kinetics have not been well constrained within this environment. Here we evaluate the effects of key environmental variables on SR kinetics in a hydrothermal flange recovered from the Grotto vent in the Main Endeavor Field, Juan de Fuca ridge. Microbial SR rates were measured by ^{35}S-tracer techniques over a range of environmentally relevant chemical conditions (pH, H_2S, SO_4^{2-}, and organic carbon concentrations) and temperatures (4, 50 and 90°C). SR rates were greatest at 50°C, and SR rates had significant, positive correlations with increasing exogenous hydrogen sulfide, pH and sulfate. Temperature exhibited the greatest influence on the magnitude of SR rates, followed by pH. The apparent Monod constant (K_m) for SR at pH 6 (7.1 mM) was higher than at pH 4 (2.5 mM), even though the maximum rate (V_{max}) remained constant (298 nmol g^{-1} day^{-1}) at both conditions. As organic carbon amendments had no measureable effect on SR rates, rates were likely fueled by mineral associated endogenous organic matter. In these experiments neither sulfate nor organic carbon were the primary drivers of SR rates, though the extent of their influence may vary with the geochemical setting. Experiments such as these illustrate how the availability of primary substrates may not always govern kinetics, and they help constrain parameters for modeling the spatial contribution of heterotrophic sulfate along the complex gradients inherent to hydrothermal deposits.

4.2 Introduction

Sulfate reducing bacteria and archaea gain energy for cell synthesis and growth by mediating the anaerobic oxidation of organic and inorganic substrates using sulfate as an electron acceptor. The electron donors utilized by sulfate reducers are quite variable, ranging from molecular hydrogen to aromatic compounds, although simple organic compounds, commonly used, including acetate, lactate, pyruvate and ethanol that are prevalent in anaerobic environments as a result of the fermentative breakdown of biomass (Rabus *et al*. 2006; Tarpgaard *et al.* 2011; Amend & Edwards 2004).

Due to the high concentrations of sulfate in seawater (28 mM; Dittmar 1884), SR is an ubiquitous metabolism in hypoxic to anoxic marine habitats (Muyzer & Stams 2008) such as oxygen minimum zone waters (Canfield *et al*. 2010), marine sediments (Kallmeyer *et al*. 2002; Robador *et al*. 2009), hydrocarbon seeps (Joye *et al*. 2004; Orcutt *et al*. 2005), marine hydrothermal vents (Jørgensen *et al*. 1992; Elsgaard *et al*. 1994a; Weber & Jørgensen 2002), and the deep subsurface (D'Hondt *et al*. 2004; Edwards *et al*. 2004). SR rates have been shown to be highly heterogeneous within marine sediments due to variations in substrate and organic carbon availability, as well as other geochemical and physical factors (Isaksen *et al*. 1994; Orcutt *et al*. 2005; Treude *et al*. 2009; Holmkvist *et al*. 2011; Canfield 1989; Kallmeyer *et al*. 2002). Indeed, previous studies of SR in marine sediments have revealed that temperature, pH, sulfate, organic carbon, and sulfide concentrations all influence SR rates and can have an impact on SR sufficient to influence the global carbon budget (Canfield 1989; Westrich & Berner 1984).

SR is also proposed to be one of the more thermodynamically favorable metabolic processes driving hydrothermal vent ecosystems (McCollom & Shock 1997; Tivey 2000). Indeed, many of the organisms isolated from hydrothermal vents have been shown to utilize SR (Alazard *et al*. 2003; Huber *et al*. 1997; Jeanthon *et al*. 2002; Audiffrin *et al*. 2003). Mass specific SR rates in hydrothermal-influenced sediments (25-6600 nmol g^{-1} day^{-1}, converted here for comparison assuming an average sediment density of 2 g cm^{-3}; Elsgaard *et al.* 1994a, 1994b; Weber & Jørgensen 2002; Kallmeyer & Boetius 2004) are measurably higher than those typically observed in non hydrothermal deep-sea sediments (0.1-10 nmol g^{-1} day^{-1}; Elsgaard *et al*. 1994; Weber & Jørgensen 2002; Joye *et al.* 2004) and are significantly affected by temperature (Weber & Jørgensen 2002; Jørgensen *et al*. 1992; Elsgaard *et al*. 1994a, 1994b, 1995; Kallmeyer & Boetius 2004). While it remains to be determined, the difference in SR rates between hydrothermal and non-hydrothermal systems could be reflective of the availability of key constituents (e.g., their concentrations, biological availability, or net flux), or physical parameters (e.g., temperature, porosity, pressure).

Deep-sea hydrothermal vent ecosystems are complex and dynamic marine habitats characterized by steep gradients in temperature and geochemistry (Jannasch & Mottl 1985). A prominent feature of deep-sea ecosystems is the chimney structures that develop as hydrothermal fluid mixes with cold seawater. The walls of these structures form permeable mineral matrices that span the transition from hot reduced vent fluid to ambient oxidized seawater, providing small but highly localized niches for prokaryotic communities to exploit and thrive (Schrenk *et al*. 2003). In contrast to the numerous studies of SR in hydrothermally influenced sediments, studies of SR in hydrothermal chimney deposits are few (Frank *et al*.

2013a; Bonch-Osmolovskaya *et al*. 2011), due in part to the challenges associated with sampling and studying the heterogeneous and consolidated mineral deposits typical of hydrothermal vent chimneys. Analyses of key SR genes suggest there is a high diversity of sulfate reducing organisms at vents, higher than predicted via 16S rRNA gene analyses alone (Nakagawa *et al.* 2004b; Nercessian *et al.* 2005). Here, the microorganisms within a hydrothermal chimney are exposed, in various degrees, to the dynamic and combined effects of high temperature, low pH, high concentrations of hydrogen sulfide, fluctuating amounts of carbon, and varying energy sources. While there are data that illustrate differences in prokaryotic populations across individual chimney structures (Harmsen *et al.* 1997; Schrenk *et al*. 2003; Kormas *et al*. 2006; Takai *et al.* 2001; Page *et al.* 2008), we know little about how physico-chemical gradients influence the rates of most key microbial metabolisms, including SR. Cell-specific SR rates among 33 diverse sulfate reducing microbial isolates, spanning the total temperature range of environments from which sulfate reducers have been isolated, vary by orders of magnitude (0.9 fmol $cell^{-1}$ day^{-1} for *Desulfospira joergensenii* and 4,340 fmol $cell^{-1}$ day^{-1} for *Desulfohalobium redbaense*; Detmers *et al.* 2001). In marine sediments, the cell-specific rate of sulfate reducers (as determined by comparing SR rates with viable cell counts) exceed those of pure cultures by orders of magnitude (though, true cell counts are also thought to be underestimated by similar orders of magnitude; Jørgensen & Bak 1991; Leloup *et al*. 2007; Orcutt *et al*. 2005). The Monod constant (or K_m, defined as the sulfate concentration at which the reaction rate is at half-maximum) of SR in marine sediments ranges from 0.204 mM–1.63 mM (Roychoudhury 2004; Roychoudhury *et al*. 2003; Kostka & Roychoudhury 2002; Boudreau & Westrich 1984; Pallud & Van Cappellen 2006), which are much larger than those reported

from low sulfate environments (10–70 µM; Ingvorsen *et al.* 1981; Lovley *et al.* 1982). The highest reported K_m value for thermophilic SR in a natural environment, 3.17 ± 1.02 mM obtained from Mushroom Springs at Yellowstone National Park (Roychoudhury 2004) is one to three orders of magnitude larger than K_m values known for marine sulfate reducers in pure culture (3.0- 330 µM; Sonne-hansen & Westermann 1999; Ingvorsen *et al.* 1984; Ingvorsen & Jørgensen 1984). Studies on reaction kinetics of SR with natural microbial communities under environmentally relevant conditions are few (Roychoudhury 2004) and often assume sulfate to be the limiting variable to SR. At hydrothermal vents, however, with high concentrations of seawater derived sulfate, we posit that sulfate is less likely to be the limiting factor for SR, and that other factors –such as organic carbon availability - may be the first order determinant of SR rates. Furthermore, temperature should place strict constraints on SR rates as a function of the phylogenetic composition of the native sulfate reducing community.

To better understand the parameters that affect SR rates, we conducted a series of experiments that examined rates of microbial heterotrophic SR in batch incubations over a range of environmentally relevant chemical conditions (pH, H_2S, SO_4^{2-} and organic carbon) and temperatures (4, 50 and 90°C) from flange material recovered from the Grotto hydrothermal deposit at the Main Endeavor Field, Juan de Fuca ridge. This vent was specifically selected to be the focus of this study because of its geology, mineralogy (pyrrhotite and pyrite based) and end-member fluid chemistry (pH of 4.2, 12.6 mmol kg^{-1} CO_2, 633 µmol kg^{-1} NH_3, 5.4 mmol kg^{-1} H_2S, 11 µM DOC) have been extensively studied over the past decade (Tivey & Delaney 1986; Delaney *et al*. 1992; Tivey 2000; Butterfield *et al.* 1994; Tivey *et al*. 2002; Zhu *et al*. 2007; Tivey *et al.* 1999; Lang *et al.* 2006). The metabolic energy available for SR can be influenced by the

physical structure of the sulfide deposit, the mixing regime (e.g. diffuse or turbulent), and the composition of the end-member fluids and the ambient seawater (Tivey 1995; Zhu *et al*. 2007; Tivey 2000). The range of experimental conditions tested was determined from published concentration profiles of aqueous species modeled as functions of temperature and position within the Grotto vent (Tivey 2000).

4.3. Materials and Methods

4.3.1 *Geologic Setting and Sampling of hydrothermal chimney deposits*

The Main Endeavor vent field is located at 47°57’ N and 129°06 W (Tivey & Delaney 1986) at a depth of 2220 m, the most shallow portion of the Endeavour segment of the Juan de Fuca ridge. This vent field is comparable in size and quantity of hydrothermal chimneys to most other hydrothermal areas, and is characterized by many (> 15) large steep-walled active chimney structures (containing multiple high temperature spires and diffusing flanges) surrounded by a scattering of smaller inactive hydrothermal chimney structures in a roughly 400 m^2 area (Delaney *et al.* 1992; Robigou *et al*. 1993).

Pieces of hydrothermal deposits were recovered from a flange on the Grotto vent (47.949, -129.098) at a depth of 2188.3 m (Dive J2-575, AT-18-08, *R/V Atlantis*) and brought up to the surface in the basket of the *ROV Jason II*. Flanges, like the one sampled, form as lateral outgrowths from massive hydrothermal deposits trapping pools of buoyant high temperature fluids beneath them, often creating a visible mirror-like interface (Tivey 2000). This sample will be hereafter referred to as a flange. Once on board ship, aggregates of tubeworms and other macrofauna were removed from the flange sample and the large pieces were broken into

manageable fragments (~4-6 cm^3) with a sterile chisel and sledgehammer. Samples were then transferred to 0.2 µm-filtered anaerobic seawater. Samples were further broken down into smaller sizes while in anaerobic water and subsamples were immediately transferred to gastight jars (Freund Container Inc.) filled with sterile anaerobic seawater containing 2 mM sodium sulfide at pH 6, and stored at 4°C (for up to 1 year) for future incubations and analyses. The sterile sulfidic seawater in the gastight jars were refreshed periodically during storage at 4°C. Though majority of the experiments (80%) were set up immediately on the ship using freshly collected samples, there is the possibility in the remaining samples that these storage conditions could result in artifacts. However, better storage techniques are currently prohibitive at this time.

Small subsamples (~1 cm^3) of the flange were preserved aboard ship in gluteraldehyde (2.5% in phosphate buffered saline, PBS), then prepared for electron microscopy via ethanol dehydration and critical point drying before being sputtered with a thin layer of gold-palladium to improve image resolution. Samples were imaged with a Zeiss model EVO Scanning Electron Microscope (SEM).

4.3.2. *Measuring sulfate reduction rates*

4.3.2.1 Experimental Design and Incubation

Hydrothermal flange deposits were homogenized by hand with a sterile sledgehammer in sterile seawater actively bubbled with nitrogen immediately prior to incubations (our mechanical homogenizer failed, resulting in hand homogenization). This was done anaerobically for about 1 hour per sample to minimize fine-scale geological and microbial heterogeneity and

facilitate more accurate experimental replication (akin to slurry experiments in sediments; Fossing & Jørgensen 1989; Weber & Jørgensen 2002; Jørgensen *et al.* 1992). For each independent treatment, aliquots of 7.5 mL flange slurry (approx. 29 g wet weight and 20 g dry weight) were transferred into Balch tubes in an anaerobic chamber, and supplemented with 15 mL of sterile artificial seawater media designed to mimic the geochemical conditions within a hydrothermal flange (400 mM NaCl, 25 mM KCl, 30 mM $CaCl_2$, 14mM SO_4^{2-}, 2.3 mM $NaHCO_3$, 1 mM H_2S, and 50 µM dissolved organic carbon - consisting of equimolar proportions 10 µM of pyruvate, citrate, formate, acetate, lactate – pH 6) under a pure nitrogen headspace.

Concentrations of sulfide, sulfate and dissolved organic carbon (DOC) were varied independently to investigate concentration dependent effects on the rates of SR. The range of experimental conditions tested was determined from previously published concentration profiles of aqueous species modeled as functions of temperature and position within the Grotto vent structure (Tivey 2000). Concentrations were varied by orders of magnitude within the modeled ranges to simulate conditions representative of different mixing regimes between seawater and vent fluid (Table 4.1). The range of DOC (which we approximate as pyruvate, citrate, formate, acetate, lactate – most of which have been identified to varying degrees within vent fluid and are known carbon sources for heterotrophic SR in culture) concentrations tested were based on the average DOC concentrations measured within diffuse fluids at the Main Endeavor Field (Lang *et al.* 2006, 2010). Hydrogen sulfide was present as H_2S (pK_a in seawater of 6.60) across all the conditions tested (Amend & Shock 2001). All incubations were carried out at pH 4 (to simulate the pH of end-member Grotto vent fluid and the average calculated pH of

Table 4.1: Experimental Media Conditions

Experiment	[H2S]	[Sulfate]	[DOC][1]	pH[2]	Temperature °C	Innoculum[3]
Δ [Sulfide]	**0mM**	14mM	50µM	**4, 6**	**4, 50, 90**	Fresh
	10µM	14mM	50µM	**4, 6**	**4, 50, 90**	Fresh
	100µM	14mM	50µM	**4, 6**	**4, 50, 90**	Fresh
	1mM	14mM	50µM	**4, 6**	**4, 50, 90**	Fresh
Δ [DOC]	1mM	14mM	**0**	**4, 6**	**4, 50, 90**	Stored
	1mM	14mM	**50µM**	**4, 6**	**4, 50, 90**	Stored
	1mM	14mM	**5µM**	**4, 6**	**4, 50, 90**	Stored
	1mM	14mM	**0.5µM**	**4, 6**	**4, 50, 90**	Stored
Δ [Sulfate]	1mM	**1mM**	50µM	**4, 6**	**50**	Stored
	1mM	**100µM**	50µM	**4, 6**	**50**	Stored
	1mM	**10µM**	50µM	**4, 6**	**50**	Stored
	1mM	**1µM**	50µM	**4, 6**	**50**	Stored
	1mM	**10nM**	50µM	**4, 6**	**50**	Stored

The base for each experiment was artificial seawater mix (KCl, CaCl2, NaCl) and 2.3mM bicarbonate.

1. Dissolved organic carbon amendments consisted of equimolar proportions of pyruvate, citrate, formate, acetate and lactate.

2. pH of media added to incubations

3. Homogenized sulfide chimney used fresh (ie. immediately after collection on the boat), or stored (used within 1 year of collection, storage in anaerobic sulfidic seawater. Sulfate reduction rates measured 1 year after collection (stored) were not statistically different from sulfate reduction measurements made immediately after collection, fresh)

mixed fluids in highly reduced zones within the flange; Tivey 2000) as well as pH 6 (representative of the calculated pH in relatively oxidized zones; Tivey 2000). Sufficient $^{35}SO_4^{2-}$ was added to achieve 15 µCi of activity. Samples were incubated anaerobically for 1, 3 or 7 days at ambient seawater (4°C), thermophilic (50 °C) and hyperthermophilic (90 °C) temperatures. The range of temperatures considered was representative of different thermal regimes associated with the surface, outer layer and middle regions of hydrothermal chimneys (Tivey 2000; Kormas *et al.* 2006; Schrenk *et al*. 2003; Frank *et al.* 2013c). Negative controls consisted

of samples amended with 28 mM molybdate to inhibit SR (Saleh *et al*. 1964; Newport & Nedwell 1988). Three biological replicates were run for each treatment, and two biological replicates for each control.

Upon completion, reactions were quenched with the injection of 5 mL 25% zinc acetate, at pH 8 (i.e. 20-fold excess Zn), and all samples were frozen at -20° C for further analysis. 80% of incubations were performed shipboard with freshly collected samples and the remaining 20% of incubations were completed within one year of collection. Select incubations performed on ship and replicated in the laboratory within one year of collection revealed no significant shift in observed SR rates due to the storage conditions. However, even though the rates seemed unaffected, we have no data on the taxonomic composition of the sulfate reducing communities and cannot exclude the possibility that communities may have shifted during storage as has been shown to be the case for stored sediment cores (Lin *et al*. 2010).

4.3.2.2 Chromium Distillation Analysis

To determine SR rates, samples were thawed and the supernatant was removed and filtered through a 0.2 µm syringe filter. The homogenized flange that remained in the tube was washed three times with deionized water to remove any remaining sulfate. One gram (wet weight) of flange material was added to 10 mL of a 1:1 ethanol to water solution in the chromium distillation apparatus, and then degassed with nitrogen for 15 minutes to drive the environment anoxic. Hydrogen sulfide gas was evolved after the anaerobic addition of 8 mL of 12 N HCl and 10 mL of 1 M reduced chromium chloride, followed by 3 hours of heating. The resulting hydrogen sulfide gas was carried via nitrogen gas through a condenser to remove HCl,

and was then trapped as zinc sulfide in a 25% zinc acetate solution. The radioactivity of the resulting sulfide ($Zn^{35}S$) and the remaining sulfate from the supernatant ($^{35}SO_4^{2-}$) were measured via liquid scintillation counter in Ultima Gold scintillation cocktail (ThermoFisher Inc., Waltham, MA).

4.3.2.3 Calculating Sulfate Reduction Rates

Rates were determined using the following calculation as in (Frank *et al.* 2013a).

$$SRR = \frac{nSO_4^{2-} \cdot a \cdot 1.06}{(a+A) \cdot t} \quad \text{Eq.1}$$

Where nSO_4^{2-} is the quantity (in moles) of sulfate added to each incubation (14 mM * 15 mL = 210 µmol), *a* is the activity (dpm) of the trapped sulfide, 1.06 is the fractionation factor between the hydrogen sulfide and sulfate pools (Jørgensen & Fenchel 1974), *A* is the activity of the sulfate pool at the completion of the incubation and t is the incubation time (days). The rates are presented in units of nmol S g^{-1} day^{-1}.

4.3.2.4 Calculating V_{max} *and* K_m, and assumptions

The Monod kinetic parameters of maximum rate (V_{max}) and half-saturation constant (K_m) were determined using a linearization of SR rate (V) vs. sulfate concentration [S] data via the Hanes Woolf plot (Eq. 2),

$$\frac{[S]}{V} = \frac{V_{max}[S]}{K_m + [S]} \quad \text{Eq.2}$$

which is more accurate than the double reciprocal Lineweaver-Burk plot(Leskovac 2003). The slope and X-intercept of the Hanes Woolf plot yield $\frac{1}{V_{max}}$ and K_m respectively. Sulfate

concentrations plotted were initial concentrations as has been historically used when incubation conditions were short and sulfate concentrations were not depleted such that they significantly influenced SR rates (Pallud & Van Cappellen 2006). Based on our previous study (Frank *et al.* 2013a), we anticipated that the magnitude of SR rates would be on the order of nmol g^{-1} day^{-1}. Given that the input sulfate concentrations range from µM to mM-three orders of magnitude greater than the burn rate-the maximum input of SR activity on the concentration of sulfate is 0.03%. Consequently, we use the initial concentration here without concern.

4.4 Results and Discussion

4.4.1 *Physical characteristics and microscopy of the study site*

Diffuse hydrothermal flow was observed on the surface of the hydrothermal chimney Grotto ranging in temperature from 4.2°C – 18.1°C, while hot hydrothermal fluid (T_{max} = 215.6°C) was observed in pools accumulating on the underside of an overhanging flange. Sulfide minerals nearest to the hottest fluid were relatively friable, whereas the majority of the flange sampled was relatively solid likely due to the precipitation of pyrrhotite, pyrite and silica (Tivey & Delaney 1986) in pore spaces at lower temperatures. An inner conduit-like channel was clearly present and densely lined with pyrite. Thick veins of anhydrite and channels of marcasite were also observed throughout the samples. Crystals of these minerals were imaged using scanning electron microscopy. Microbial cells were observed associated with mineral surfaces in low abundance (Supplementary Figure C4.1). There was no visual evidence of dense biofilms within the sample.

4.4.2 *Sulfate Reduction Rates*

Sulfate reduction was detected at temperatures of 4, 50 and 90 °C over a range of environmentally relevant chemical conditions (pH, H_2S, SO_4^{2-}, and organic carbon concentrations) in flange material recovered from the Grotto vent. Measured rates (except for those at low sulfate concentrations) are comparable in magnitude to those previously observed in hydrothermally influenced sediments (e.g. Guaymas Basin or Lake Tanganyika; Weber & Jørgensen 2002; Kallmeyer & Boetius 2004; Elsgaard, Isaken *et al*. 1994a, 1994b). Among all treatments, the highest observed rate (3940 nmol g^{-1} day^{-1}) occurred at 100 µM H_2S, 14 mM SO_4^{2-}, 50 µM DOC at pH 6 and 50°C. The lowest observed rates (120 fmol g^{-1} day^{-1} – 1.5 nmol g^{-1} day^{-1}) were under conditions of severe sulfate limitation (10 nM – 100 µM) in the presence of 1 mM H_2S, pH 4 and 6 at 50°C. SR rates measured in samples amended with molybdate (as an inhibitory control) were all lower than experimental samples (Mann-Whitney-Wilcox test, p=0.1). Rates from 3-day and 7-day incubations were not significantly different from one another (n=271; Mann-Whitney-Wilcoxon, p=0.728) and will therefore be treated as pseudo-replicates. As has been previously observed (Frank *et al.* 2013a), SR rates exhibited large standard deviations presumably due to microscale sample heterogeneity (despite efforts to homogenize, mineral clasts ranged in size from 0.003 mm^3 - 80 mm^3) among biological replicates (n=3 for experiments, n=2 for SR-inhibited samples). Notably, even though Middle Valley samples were mechanically homogenized (with mineral sizes 0.001 mm^3 – 7 mm^3), data from both papers suggest that mechanical homogenization is not efficient enough to adequately disperse chimney microbial communities.

4.4.2.1 Effect of Temperature on Rates of Sulfate Reduction

The highest rates across all conditions tested were observed at 50°C (Figure 4.1). The average SR rates with 14mM sulfate were 18.5 nmol g^{-1} day^{-1} at 4°C, 273 nmol g^{-1} day^{-1} at 50°C, and 9.93 nmol g^{-1} day^{-1} at 90°C. The SR rates range from 1.8 - 174 nmol g^{-1} day^{-1} at 4°C, 2.6 - 3940 nmol g^{-1} day^{-1} at 50°C, and 0 – 142 nmol g^{-1} day^{-1} at 90°C. SR rates observed at 50°C were significantly higher than those measured at 4°C (n=152; Mann-Whitney-Wilcoxon, $p<0.0001$) and 90°C (n=151; Mann-Whitney-Wilcoxon, $p<0.0001$). Our data show that when temperature is varied independently from chemistry (under thermodynamically favorable conditions of excess sulfate and no oxygen), the highest rates of SR occurs at 50°C. Additionally, the maximum rates of SR occur at 50°C independent of pH, sulfide concentration or exogenous DOC additions.

The distribution of rates with respect to temperature resembled the distribution observed in vent sediments (Weber & Jørgensen 2002; Elsgaard *et al.* 1994a; Jørgensen *et al.* 1992) but differed from those measured in vent structures from Middle Valley (Frank *et al*. 2013a). Because SR rates from Grotto and Middle Valley were measured under identical conditions, differences in the thermal optimum of SR between Grotto and Middle Valley deposits are likely due to differences in the prokaryotic abundance and phylogenetic composition of associated consortia (Frank *et al*. 2013a; Olins *et al*. 2013). These differences in density and composition are, in turn, a reflection of the availability of relevant substrates, and the physico-chemical conditions at each site. For example, the Middle Valley vents sampled were much smaller than Grotto, composed of primarily anhydrite with no inner conduit like structures and were exposed to higher temperature end-member fluid (261°C) selecting for a

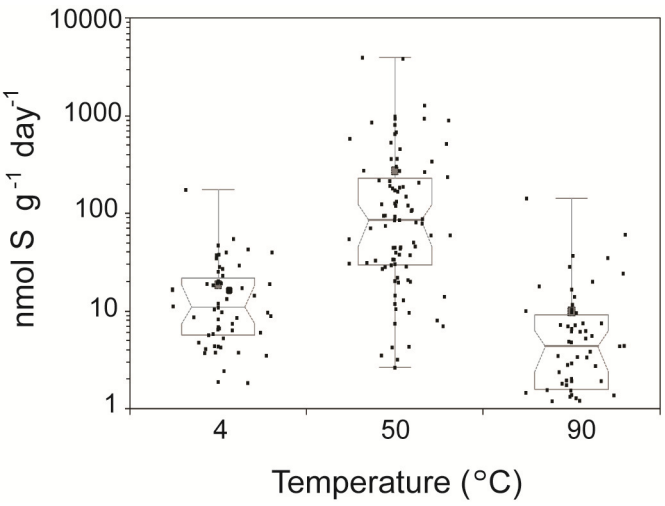

Figure 4.1: **Temperature dependence of sulfate reduction rates** in crushed hydrothermal flange material from Grotto vent (Main Endeavor, JdF). The median of 213 samples is plotted as a line, the 1st and 3rd quartiles as a box, and the minimum and maximum as whiskers with end caps. The 95% confidence interval of the median is plotted as a notch on the box. The mean of the 213 samples is depicted as a blue square. Rates measured from sulfate gradient experiments were excluded in this figure because those experiments were only done at 50°C.

hyperthermophilic community dominated by *Thermodesulfovibro* (Frank *et al*. 2013a) or *Archaeoglobus*-like (Olins *et a*l. 2013) organisms. Though microbial community analyses were beyond the scope of this study, our data suggests that the sulfate reducing consortia of Grotto flange is dominated by thermophilic organisms, and the majority of SR in the Grotto flange occurs at thermophilic temperatures in the outer to middle region of the flange. This finding corroborates recent metagenomic data that reveals genes for the complete SR pathway are enriched in the outer region of a hydrothermal exposed to average *in situ* temperatures of ~50°C (Frank *et al.* 2013c). Future research should utilize ribotype specific and functional gene

qPCR to characterize the expression of SR genes and identify dominant sulfate reducing community members under different conditions.

4.4.2.2 Effect of pH on Rates of Sulfate Reduction

SR rates observed at pH 6 were significantly higher than those measured at pH 4 (n=271; Mann-Whitney-Wilcoxon, p=0.0267). The average SR rates at pH 6 were 152 nmol g^{-1} day^{-1} compared to 37.8 nmol g^{-1} day^{-1} at pH 4. Published SR rates (observed at varying pH) in hydrothermal sediment of Lake Tanganyika show that maximum rates of SR occur at a pH closer to the pH of the hydrothermal fluids than to the pH of the ambient lake water (Elsgaard *et al.* 1994b). Here, Grotto endmember fluids have pH of 4.2 (Butterfield *et al.* 1994) and published models predict pH 8 at 4°C and pH < 3 at temperatures greater than 27°C if mixing is conservative; pH 8 at 4°C, pH 6 at 50°C and pH < 3 if seawater is advecting in; pH 6 at 4°C and pH< 3 at temperature above 13°C if vent fluid is advecting out; and pH 4.2 across all temperatures if fluid is conductively cooled (Tivey 2000). Despite the predictions of low pH conditions across the flange, our data illustrate that while SR does occurs at pH 4, rates are higher at pH 6. The speciation of various metabolites (like H_2S, organic acids and metals) into more toxic forms at low pH may partially explain lower rates observed at pH 4 (Gadd & Griffiths 2013; Giller *et al*. 1998; Oleszkiewicz *et al*. 1989; Ghose & Wiken 1955). For example at low pH, the carboxyl groups of simple organic acids (amended in most reactions at 50 µM) occur mainly in the undissociated form allowing them to pass into the cell membrane where they can uncouple electrochemical gradients (Ghose & Wiken 1955). Additionally, because sulfate reducing organisms are embedded within a metal sulfide matrix, incubating slurries at pH 4

likely results in elevated concentrations of dissolved metals such as zinc and copper that might be toxic to bacteria (Johnson 1998; Utgikar *et al*. 2003). Furthermore, insoluble metal sulfides that precipitate under low pH conditions have also been shown to reversibly inhibit sulfate reducing activity by acting as barriers to prevent the access of reactants into the cell (Utgikar *et al.* 2002). Toxicity of metabolites is also the main factor affecting decreasing rates in suspended batch bioreactors (Colleran *et al*. 1995; Koschorreck 2008). These data further supports our hypothesis that the majority of SR occurs in the outer region of the chimney, where pH is likely to be less acidic.

Competition for substrate with microorganisms utilizing alternate metabolisms is another feasible explanation for the reduced rates of SR observed at pH 4. It has been well documented that naturally occurring sulfate reducing consortia compete with fermenting bacteria, hydrogen-producing syntrophic bacteria, homoacetogens, denitrifiers, iron reducing bacteria and methanogenic bacteria for electron donors (Colleran *et al*. 1995; Weijma *et al*. 2000; Lovley & Klug 1986; Oremland & Polcin 1982; Oremland & Taylor 1977). Because these experiments were incubated in the absence of nitrate and hydrogen, potential competition with denitrifiers or any autotrophic metabolisms can be excluded. Furthermore, considering how sulfate reduction and methanogenesis compete for reductants in natural and human-made systems, data from numerous studies suggest that under these experimental conditions heterotrophic sulfate reducers would outcompete methanogenic bacteria (Weijma *et al*. 2000; Lovley & Klug 1986; Oremland & Polcin 1982; Oremland & Taylor 1977).

In several hydrothermal environments, end-member fluid compositions, including Fe(aq), H_2S, and H_2, are consistent with buffering by the pyrrhotite-pyrite-magnetite mineral

assemblage (Shock & Schulte 1998; Shock *et al*. 1995; Von Damm 1988). Assuming the presence of dissolved iron from the dissolution of pyrrhotite and pyrite a low pH (Grotto end-member fluid has an iron concentrations of 915 µmol kg^{-1}; Butterfield *et al*. 1994), iron reduction is likely favorable under experimental conditions (McCollom & Shock 1997). If the concentration of dissolved iron is high enough, the energy yield of microbial iron reduction and SR at low pH is comparable (Blodau & Peiffer 2003). In shallow hydrothermal systems, heterotrophic respiration coupled to iron reduction is more favorable (29–91 kJ/ mol e^-) than coupled to sulfate reduction (6–34 kJ/mol e^-), though dissolved iron concentrations are higher than those observed in Grotto end-member fluids (Rogers & Amend 2006). Many organisms capable of iron reduction have been isolated from vents (Slobodkina *et al.* 2009; Sokolova *et al.* 2007; Takai *et al.* 2000b; Kashefi *et al*. 2002; Hirayama *et al*. 2007) and iron reducers have been shown to be more abundant within the interior of the chimney where pH is assumed to be low (Ver Eecke *et al*. 2009).

4.4.2.3 Effect of Hydrogen Sulfide Concentration on Rates of Sulfate Reduction

To replicate relevant *in situ* conditions and microniches available within the mineral matrix of a flange based on varying mixing regimes, the effect of exogenous hydrogen sulfide on SR rates was evaluated at several concentrations less than 1 mM (0, 10uM, 100uM, 1mM). Overall, the 216 SR rates (ranging from 1.9 nmol g^{-1} day^{-1} to 3936 nmol g^{-1} day^{-1}) had a positive correlation (Pearson's correlation, $p=0.04$) with H_2S additions (Figure 4.2). SR rates had a strong correlation with hydrogen sulfide concentration (Table 4.2) at pH 4 at temperatures 4°C ($p<0.0001$) and 50°C ($p<0.0001$) with rates increasing between one and two orders of

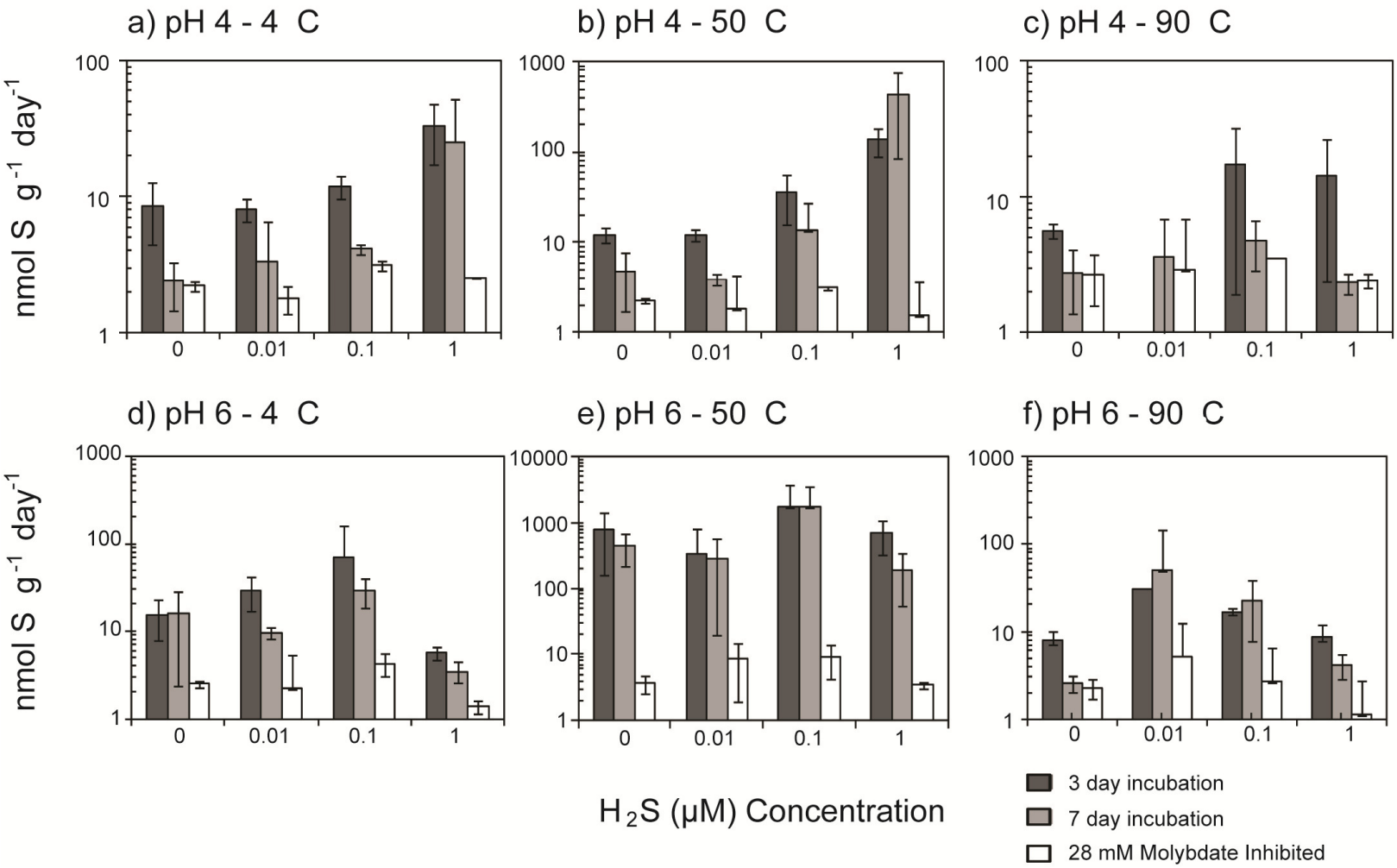

Figure 4.2: Effect of sulfide concentration on sulfate reduction rates in crushed Grotto flange. The crushed flange was incubated for 3 days (■) and 7 days (■) in media of (a) pH 4 at 4°C, (b) pH 4 at 50°C, (c) pH 4 at 90°C, (d) pH 6 at 4°C, (e) pH 6 at 50°C and (f) pH 6 at 90°C. 28mM molybdate amended samples were incubated under all conditions (white) as abiotic controls. Error bars represent 1 standard deviation.

Table 4.2: Pearson's correlation p values

Gradient:	Sulfide: 0-1 mM		Sulfate: 10 nM – 14 mM		DOC: 0 - 50 µM	
Temperature	pH 6	pH 4	pH 6	pH 4	pH 6	pH 4
4 °C	p=0.057	p<0.0001	p=0.1260	-	-	-
50 °C	p=0.5156	p<0.0001	p=0.9659	p=0.5038	p<0.0001	p<0.0001
90 °C	p=0.5306	p=0.4340	p=0.5654	-	-	-
All data	p=0.0004		p=0.5301		p<0.0001	

magnitude with increasing hydrogen sulfide concentration from 0 to 1 mM. In contrast, SR rates were not significantly correlated with exogenous hydrogen sulfide concentration at pH 6 (Pearson's correlation, p=0.354).

Basic thermodynamic models of ΔG_r for SR at conditions within incubations (calculations based on Amend & Shock, 2001) show that the increasing H_2S concentration decreases the favorability of SR (Table 4.3). For example at 55°C and pH 6, ΔG_r for SR is -276 kJ mol^{-1} at 0 mM H_2S but increases to -106 kJ mol^{-1} at 1 mM H_2S. However, our data show that increased concentrations of H_2S do not significantly decrease SR rates. While some SR isolates can be inhibited by elevated H_2S (2-15mM), the Grotto microbial communities may be more tolerant because of the high H_2S concentrations in Grotto end-member fluids (5.4 mmol/kg at pH=4.2; Butterfield *et al.* 1994). Vent microbes are likely adapted to tolerate a wide range of sulfide concentrations (as H_2S naturally fluctuates). For example, archaea isolated from of deep-sea hydrothermal vents such as *Methanocaldococcus jannaschii, Archaeoglobus profundus, Thermococcus fumicolans,* and isolates from the genus *Pyrococcus* and *Desulfurococcus* have high tolerance to hydrogen sulfide concentrations in the range of 40 - 100 mM (Jannasch *et al*. 1988; Lloyd *et al*. 2005). As all experiments were incubated at concentrations below the range reported for significant SR inhibition (Reis *et al.* 1992; Okabe *et al*. 1995; Koschorreck 2008),

variation in rates as a function of sulfide concentration is likely not due to the effects of H_2S toxicity.

Table 4.3: ΔG_r (kJ mol^{-1}) of heterotrophic sulfate reduction at incubation conditions

$$CH_3COOH\ (aq) + SO_4^{2-} + 2\ H^+ \rightarrow\ 2CO_2 + H_2S(aq) + 2H_2O$$

[H_2S] (μM)	pH	2°C	55°C	100°C
0	4	-238	-276	-313
	6	-217	-251	-285
10	4	-107	-119	-135
	6	-85.8	-94.1	-107
100	4	-101	-112	-128
	6	-80.5	-87.9	-99.5
1000	4	-96.3	-106	-120
	6	-75.2	-81.6	-92.4

The positive correlation of SR with H_2S concentration at pH 4 is likely driven by effects of the chemical speciation of metals and H_2S. For example, hydrogen sulfide may be required to poise the environment at a favorable redox potential for SR to occur. The general range of E_h commonly associated with SR is -0.3 to 0.0 V at circumneutral pH (Lovley & Goodwin 1988) and is suggested to be slightly more positive at lower pH values (Church *et al*. 2007). Another possibility is that the activity of hydrogen sulfide is lower than the activity we assumed (based on the concentration of sulfide, salinity, and assumed mineral composition of media) due to oxidation with trace amounts of oxidants in the media, ion pairing with cations (e.g. FeS(aq), CuS(aq) etc.) or adsorption to mineral surfaces (Morse *et al.* 1987). Furthermore, the formation of metal-sulfide complexes may provide the sulfate reducing community a degree of protection against toxic heavy metals (Bharathi *et al.* 1990; Colleran *et al*. 1995). In pure cultures of

Thermococcus fumicolans, *Pyrococcus* strain GB-D, *Methanocaldococcus jannaschii*, sulfide additions were shown to attenuate the toxic effects of metal cations by forming metal-sulfide complexes (Edgcomb *et al*. 2004).

4.4.2.4 Effect of Sulfate Concentration on Rates of Sulfate Reduction

Sulfate reduction rates were positively correlated ($p<0.0001$) with sulfate concentration at both pH 6 and pH 4 (Figure 4.3). Monod Kinetics parameters determined using the Hanes-Woolf linearized form of the Monod rate equation (Eq. 2) revealed a K_m value 7.1 mM and V_{max} of 298 nmol g^{-1} day^{-1} for SR at pH 6 (r^2=0.441) and a K_m value of 2.5 mM and V_{max} of 298 nmol g^{-1} day^{-1} at pH 4 (r^2=0.513). Remember, K_m is defined as the sulfate concentration at which SR rate is at half-maximum and the larger the K_m value the lower the affinity for sulfate. The K_m values calculated for Grotto are higher than the range of K_m values calculated for SR in marine sediments (Roychoudhury 2004; Roychoudhury *et al.* 2003; Kostka & Roychoudhury 2002; Boudreau & Westrich 1984; Pallud & Van Cappellen 2006). Furthermore, the apparent K_m value for SR at pH 6 is higher than the highest reported K_m values for thermophilic SR (3.17 ± 1.02 mM) from Yellowstone Mushroom Springs (Roychoudhury 2004). Interestingly the apparent K_m values for SR at pH 6 are higher than pH 4 even though V_{max} remains constant under both conditions. Due to the low r^2 values for linear regressions, future experiments should consider a wider range of sulfate concentrations to validate these values.

One possible reason why K_m values for hydrothermal SR are higher than in other marine systems, is that the cellular uptake of sulfate is less efficient in hydrothermal sulfate reducers. Since all the enzymes required to catalyze sulfate into hydrogen sulfide are located in the

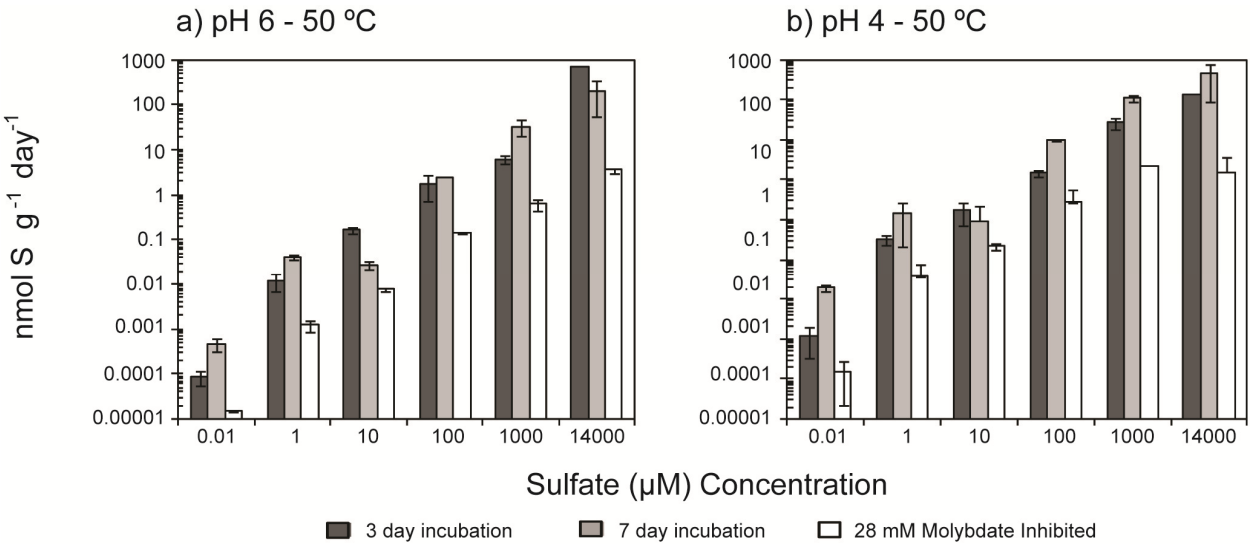

Figure 4.3: Effect of sulfate concentration on sulfate reduction rates in crushed Grotto flange. Crushed flange was incubated for 3 days (■) and 7 days (■) at 50°C at (a) pH 6 or (b) pH 4. 28mM molybdate amended samples were incubated under all conditions (white) as abiotic controls. Error bars represent 1 standard deviation.

interior of a cell (cytoplasm or associated with the inner surface of the cytoplasmic membrane), sulfate must be transported into the cells in order to be utilized. Due to the high sulfate concentration in seawater, marine SR communities often utilize low affinity transport mechanisms such as cation dependent passive transport (Cypionka & Konstanz 1989; Kreke *et al.* 1995; Kreke & Cypionka 1992, 1994) but can switch to active transport via sulfate permeases (Piłsyk & Paszewski 2009) under sulfate limitation (Tarpgaard *et al.* 2011). In comparison to marine systems, hydrothermal chimney structures have higher metal and H_2S loads, lower sulfate and experience higher temperature and lower pH fluids. Higher K_m values at vents may

be a result of insoluble metal sulfides acting as barriers to prevent the transport of sulfate (or other substrate) into the cell (Utgikar *et al.* 2002). Hydrothermal communities may mediate the potentially inhibitory effects of high temperature, low pH and sulfate limitation by increasing the number or type of sulfate permeases per cell. Recent metagenomic data shows a greater number of sulfate permease genes in communities from the middle zones of a chimney structure as compared to those from the outer regions of the structure (Frank *et al*. 2013c). Our data suggests that sulfate reducers have a higher affinity for sulfate at pH 4 than at pH 6 and may utilize different mechanisms (like increasing the number or type of sulfate permeases utilized) to overcome pH-induced constraints to maintain constant rates of SR. Interestingly, the measured rates at 14mM sulfate are comparable in magnitude to hydrothermally influenced sediments at Guaymas (high sulfate; Jørgensen *et al*. 1990; Elsgaard *et al*. 1994a) and Lake Tanganyika (low sulfate; Elsgaard *et al.* 1994b), which have strikingly different sulfate concentrations, suggesting that sulfate concentration may not govern the kinetics of SR.

4.4.2.5 Effect of Dissolved Organic Carbon on Rates of Sulfate Reduction

Sulfate reduction rates of samples incubated in the absence of an exogenous DOC were not significantly different from the rates of samples incubated with DOC (pyruvate, citrate,formate, acetate and lactate) concentrations up to 50 µM (Pearsons correlation, p=0.565; Figure 4.4). The favorability ($\Delta G_r°$) of SR utilizing these different low molecular weight carbon amendments varies from -146.6 kJ mol sulfate^{-1} with formate to -47.6 kJ mol sulfate^{-1} with acetate (Table 4.4), though the favorability of a given carbon compound is largely irrelevant when ΔG_r is normalized to the number of moles of C transferred (Rogers & Amend

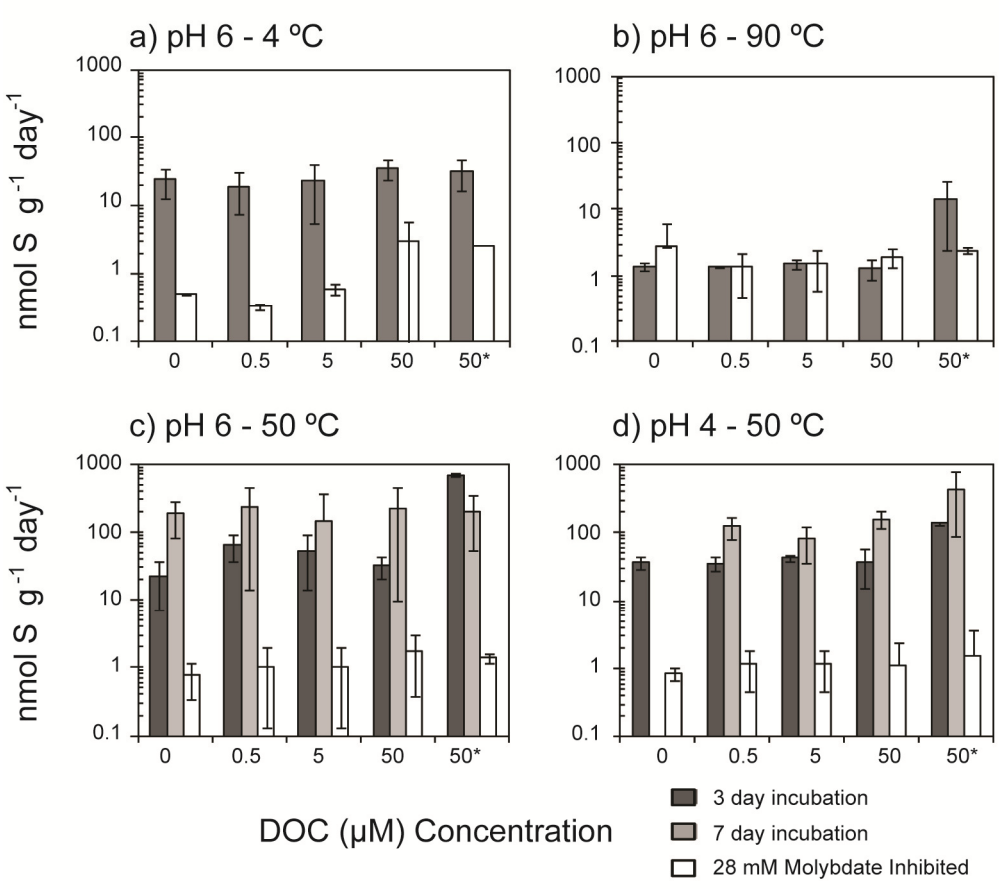

Figure 4.4: Effect of dissolved organic carbon (DOC) concentrations on sulfate reduction rates in crushed Grotto flange. Crushed flange was incubated for 3 days (■) in media of (a) pH 6 at 4°C, (b) pH 6 at 90°C, and 7 days (■) in media of (c) pH 6 at 50°C and (d) pH 4 at 50°C. While most of experiments were performed in laboratory using stored samples, concentrations identified with an asterisk (*) were done shipboard immediately after collection of hydrothermal chimney. 28mM molybdate amended samples were incubated under all conditions (white) as abiotic controls. Error bars represent 1 standard deviation.

2006). Most of the SR rates observed at 50°C were greater than could be supported by the exogenous DOC concentration provided in batch reactions for 7 days (Table 4.4) consistent with an endogenous carbon source. The observed rates suggest that even in non-DOC amended

samples, communities were not carbon limited. Mineral associated products of microbial respiration or fermentation, lysed cells and remnants from associated macrofauna (the surface of the flange was heavily colonized by tube worms) are likely sources of endogenous organic carbon. The total organic carbon (TOC) content of sediments from across the Juan de Fuca Ridge vary between 0.06 – 0.83% and hydrolysable amino acids account for up to 3.3% of this organic carbon (Andersson *et al*. 2000). Heterotrophic SR utilizing these carbon sources has been shown to be thermodynamically favorable in hydrothermal environments based on concentrations in diffuse fluid (Rogers & Amend 2006). Unfortunately, concentrations of mineral associated carbon (or total organic carbon) have not been evaluated, due to technical complications, in this environment. These data suggest that hydrothermal chimneys contain a substantially greater amount of biologically available endogenous carbon to support heterotrophic metabolisms than has previously been considered by bioenergetic models. DOC and TOC measurements at vents are relatively sparse and a more thorough documentation of these values across vent fields would be incredibly valuable to re-evaluate the potential energy yields of heterotrophic metabolisms in hydrothermal systems.

Table 4.4: Heterotrophic Sulfate reduction metabolism with particular carbon species.

Carbon Source	Reaction	$\Delta G_r°$ (kJ/ mol SO_4^{2-})	Max Rates* nmol/day
Acetate	$CH_3COO^- + SO_4^{2-} \rightarrow 2HCO_3^- + HS^-$	-47.6	21
Formate	$4HCO_2^- + SO_4^{2-} \rightarrow 2HCO_3^- + HS^-$	-146.6	5
Lactate	$2\ CH_3CHOHCOO^- + SO_4^{2-} \rightarrow 2\ CH_3CHOO^- + 2\ HCO_3^- + HS^- + H^+$	-160	11
	$2\ CH_3CHOHCOO^- + 3SO_4^{2-} \rightarrow 6HCO_3^- + 3HS^- + H^+$	-85	32

*Maximum rates 10µM of these organic carbon substrates could support in 7 day batch reactions

Another, though unlikely, possibility is the production of hydrogen by inorganic reactions thereby providing favorable conditions for autotrophic SR. Abiotic generation of hydrogen, dependent on the relative abundance of FeS and H_2S and temperature, has been documented above 50°C under similar anaerobic conditions (Heinen & Lauwers 1996). Given buffering by the pyrrhotite-pyrite-magnetite mineral assemblage (Shock & Schulte 1998; Shock *et al*. 1995; Von Damm 1988), abiotic production of H_2 is likely limited and rates of autotrophic SR in these reactions are negligible.

4.5 Conclusion

These experiments demonstrate the physiological properties of hydrothermally hosted sulfate reducing bacteria and archaea, revealing the potential for heterotrophic SR within Main Endeavor hydrothermal deposits. Variability in temperature, pH, sulfate concentration, and hydrogen sulfide concentration all contribute to the variable sulfate reducing activity, though the extent of their influence may vary with the geochemical setting. Despite the fact that bioenergetic models predict thermodynamic favorability of certain reactions, these calculations only place bounds on the potential activity but do not explain SR kinetics. Instead, the variability of SR rates (kinetics) is most likely governed by the abundance and composition of the active microbial consortia in response to these environmental stresses. Our data suggests that the Grotto flange has an active thermophilic sulfate reducing consortia and that majority of SR likely occurs within the outer to middle region of the flange.

Our data show that temperature is the primary factor that controls the magnitude of SR rates with the greatest effects observed at 50°C across all conditions tested. This is ecologically

consistent with temperature being one of the main driving forces that shape the composition and abundance of native microbial communities (Frank *et al*. 2013c). Additionally, pH served as a secondary factor in controlling rates, presumably mediating the availability of tertiary factors such as organic matter or sulfate and the speciation of potentially toxic compounds (ie. dissolved metals such as zinc and copper; Johnson 1998; Utgikar *et al*. 2003). Additionally, reduced SR rates at low pH may be a reflection of substrate competition with iron reducers. Sulfate reducers in this system were also shown to have lower affinity for sulfate than those in marine systems, possibly due to inefficient sulfate transport mechanisms. Hydrothermal communities may mediate the potentially inhibitory effects of high temperature, low pH and sulfate limitation by increasing the number or type of sulfate permeases per cell. DOC additions did not affect SR rates suggesting that these chimney samples are not carbon limited and contain a significant amount of endogenous carbon available for SR. While the factors governing SR *in situ* are likely far more complex than what is discussed here, kinetic experiments such as these can help constrain parameters for modeling the spatial contribution of heterotrophic sulfate to the carbon budget along the complex gradients inherent to hydrothermal deposits.

4.6 Acknowledgments

Financial support for this research was provided by the Nation Science Foundation (OCE-0838107 and OCE-1061934 to P.R. Girguis), the National Aeronautic and Space Administration (NASA-ASTEP NNX09AB78G to C. Scholin and P. R. Girguis and NASA-ASTEP NNX07AV51G to A. Knoll and P. R.Girguis) and the Center for Dark Energy Biosphere Investigations (C-DEBI

graduate fellowship support to K. L. Frank). We are grateful for the expert assistance of the *R/V Atlantis* crews and the pilots and team of the *DSV Alvin* for enabling the collections of hydrothermal deposits used in our experiments. We also thank Steve Sansone, Dr. Joseph Ring, Ms. Julie Hanlon, Dr. Jan Amend, Heather Olins and John Skutnik for providing assistance with various technical aspects of the experiments.

CHAPTER 5:

Conclusions

Collectively these data presented in this dissertation provide the first comprehensive assessment of endolithic microbial communities at vents, from diversity to activity, which refines our understanding of biogeochemical sulfur and carbon cycling. Chapter two provides insight on the detailed spatial relationships between vent geochemistry and the abundance, distribution, and metabolic characteristics of endolithic hosted communities. This sets the stage for chapters three and four, which examine heterotrophic sulfate reduction at vents, as well as the relationship between sulfate reduction rates, temperature, microbial biomass and community density and composition. As the conclusions for each project are presented in each respective chapter, here I will briefly discuss and consider how these data can be used to further contribute to our understanding of hydrothermal microbial ecology, and the implications for carbon and sulfur cycling at vents and in the greater ocean.

Bioenergetic modeling is a powerful means of examining (or even establishing) linkages between microbial phylogeny, microbial function, and biogeochemistry, and should be used to constrain the spatial distribution of sulfur metabolisms within the vent environment. Few corresponding data sets exist that correlate metabolic reaction energetics with reaction rates and taxonomy. Energy yields (ΔG_r^0) of different metabolic reactions (i.e. sulfate reduction and sulfide oxidation) can be calculated from *in situ* temperature and chemical conditions of environments discussed in chapters two through four. Integrating data on the microbial community composition and structure, metagenomic reconstructions of energy metabolisms, measured rates of metabolic activities of hydrothermal chimney microbes can provide specific evidence to test energetic hypothesizes. Only by concurrently assessing these biological and the geochemical data can we begin to understand the relationship between vent geochemistry and

the prolific and diverse communities observed therein, as well as their impact on global biogeochemical cycles. Additionally, natural sulfur isotopic data would be invaluable to further constrain the localization of different pathways of the sulfur cycle within hydrothermal chimneys and can provide a historical context of metabolisms utilized throughout the lifetime of a chimney. This approach could facilitate our comprehension of modern biogeochemical cycles at vents and help to decipher the significance of historical geological patterns.

Data presented in this dissertation further highlight the importance of designing experiments at the appropriate sampling scale within hydrothermal environments. Data from chapter two clearly show that the intrinsic heterogeneity of chimneys leads to heterogeneous quantitative (density), qualitative (diversity) and functional (activity) distribution of microorganisms. As evident here, *in situ* microbial incubation devices carefully designed to sample communities at high spatial resolution (with modifications to decrease any potential artifacts based on fluid dynamics within individual chambers) are an incredible technological advancement to the field, allowing replicated sampling at ecologically appropriate scales. In the future, devices like these can help to address if sulfide-associated microbiota experience transient responses to tidal associated changes in temperature and chemistry-a parameter never before considered in this environment-and to investigate the upper thermal limit of life.

The design of the experiments presented within this dissertation attempted to mitigate some of the issues (i.e. lack of appropriate replication, controls or co-registered thermal, chemical and microbiological measurements) associated with the difficulty in sampling hydrothermal environments. For example, chapter two presents the first statistically robust comparison of community composition across sulfides within a hydrothermal vent field, as well

as a metagenomic framework for discussing metabolic potential across redox gradients of a chimney (with co-registered temperature measurements). Data from chapter three and four present the first sulfate reduction rates measured within hydrothermal chimneys and underscore that thermodynamics (which constrains potential metabolic energy yields) does not necessarily describe the kinetics of vent microbial communities. Indeed, these data suggest that temperature and chemistry, as well as other geochemical factors, may significantly influence enzyme kinetics or the availability of substrates to microbes, thereby influencing rates. Together, chapters three and four (along with work like Olins *et al*. 2013) emphasize the importance of quantifying metabolic rates in hydrothermal structures and hopefully pave the way for future rate measurements in these systems.

These chapters also shed light on the technical challenges that remain associated with this field. While sampling methodology has advanced since the discovery of hydrothermal vents, many techniques for sampling fluid chemistry within a chimney or even maintaining and replicating conditions within the laboratory are currently prohibitive. For example, in the absence of convenient and transportable storage devices (that would ideally maintain pressurized gradients of temperature and chemistry), currently accepted storage methods of live vent samples (i.e. gastight jars filled with filtered anaerobic seawater) may induce shifts in community composition. Data in chapter three reveals that even mechanical homogenization will not always results in homogeneity of chimney materials for rate incubation experiments. Also, experiments are often not performed at physiologically relevant pressures, given the difficulty and that pressure doesn't significantly influence the thermodynamic favorability of reactions.

Equally important, the data presented herein underscore the relevance of sulfate reduction in hydrothermal ecosystems and the need for continued studies of sulfur cycling along ridge systems. Ideally future studies should attempt to couple fine-scale *in situ* redox measurements and microbial sampling with bioenergetic modeling and direct measurements of metabolic rates in order to more explicitly constrain microbial niches across steep redox gradients. The metabolic processes occurring within these systems are of importance because they may be analogs of the first living systems to evolve on Earth and ecosystems on other planets. Understanding the microbial communities' activities within hydrothermal environments will aid in the understanding of when and where life may have evolved on a hot early Earth; the depth to which life may exist in the Earth's subsurface; and the potential for life in extraterrestrial environments.

REFERENCES

Alain, K., Marteinsson, V. T., Miroshnichenko, M. L., Bonch-osmolovskaya, E. A., Prieur, D., & Birrien, J. (2002a). Marinitoga piezophila sp. nov., a rod-shaped, thermo-piezophilic bacterium isolated under high hydrostatic pressure from a deep-sea hydrothermal vent. *International Journal of Systematic and Evolutionary Microbiology*, *52*, 1331–1339.

Alain, K., Pignet, P., & Crassous, P. (2002b). Caminibacter hydrogeniphilus gen. nov., sp. nov., a novel thermophilic , hydrogen-oxidizing bacterium isolated from an East Pacific Rise hydrothermal vent. *International Journal of Systematic and Evolutionary Microbiology*, *52*, 1317–1323.

Alazard, D., Dukan, S., Urios, A., Verhe, F., Bouabida, N., Morel, F., … Ollivier, B. (2003). Desulfovibrio hydrothermalis sp nov., a novel sulfate-reducing bacterium isolated from hydrothermal vents. *International Journal of Systematic and Evolutionary Microbiology*, *53*, 173–178.

Altschul, S. F., Madden, T. L., Schäffer, a a, Zhang, J., Zhang, Z., Miller, W., & Lipman, D. J. (1997). Gapped BLAST and PSI-BLAST: a new generation of protein database search programs. *Nucleic Acids Research*, *25*(17), 3389–3402.

Amend, J P, & Shock, E. L. (2001). Energetics of overall metabolic reactions of thermophilic and hyperthermophilic Archaea and Bacteria. *FEMS Microbiology Reviews*, *25*(2), 175–243.

Amend, Jan P, & Edwards, K. J. (2004). Microbially mediated sulfur-redox: energetics in marine hydrothermal vent systems. In Jan P. Amend, K. J. Edwards, & T. W. Lyons (Eds.), *Sulfur Biogeochemistry: Past and Present* (pp. 17–34).

Anderson, R. E., Beltrán, M. T., Hallam, S. J., & Baross, J. A. (2012). Microbial community structure across fluid gradients in the Juan de Fuca Ridge hydrothermal system. *FEMS Microbiology Ecology*, *83*, 324–339.

Andersson, E., Simoneit, B. R. T., & Holm, N. G. (2000). Amino acid abundances and stereochemistry in hydrothermally altered sediments from the Juan de Fuca Ridge, northeastern Pacific Ocean. *Applied Geochemistry*, *15*, 1169–1190.

Angelis, M. A. De, Baross, J. A., Lilley, M. D., Limnology, S., & May, N. (1991). Enhanced Microbial Methane Oxidation in Water from a Deep-Sea Hydrothermal Vent Field at Simulated in Situ Hydrostatic Pressures. *Limnology and Oceanography*, *36*(3), 565–570.

Audiffrin, C., Cayol, J. L., Joulian, C., Casalot, L., Thomas, P., Garcia, J. L., & Ollivier, B. (2003). Desulfonauticus submarinus gen. nov., sp nov., a novel sulfate-reducing bacterium isolated

from a deep-sea hydrothermal vent. *International Journal of Systematic and Evolutionary Microbiology*, *53*, 1585–1590.

Bae, S. S., Kim, Y. J., Yang, S. H., Lim, J. K., Jeon, J. H., Lee, H. S., Lee, J. H. (2006). Thermococcus onnurineus sp nov., a hyperthermophilic Archaeon isolated from a deep-sea hydrothermal vent area at the PACMANUS field. *Journal of Microbiology and Biotechnology*, *16*(11), 1826–1831.

Baker, B. J., Lesniewski, R. A., & Dick, G. J. (2012). Genome-enabled transcriptomics reveals archaeal populations that drive nitrification in a deep-sea hydrothermal plume. *The ISME Journal*, *6*(12), 2269–2279.

Barton, L. L., Hamilton, W. A., Thauer, R. K., Stackebrandt, E., Legall, J., Odom, J. M., & Peck, H. D. (2003). Energy metabolism and phylogenetic diversity of sulphate-reducing bacteria. In W. A. Hamilton & L. L. Barton (Eds.), *Sulphate-Reducting Bacteria: Environmental and Engineered Systems* (pp. 1–10). Cambridge University Press.

Belkin, S., Jannasch, H. W., & Hole, W. (1985). A new extremely thermophilie, sulfur-reducing heterotrophie, marine bacterium. *Archives of Microbiology*, *141*, 181–186.

Berg, I. A. (2011). Ecological aspects of the distribution of different autotrophic CO2 fixation pathways. *Applied and Environmental Microbiology*, *77*(6), 1925–36.

Besemer, K., Singer, G., Limberger, R., Chlup, A.K., Hochedlinger, G., Hödl, I., Battin, T. J. (2007). Biophysical controls on community succession in stream biofilms. *Applied and Environmental Microbiology*, *73*(15), 4966–4974.

Bharathi, P. A., Sathe, V., & Chandramohan, D. (1990). Effect of lead, mercury and cadmium on a sulphate-reducing bacterium. *Environmental Pollution*, *67*(4), 361–374.

Biddle, J. F., Cardman, Z., Mendlovitz, H., Albert, D. B., Lloyd, K. G., Boetius, A., & Teske, A. (2012). Anaerobic oxidation of methane at different temperature regimes in Guaymas Basin hydrothermal sediments. *The ISME Journal*, *6*(5), 1018–31.

Blöchl, E., Rachel, R., Burggraf, S., Hafenbradl, D., Jannasch, H. W., Stetter, K. O., & Blochl, E. (1997). Pyrolobus fumarii, gen. and sp. nov., represents a novel group of archaea, extending the upper temperature limit for life to 113 degrees C. *Extremophiles*, *1*, 14–21.

Blodau, C., & Peiffer, S. (2003). Thermodynamics and organic matter: constraints on neutralization processes in sediments of highly acidic waters. *Applied Geochemistry*, *18*(1), 25–36.

Bonch-Osmolovskaya, E. A., Perevalova, A. A., Kolganova, T. V, Rusanov, I. I., Jeanthon, C., & Pimenov, N. V. (2011). Activity and distribution of thermophilic bacteria and archaea in

hydrothermal fluid, sulfidic structures, and sheaths of alvinellids (East Pacific Rise, 13°N). *Applied and Environmental Microbiology*, *77*(8), 2803–2806.

Bostick, B. C., Fendorf, S., & Helz, G. R. (2003). Differential adsorption of molybdate and tetrathiomolybdate on pyrite (FeS2). *Environmental Science & Technology*, *37*(2), 285–91.

Boudreau, B., & Westrich, J. (1984). The dependence of bacterial sulfate reduction on sulfate concentration in marine sediments. *Geochimica et Cosmochimica*, *48*, 2503–2516.

Bowien, B., & Schlegel, H. G. (1981). Physiology and Biochemistry of aerobic hydrogen-oxidizing bacteria. *Annual Review of Microbiology*, *35*, 405–452.

Braun, M. K. F., Dirmeier, R., & Hafenbradl, D. (1995). Thermococcus alcaliphilus sp. nov., a new hyperthermophilic archaeum growing on polysulfide at alkaline pH. *Archives of Microbiology*, *164*, 390–395.

Brazelton, W J, Schrenk, M. O., Kelley, D. S., & Baross, J. A. (2006). Methane- and sulfur-metabolizing microbial communities dominate the Lost City hydrothermal field ecosystem. *Applied and Environmental Microbiology*, *72*(9), 6257–6270.

Brazelton, William J, Ludwig, K. A., Sogin, M. L., Andreishcheva, E. N., Kelley, D. S., Shen, C. C., Baross, J. A. (2010). Archaea and bacteria with surprising microdiversity show shifts in dominance over 1,000-year time scales in hydrothermal chimneys. *Proceedings of the National Academy of Sciences*, *107*(4), 1612–1617.

Butterfield, D. A., Mcduff, R. E., Franklin, J., & Wheat, C. G. (1994). Geochemistry of hydrothermal vent fluids from Middle Valley, Juan de Fuca ridge. *Proc ODP Sci Res*, *139*, 395–410.

Butterfield, D. A., McDuff, R. E., Mottl, M. J., Lilley, M. D., Lupton, J. E., Massoth, G. J., Massoth, J. (1994). Gradients in the composition of hydrothermal fluids from the Endeavour segment vent field: Phase separation and brine loss. *Joural of Geophysical Research*, *99*(B5), 9561–9583.

Byrne, N., Strous, M., Crépeau, V., Kartal, B., Birrien, J.-L., Schmid, M., Godfroy, A. (2009). Presence and activity of anaerobic ammonium-oxidizing bacteria at deep-sea hydrothermal vents. *The ISME Journal*, *3*(1), 117–123.

Campbell, B. J., Engel, A. S., Porter, M. L., & Takai, K. (2006). The versatile epsilon-proteobacteria: key players in sulphidic habitats. *Nature reviews. Microbiology*, *4*(6), 458–468.

Canfield, D E. (1989). Sulfate Reduction and oxic respiration in marine- sediments- Implications for organic-carbon preservation in euxinic envrionments. *Deep Sea Research Part A Oceanographic Research Papers*, *36*(1), 121–138.

Canfield, Don E, Stewart, F. J., Thamdrup, B., De Brabandere, L., Dalsgaard, T., Delong, E. F., Ulloa, O. (2010). A cryptic sulfur cycle in oxygen-minimum-zone waters off the Chilean coast. *Science*, *330*(6009), 1375–1378.

Chauhan, A., Cherrier, J., & Williams, H. N. (2009). Impact of sideways and bottom-up control factors on bacterial community succession over a tidal cycle. *Proceedings of the National Academy of Sciences of the United States of America*, *106*(11), 4301–4306.

Chen, R. F., Bada, J. L., & Suzuk, Y. (1993). The relationship between dissolved organic carbon (DOC) and fluorescence in anoxic marine porewaters: Implications for estimating benthic DOC fluxes. *Geochimica et Cosmochimica Acta*, *57*, 2149–2153.

Christophersen, C. T., Morrison, M., & Conlon, M. A. (2011). Overestimation of the abundance of sulfate-reducing bacteria in human feces by quantitative PCR targeting the Desulfovibrio 16S rRNA gene. *Applied and Environmental Microbiology*, *77*(10), 3544–3546.

Church, C. D., Wilkin, R. T., Alpers, C. N., Rye, R. O., & McCleskey, R. B. (2007). Microbial sulfate reduction and metal attenuation in pH 4 acid mine water. *Geochemical Transactions*, *8*, 10.

Cole, J. R., Chai, B., Farris, R. J., Wang, Q., Kulam, S. a, McGarrell, D. M., Tiedje, J. M. (2005). The Ribosomal Database Project (RDP-II): sequences and tools for high-throughput rRNA analysis. *Nucleic acids research*, *33*(Database issue), D294–6.

Colleran, E., Finnegan, S., & Lens, P. (1995). Anaerobic treatment of sulphate-containing waste streams. *Antonie van Leeuwenhoek*, *67*(1), 29–46.

Cord-ruwisch, R., Seitz, H., & Conrad, R. (1988). The capacity of hydrogenotrophic anaerobic bacteria on the redox potential of the terminal electron acceptor. *Archives of Microbiology*, *149*, 350–357.

Costerton, J. W., Lewandowski, Z., Debeer, D., Caldwell, D., Korber, D., & James, G. (1994). Biofilms, the Customized Microniche. *Journal of Bacteriology*, *176*(8), 2137–2142.

Costerton, J. W., Lewandowski, Z., Caldwell, D. E., Korber, D. R., & Lappin-scott, H. M. (1995). Microbial biofilms. *Annual Review of Microbiology*, *49*, 711–745.

Crill, P. M., & Martens, C. S. (1986). Methane production from bicarbonate and acetate in an anoxic marine sediment. *Geochimica et Cosmochimica Acta*, *50*(9), 2089–2097.

Cruse, A. M., & Seewald, J. S. (2006). Geochemistry of low-molecular weight hydrocarbons in hydrothermal fluids from Middle Valley, northern Juan de Fuca Ridge. *Geochimica et Cosmochimica Acta*, *70*(8), 2073–2092.

Cypionka, H., & Konstanz, U. (1989). Characterization of sulfate transport in Desulfovibrio desulfuricans. *Archives of Microbiology*, *152*, 237–243.

D'Hondt, S., Jørgensen, B. B., Miller, D. J., Batzke, A., Blake, R., Cragg, B. A., Guerin, G. (2004). Distributions of microbial activities in deep subseafloor sediments. *Science*, *306*(5705), 2216–2221.

Dahle, H., Roalkvam, I., Thorseth, I. H., Pedersen, R. B., & Steen, I. H. (2013). The versatile in situ gene expression of an Epsilonproteobacteria-dominated biofilm from a hydrothermal chimney. *Environmental Microbiology Reports*, *5*(2), 282–290.

Dekas, A. E., Poretsky, R. S., & Orphan, V. J. (2009). Deep-sea archaea fix and share nitrogen in methane-consuming microbial consortia. *Science*, *326*, 422–426.

Delaney, J. R., Robigou, V., McDuff, R. E., & Tivey, M. K. (1992). Geology of a vigorous hydrothermal system on the Endeavor segment, Juan de Fuca ridge. *Journal of Geophysical Research-Solid Earth*, *97*(B13), 19663–19682.

Detmers, J., Brüchert, V., & Habicht, K. S. (2001). Diversity of Sulfur Isotope Fractionations by Sulfate-Reducing Bacteria and archaea Diversity of Sulfur Isotope Fractionations by Sulfate-Reducing Bacteria and archaea. *Applied and Environmental Microbiology*, *67*(2), 888–894.

Dick, G. J., Lee, Y. E., & Tebo, B. M. (2006). Manganese (II) -Oxidizing Bacillus Spores in Guaymas Basin Hydrothermal Sediments and Plumes. *Applied and Environmental Microbiology*, *72*(5), 3184–3190.

Dillon, J. G., Miller, S., Bebout, B., Hullar, M., Pinel, N., & Stahl, D. A. (2009). Spatial and temporal variability in a stratified hypersaline microbial mat community. *FEMS Microbiology Ecology*, *68*(1), 46–58.

Dirmeier, R., Keller, M., Hafenbradl, D., Braun, F. J., Rachel, R., Burggraf, S., & Stetter, K. O. (1998). Thermococcus acidaminovorans sp. nov., a new hyperthermophilic alkalophilic archaeon growing on amino acids. *Extremophiles*, *2*(2), 109–114.

Distel, D. L., Lee, H. K., & Cavanaugh, C. M. (1995). Intracellular coexistence of methano- and thioautotrophic bacteria in a hydrothermal vent mussel. *Proceedings of the National Academy of Sciences of the United States of America*, *92*(21), 9598–9602.

Dittmar, W. (1884). Report on researches into the composition of ocean water, collected by the HMS Challenger, during the years 1873-1876. *Report on the Scientific Results Voyage H.M.S. Challenger (Phys And Chem)*, *1*, 1–251.

Donlan, R. M., & Costerton, J. W. (2002). Biofilms: Survival Mechanisms of Clinically Relevant Microorganisms. *Clinical Microbiology Reviews*, *15*(2), 167–193.

Dowd, S. E., Sun, Y., Secor, P. R., Rhoads, D. D., Wolcott, B. M., James, G. A, & Wolcott, R. D. (2008). Survey of bacterial diversity in chronic wounds using Pyrosequencing, DGGE, and full ribosome shotgun sequencing. *BMC Microbiology*, *8*(43), 1-15.

Duffaud, G. D., D'Hennezel, O. B., Peek, A. S., Reysenbach, A. L., & Kelly, R. M. (1998). Isolation and characterization of Thermococcus barossii, sp. nov., a hyperthermophilic Archaeon isolated from a hydrothermal vent flange formation. *Systematic and Applied Microbiology*, *21*(1), 40–49.

Durand, P., Reysenbach, A., Prieur, D., & Pace, N. (1993). Isolation and characterization of Thiobacillus hydrothermalis sp. nov., a mesophilic obligately chemolithotrophic bacterium isolated from a deep-sea hydrothermal vent in Fiji Basin. *Archives of Microbiology*, *159*, 39–44.

Edgcomb, V. P., Molyneaux, S. J., Saito, M. A., Lloyd, K., Wirsen, C. O., Atkins, M. S., Carolina, N. (2004). Sulfide Ameliorates Metal Toxicity for Deep-Sea Hydrothermal Vent Archaea. *Applied and Environmental Microbiology*, *70*(4), 2551–2555.

Edwards, K. J., Rogers, D. R., Wirsen, C. O., & Mccollom, T. M. (2003). Isolation and Characterization of Novel Proteobacteria from the Deep Sea Isolation and Characterization of Novel Psychrophilic , Neutrophilic , Fe-Oxidizing , Chemolithoautotrophic α - and γ - Proteobacteria from the Deep Sea. *Applied and Environmental Microbiology*, *69*(5), 2906–2913.

Edwards, Katrina J, Bach, W., & McCollom, T. M. (2005). Geomicrobiology in oceanography: microbe-mineral interactions at and below the seafloor. *Trends in Microbiology*, *13*(9), 449–56.

Edwards, Katrina J., Bach, W., McCollom, T. M., & Rogers, D. R. (2004). Neutrophilic Iron-Oxidizing Bacteria in the Ocean: Their Habitats, Diversity, and Roles in Mineral Deposition, Rock Alteration, and Biomass Production in the Deep-Sea. *Geomicrobiology Journal*, *21*(6), 393–404.

Ehrhardt, C. J., Haymon, R. M., Lamontagne, M. G., & Holden, P. A. (2007). Evidence for hydrothermal Archaea within the basaltic flanks of the East Pacific Rise. *Environmental Microbiology*, *9*(4), 900–912.

Elderfield, H., & Schultz, A. (1996). Mid-Ocean Ridge Hydrothermal Fluxes and the Chemical Composition of the Ocean. *Annual Review of Earth and Planetary Sciences*, *24*(1), 191–224.

Elsaied, H. E., Kimura, H., & Naganuma, T. (2007). Composition of archaeal, bacterial, and eukaryal RuBisCO genotypes in three Western Pacific arc hydrothermal vent systems. *Extremophiles*, *11*(1), 191–202.

Elsaied, H., & Naganuma, T. (2001). Phylogenetic Diversity of Ribulose-1 , 5-Bisphosphate Carboxylase/Oxygenase Large-Subunit Genes from Deep-Sea Microorganisms. *Applied and Environmental Microbiology*, *67*(4), 1751–1765.

Elsgaard, L., Guezennec, J., Benbouzidrollet, N., & Prieur, D. (1995). Mesophilic sulfate-reducing bacteria from 3 deep-sea hydrothermal vent sites. *Oceanologica Acta*, *18*(1), 95–104.

Elsgaard, L., Isaksen, M. F., Jørgensen, B. B., Alayse, A. M., & Jannasch, H. W. (1994a). Microbial sulfate reduction in deep-sea sediments at the Guaymas Basin hydrothermal vent area: Influence of temperature and substrates. *Geochimica et Cosmochimica Acta*, *58*(16), 3335–3343.

Elsgaard, L., Prieur, D., Mukwaya, G. M., & Jørgensen, B. B. (1994b). Thermophilic sulfate reduction in hydrothermal sediment of lake tanganyika, East Africa. *Applied and Environmental Microbiology*, *60*(5), 1473–1480.

Erauso, G., Reysenbach, A., Godfroy, A., Meunier, J., Crump, B., Partensky, F., Prieur, D. (1993). Pyrococcus abyssi sp. nov., a new hyperthermophilic archaeon isolated from a deep-sea hydrothermal vent. *Archives of Microbiology*, *160*, 338–349.

Fernandes, S. O., Krishnan, K. P., Khedekar, V. D., & Loka Bharathi, P. A. (2005). Manganese oxidation by bacterial isolates from the Indian ridge system. *Biometals : an International Journal on the Role of Metal Ions in Biology, Biochemistry, and Medicine*, *18*(5), 483–492.

Ferrera, I., Longhorn, S., Banta, A. B., Liu, Y., Preston, D., & Reysenbach, A. L. (2007). Diversity of 16S rRNA gene, ITS region and aclB gene of the Aquificales. *Extremophiles :Life Under Extreme Conditions*, *11*(1), 57–64.

Fitz, R., & Cypionka, H. (1991). Generation of a proton gradient in Desulfovibrio vulgaris. *Archives of Microbiology*, *155*(5), 444–448.

Fossing, H, & Jørgensen, B. B. (1989). Measurment of bacterial sulfate reduction in sediments-evaluation of a single-step chromium reduction method. *Biogeochemistry*, *8*(3), 205–222.

Fossing, Henrik, & Jørgensen, B. B. (1989). Chromium Reduction Method of bacterial sulfate reduction in sediments: Measurement reduction of a single-step chromium method Evaluation. *Biogeochemistry*, *8*(3), 205–222.

Fourçans, A., Ranchou-Peyruse, A., Caumette, P., & Duran, R. (2008). Molecular analysis of the spatio-temporal distribution of sulfate-reducing bacteria (SRB) in Camargue (France) hypersaline microbial mat. *Microbial ecology*, *56*(1), 90–100.

Frank, K. L., Rogers, D. R., Olins, H. C., Vidoudez, C., & Girguis, P. R. (2013a). Characterizing the distribution and rates of microbial sulfate reduction at Middle Valley hydrothermal vents. *ISME*, *7*, 1391–1401.

Frank, K. L., Rogers, D. R., Rogers, K. L., Johnston, D. T., & Girguis, P. R. (2013b). Key factors influencing rates of heterotrophic sulfate reduction in hydrothermal massive sulfide deposits. *In Prep for Geochimica et Cosmochimica*.

Frank, K., Schrenk, M., Lilley, M. D., Wheat, G., Kelley, D., & Girguis, P. R. (2013c). Breaks in the physiochemical environment correlate with sharp biological boundaries within an active hydrothermal vent chimney Roane. *Unpublished-Dissertation*, *Chapter 2*.

Frias-lopez, J., Zerkle, A. L., Bonheyo, G. T., & Fouke, B. W. (2002). Partitioning of Bacterial Communities between Seawater and Healthy , Black Band Diseased , and Dead Coral Surfaces. *Applied and Environmental Microbiology*, *68*(5), 2214–2228.

Fujiwara, Y., Takai, K., Uematsu, K., Tsuchida, S., Hunt, J., & Hashimoto, J. (2000). Phylogenetic characterization of endosymbionts in three hydrothermal vent mussels: influence on host distributions. *Marine Ecology Progress Series*, *208*, 147–155.

Gadd, G. M., & Griffiths, A. J. (2013). Microorganisms and Heavy Metal Toxicity. *Microbial Ecology*, *4*(4), 303–317.

Garrity, G. M., & Holt, J. G. (2001). The road map to the Manual. In R. W. Castenholz & G.. Garrity (Eds.), *Bergys Manual of Systematic Bacteriology* (2nd ed., pp. 119–166). New York: Springer.

Ghose, T., & Wiken, T. (1955). Inhibition of Bacterial Sulphate-Reduction in Presence of Short Chain Fatty Acids. *Physiologia Plantarum*, *8*, 116–134.

Giller, K. E., Witter, E., & Mcgrath, S. P. (1998). Toxicity of heavy metals to microorganisms and microbial processes in agricultural soils: a review. *Soil Biology and Biochemistry*, *30*(10-11), 1389–1414.

Glickson, D. A., Kelley, D. S., & Delaney, J. R. (2007). Geology and hydrothermal evolution of the Mothra Hydrothermal Field, Endeavour Segment, Juan de Fuca Ridge. *Geochemistry Geophysics Geosystems*, *8*(6), 1–23.

Godfroy, A., Meunier, J. R., Guezennec, J., Lesongeur, F., Raguenes, G., Rimbault, A., & Barbier, G. (1996). Thermococcus fumicolans sp nov, a new hyperthermophilic archaeon isolated

from a deep-sea hydrothermal vent in the North Fiji Basin. *International Journal of Systematic Bacteriology*, *46*(4), 1113–1119.

González, J. M., Masuchi, Y., Robb, F. T., Ammerman, J. W., Maeder, D. L., Yanagibayashi, M., Kato, C. (1998). Pyrococcus horikoshii sp. nov., a hyperthermophilic archaeon isolated from a hydrothermal vent at the Okinawa Trough. *Extremophiles*, *2*(2), 123–130.

Grote, R., Li, L., Tamaoka, J., Kato, C., Horikoshi, K., & Antranikian, G. (1999). Thermococcus siculi sp. nov., a novel hyperthermophilic archaeon isolated from a deep-sea hydrothermal vent at the Mid-Okinawa Trough. *Extremophiles*, *3*(1), 55–62.

Guezennec, J. Y., Raguenes, G., & Geesey, G. (1998). Bacterial colonization of artificial substrate in the vicinity of deep-sea hydrothermal vents. *FEMS Microbiology Ecology*, *26*, 89–99.

Hafenbradl, D., Keller, M., Dirmeier, R., Rachel, R., Roßnagel, P., Burggraf, S., Stetter, K. O. (1996). Ferroglobus placidus gen. nov., sp. nov., a novel hyperthermophilic archaeum that oxidizes Fe^{2+} at neutral pH under anoxic conditions. *Archives of Microbiology*, *2*, 308–314.

Hanson, R. S., & Hanson, T. E. (1996). Methanotrophic bacteria. *Microbiological Reviews*, *60*(2), 439–471.

Harmsen, H. J. M., Prieur, D., & Jeanthon, C. (1997). Distribution of microorganisms in deep-sea hydrothermal vent chimneys investigated by whole-cell hybridization and enrichment culture of thermophilic subpopulations. *Applied and Environmental Microbiology*, *63*(7), 2876–2883.

Hedrick, D. B., Pledger, R. D., White, D. C., & Baross, J. A. (1992). *In situ* microbial ecology of hydrothermal vent sediments. *FEMS Microbiology Ecology*, *101*(1), 1–10.

Heinen, W., & Lauwers, A. M. (1996). Organic sulfur compounds resulting from the interaction of iron sulfide, hydrogen sulfide and carbon dioxide in an anaerobic aqueous environment. *Origins of Life and Evolution of the Biosphere*, *26*, 131–150.

Herter, S., Fuchs, G., Bacher, A., & Eisenreich, W. (2002). A bicyclic autotrophic CO2 fixation pathway in Chloroflexus aurantiacus. *The Journal of biological chemistry*, *277*(23), 20277–20283.

Hipp, W. M., Pott, A., Thum-schmitz, N., Dahl, C., & Truper, H. G. (1997). Towards the phylogeny of APS reductases and sirohaem sulf ite reductases in sulfate-reducing and sulf ur-oxidizing bacteria and archaea. *Microbiology*, *143*, 2891–2902.

Hirayama, H., Sunamura, M., Takai, K., Nunoura, T., Noguchi, T., Oida, H., Horikoshi, K. (2007). Culture-dependent and -independent characterization of microbial communities

associated with a shallow submarine hydrothermal system occurring within a coral reef off Taketomi Island, Japan. *Applied and Environmental Microbiology*, *73*(23), 7642–7656.

Hoek, J., Banta, A., Hubler, F., & Reysenbach, A. L. (2003). Microbial diversity of a sulphide spire located in the Edmond deep-sea hydrothermal vent field on the Central Indian Ridge. *Geobiology*, *1*(2), 119–127.

Holden, J. F., Summit, M., & Baross, J. A. (1998). Thermophilic and hyperthermophilic microorganisms in 3-30-degree-C hydrothermal fluids following a deep-sea volcanic eruption. *FEMS Microbiology Ecology*, *25*, 33–41.

Holmkvist, L., Kamyshny, A., Vogt, C., Vamvakopoulos, K., Ferdelman, T. G., & Jørgensen, B. B. (2011). Sulfate reduction below the sulfate-methane transition in Black Sea sediments. *Deep Sea Research Part I: Oceanographic Research Papers*, *58*(5), 493–504.

Houghton, J. L., Seyfried, W. E., Banta, A. B., & Reysenbach, A. L. (2007). Continuous enrichment culturing of thermophiles under sulfate and nitrate-reducing conditions and at deep-sea hydrostatic pressures. *Extremophiles*, *11*(2), 371–382.

Hu, M., Wirsen, C. O., Fuchs, G., Taylor, C. D., & Sievert, S. M. (2005). Evidence for Autotrophic CO2 Fixation via the Reductive Tricarboxylic Acid Cycle by Members of the ε Subdivision of Proteobacteria. *Journal of Bacteriology*, *187*(9), 3020–3027.

Huber, H, Jannasch, H., Rachel, R., Fuchs, T., & Stetter, K. O. (1997). Archaeoglobus veneficus sp nov, a novel facultative chemolithoautotrophic hyperthermophilic sulfite reducer, isolated from abyssal black smokers. *Systematic and Applied Microbiology*, *20*(3), 374–380.

Huber, Harald, Diller, S., Horn, C., & Rachel, R. (2002). Thermovibrio ruber gen. nov., sp. nov., an extremely thermophilic , chemolithoautotrophic , nitrate-reducing bacterium that forms a deep branch within the phylum Aquificae. *International Journal of Systematic and Evolutionary Microbiology*, *52*, 1859–1865.

Huber, Harald, & Stetter, K. O. (1989). Thiobacillus prosperus sp. nov., represents a new group of halotolerant metal-mobilizing bacteria isolated from a marine geothermal field. *Archives of Microbiology*, *151*, 479–485.

Huber, Harald, Thomm, M., Konig, H., Thies, G., & Stetter, K. O. (1982). Methanococcus Thermolithotrophicus, a Novel Themophilic Lithotrophic Methanogen. *Archives of Microbiology*, *132*, 47–50.

Huber, J A, Butterfield, D. A., & Baross, J. A. (2002). Temporal changes in archaeal diversity and chemistry in a mid-ocean ridge subseafloor habitat. *Applied and Environmental Microbiology*, *68*(4), 1585–1594.

Huber, J A, Mark Welch, D., Morrison, H. G., Huse, S. M., Neal, P. R., Butterfield, D. A., & Sogin, M. L. (2007). Microbial population structures in the deep marine biosphere. *Science*, *318*(5847), 97–100.

Huber, Julie A, Johnson, H. P., Butterfield, D. A., & Baross, J. A. (2006). Microbial life in ridge flank crustal fluids. *Environmental Microbiology*, *8*(1), 88–99.

Hügler, M., Huber, H., Molyneaux, S. J., Vetriani, C., & Sievert, S. M. (2007). Autotrophic CO2 fixation via the reductive tricarboxylic acid cycle in different lineages within the phylum Aquificae: evidence for two ways of citrate cleavage. *Environmental Microbiology*, *9*(1), 81–92.

Inagaki, F. (2003). Sulfurimonas autotrophica gen. nov., sp. nov., a novel sulfur-oxidizing -proteobacterium isolated from hydrothermal sediments in the Mid-Okinawa Trough. *International Journal of Systematic and Evolutionary Microbiology*, *53*(6), 1801–1805.

Inagaki, Fumio, Takai, K., Nealson, K. H., & Horikoshi, K. (2004). Sulfurovum lithotrophicum gen. nov., sp. nov., a novel sulfur-oxidizing chemolithoautotroph within the epsilon-Proteobacteria isolated from Okinawa Trough hydrothermal sediments. *International Journal of Systematic and Evolutionary Microbiology*, *54*, 1477–82.

Ingvorsen, K, Zehnder, A. J., & Jørgensen, B. B. (1984). Kinetics of Sulfate and Acetate Uptake by Desulfobacter postgatei. *Applied and Environmental Microbiology*, *47*(2), 403–408.

Ingvorsen, K, Zeikus, J. G., & Brock, T. D. (1981). Dynamics of bacterial sulfate reduction in a eutrophic lake. *Applied and Environmental Microbiology*, *42*(6), 1029–1036.

Ingvorsen, Kjeld, & Jørgensen, B. B. (1984). Kinetics of sulfate uptake by freshwater and marine species of Desulfovibrio. *Archives of Microbiology*, *139*, 61–66.

Isaksen, M. F., Bak, F., & Jørgensen, B. B. (1994). Thermophilic sulfate-reducing bacteria in cold marine sediment. *FEMS Microbiology Ecology*, *14*(1), 1–8.

Jackson, C.R., Churchill, P. F., & Roden, E. E. (2001). Successional changes in bacterial assemblage structure during epilithic biofilm development. *Ecology*, *82*, 555–566.

Jackson, Colin R, Oikos, S., & May, F. (2003). Changes in Community Properties during Microbial Succession. *Oikos*, *101*(2), 444–448.

Jaeschke, A., Jørgensen, S. L., Bernasconi, S. M., Pedersen, R. B., Thorseth, I. H., & Früh-Green, G. L. (2012). Microbial diversity of Loki's Castle black smokers at the Arctic Mid-Ocean Ridge. *Geobiology*, *10*(6), 548–561.

James, G. A., Beaudette, L., & Costerton, J. W. (1995). Interspecies bacterial interactions in biofilms. *Journal of Industrial Microbiology*, *15*(4), 257–262.

Jannasch, H W, & Mottl, M. J. (1985). Geomicrobiology of Deep-sea Hydrothermal Vents. *Science*, *229*(4715), 717–725.

Jannasch, H W, Wirsen, C. O., Molyneaux, S. J., & Langworthy, T. A. (1988). Extremely thermophilic fermentative archaebacteria of the genus Desulfurococcus from deep-sea hydrothermal vents. *Applied and Environmental Microbiology*, *54*(5), 1203–1209.

Jannasch, H. W. (1995). Microbial interactions with hydrothermal fluids. In R. E. Thomsom (Ed.), *Seafloor Hydrothermal Systems: Physical, Chemical, Biological, and Geological Interactions* (pp. 273–296). Washington, DC: American Geophysical Union.

Jannasch, Holger W, Wirsen, C. O., Nelson, D. C., & Robertson, L. A. (1985). Thiomicrospira crunogena sp nov, a colorless, sulfur-oxidizing bacterium from a deep-sea hydrothermal vent. *International journal of systematic bacteriology*, *35*(4), 422–424.

Jeanthon, C, L'Haridon, S., Reysenbach, A. L., Corre, E., Vernet, M., Messner, P., Prieur, D. (1999). Methanococcus vulcanius sp. nov., a novel hyperthermophilic methanogen isolated from East Pacific Rise, and identification of Methanococcus sp. DSM 4213(T) as Methanococcus fervens sp. nov. *International Journal of Systematic Bacteriology*, *49*(2), 583–589.

Jeanthon, C, L'Haridon, S., Reysenbach, A. L., Vernet, M., Messner, P., Sleytr, U. B., & Prieur, D. (1998). Methanococcus infernos sp. nov., a novel hyperthermophilic lithotrophic methanogen isolated from a deep-sea hydrothermal vent. *International Journal of Systematic Bacteriology*, *48*(3), 913–919.

Jeanthon, Christian, Haridon, L., Cueff, V., Banta, A., Reysenbach, A., & Prieur, D. (2002). Thermodesulfobacterium hydrogeniphilum sp. nov., a thermophilic , chemolithoautotrophic , sulfate-reducing bacterium isolated from a deep-sea hydrothermal vent at Guaymas Basin. *International Journal of Systematic and Evolutionary Microbiology*, *52*, 765–772.

Johnson, D. B. (1998). Biodiversity and ecology of acidophilic microorganisms. *FEMS Microbiology Ecology*, *27*(4), 307–317.

Johnson, K., Beehler, C., Sakamoto-Arnold, C., & Childress, J. (1986). In situ measurements of chemical distributions in a deep-sea hydrothermal vent field. *Science*, *231*, 1139–1141.

Jones, W. J., Leigh, J. A., Woese, C. R., Wolfe, R. S., & Mayer, F. (1983). Methanococcus jannaschii sp. nov., an extremely thermophilic methanogen from a submarine hydrothermal vent. *Archives of Microbiology*, *136*, 254–261.

Jørgensen, B. B., & Fenchel, T. (1974). The Sulfur Cycle of a Marine Sediment Model System. *Marine Biology*, *24*, 189–201.

Jørgensen, B. B., Isaksen, M. F., & Jannasch, H. W. (1992). Bacterial sulfate reduction above 100-degrees-C in deep-sea hydrothermal vent sediments. *Science*, *258*, 1756–1757.

Jørgensen, B. B., Zawacki, L. X., & Jannasch, H. W. (1990). Thermophilic bacterial sulfate reduction in deep-sea sediments at the Guaymas Basin hydrothermal vent site (Gulf of California). *Deep Sea Research Part A Oceanographic Research Papers*, *37*(4), 695–710.

Jørgensen, B. B., & Bak, F. (1991). Pathways and microbiology of thiosulfate transformations and sulfate reduction in a marine sediment (Kattegat, Denmark). *Applied and Environmental Microbiology*, *57*(3), 847–856.

Jørgensen, S. L., Hannisdal, B., Lanzén, A., Baumberger, T., & Flesland, K. (2012). Correlating microbial community profiles with geochemical data in highly stratified sediments from the Arctic Mid-Ocean Ridge. *Proceedings of the National Academy of Sciences*, *109*(42), e2846–2855.

Joye, S. B., Boetius, A., Orcutt, B. N., Montoya, J. P., Schulz, H. N., Erickson, M. J., & Lugo, S. K. (2004). The anaerobic oxidation of methane and sulfate reduction in sediments from Gulf of Mexico cold seeps. *Chemical Geology*, *205*(3-4), 219–238.

Kallmeyer, J, Ferdelman, T. G., & Jørgensen, B. B. (2002). Sulfate reduction rates in deeply, buried marine sediments. *Geochimica et Cosmochimica*, *66*(15A, 1), A378.

Kallmeyer, Jens, & Boetius, A. (2004). Effects of Temperature and Pressure on Sulfate Reduction and Anaerobic Oxidation of Methane in Hydrothermal Sediments of Guaymas Basin Effects of Temperature and Pressure on Sulfate Reduction and Anaerobic Oxidation of Methane in Hydrothermal Sediments of. *Applied and Environmental Microbiology*, *70*(2), 1231–1233.

Kashefi, K., Tor, J. M., Holmes, D. E., Gaw Van Praagh, C. V, Reysenbach, A.-L., & Lovley, D. R. (2002). Geoglobus ahangari gen. nov., sp. nov., a novel hyperthermophilic archaeon capable of oxidizing organic acids and growing autotrophically on hydrogen with Fe(III) serving as the sole electron acceptor. *International Journal of Systematic and Evolutionary Microbiology*, *52*, 719–728.

Kelly, D P, Shergill, J. K., Lu, W. P., & Wood, A. P. (1997). Oxidative metabolism of inorganic sulfur compounds by bacteria. *Antonie van Leeuwenhoek*, *71*(1-2), 95–107.

Kelly, Donovan P. (1999). Thermodynamic aspects of energy conservation by chemolithotrophic sulfur bacteria in relation to the sulfur oxidation pathways. *Archives of Microbiology*, *171*(4), 219–229.

Kembel, S. W., Eisen, J. A., Pollard, K. S., & Green, J. L. (2011). The phylogenetic diversity of metagenomes. *PloS One*, *6*(8), e23214.

Klappenbach, J. A., Saxman, P. R., Cole, J. R., & Schmidt, T. M. (2001). rrndb: the Ribosomal RNA Operon Copy Number Database. *Nucleic Acids Research*, *29*(1), 181–184.

Klein, M., Friedrich, M., Roger, A. J., Hugenholtz, P., Fishbain, S., Abicht, H., Linda, L. (2001). Multiple Lateral Transfers of Dissimilatory Sulfite Reductase Genes between Major Lineages of Sulfate-Reducing Bacteria and archaea. *Applied and Environmental Microbiology*, *183*(20), 6028–6035.

Kobayashi, T., Kwak, Y. S., Akiba, T., Kudo, T., & Horikoshi, K. (1994). Thermococcus profundus sp. nov, a new hyperthermophilic archaeon isolated from a deep-sea hydrothermal vent. *Systematic and Applied Microbiology*, *17*(2), 232–236.

Kondo, R., Nedwell, D. B., Purdy, K. J., & Silva, S. Q. (2004). Detection and Enumeration of Sulphate-Reducing Bacteria in Estuarine Sediments by Competitive PCR. *Geomicrobiology Journal*, *21*(3), 145–157.

Kormas, K. A., Tivey, M. K., Von Damm, K., & Teske, A. (2006). Bacterial and archaeal phylotypes associated with distinct mineralogical layers of a white smoker spire from a deep-sea hydrothermal vent site (9 degrees N, East Pacific Rise). *Environmental Microbiology*, *8*(5), 909–920.

Koschorreck, M. (2008). Microbial sulphate reduction at a low pH. *FEMS Microbiology Ecology*, *64*(3), 329–342.

Kostka, J. E., & Roychoudhury, A. (2002). Rates and controls of anaerobic microbial respiration across spatial and temporal gradients in saltmarsh sediments. *Biogeochemistry*, *60*, 49–76.

Kowalchuk, G. A., & Stephen, J. R. (2001). Ammonia-oxidizing bacteria: a model for molecular microbial ecology. *Annual review of microbiology*, *55*, 485–529.

Kreke, Bemd, Cypionka, H., & Microbiol, A. (1995). Energetics of sulfate transport in Desulfomicrobium baculatum. *Archives of Microbiology*, (November 1994), 307–309.

Kreke, Bernd, & Cypionka, H. (1992). Protonmotive force in freshwater sulfate-reducing bacteria, and its role in sulfate accumulation in Desulfobulbus propionicus. *Archives of Microbiology*, *158*, 183–187.

Kreke, Bernd, & Cypionka, H. (1994). Role of sodium ions for sulfaate transport and energy metabolism in Desulfovibrio salexigens. *Archives of Microbiology*, *161*, 55–61.

Kristall, B., Kelley, D. S., Hannington, M. D., & Delaney, J. R. (2006). Growth history of a diffusely venting sulfide structure from the Juan de Fuca Ridge: A petrological and geochemical study. *Geochemistry Geophysics Geosystems*, *7*(7), 1–30.

Kurr, M., Huber, R., Ki, H., Jannasch, H. W., Fricke, H., Trineone, A., Stetter, K. O. (1991). Methanopyrus kandleri, gen. and sp. nov. represents a novel group of hyperthermophilic methanogens, growing at 110°C. *Archives of Microbiology*, *156*, 239–247.

L'Haridon, S., Reysenbach, A.., Banta, A., Messner, P., Schumann, P., Stackbrandt, E., & Jeanthon, C. (2003). Methanocaldococcus indicus sp. nov., a novel hyperthermophilic methanogen isolated from the Central Indian Ridge. *International Journal of Systematic and Evolutionary Microbiology*, *53*(6), 1931–1935.

Lang, S Q, Butterfield, D. A., Lilley, M. D., Johnson, H. P., & Hedges, J. I. (2006). Dissolved organic carbon in ridge-axis and ridge-flank hydrothermal systems. *Geochimica et Cosmochimica Acta*, *70*(15), 3830–3842.

Lang, Susan Q, Butterfield, D. A., Schulte, M., Kelley, D. S., & Lilley, M. D. (2010). Elevated concentrations of formate, acetate and dissolved organic carbon found at the Lost City hydrothermal field. *Geochimica et Cosmochimica Acta*, *74*(3), 941–952.

Lanzén, A., Jørgensen, S. L., Bengtsson, M. M., Jonassen, I., Ovreås, L., & Urich, T. (2011). Exploring the composition and diversity of microbial communities at the Jan Mayen hydrothermal vent field using RNA and DNA. *FEMS microbiology ecology*, *77*(3), 577–589.

Lee, Z. M.P., Bussema, C., & Schmidt, T. M. (2009). rrnDB: documenting the number of rRNA and tRNA genes in bacteria and archaea. *Nucleic Acids Research*, *37*(Database issue), 489–493.

Leloup, J., Loy, A., Knab, N. J., Borowski, C., Wagner, M., & Jørgensen, B. B. (2007). Diversity and abundance of sulfate-reducing microorganisms in the sulfate and methane zones of a marine sediment, Black Sea. *Environ. Microbiol.*, *9*(1), 131–142.

Leskovac, V. (2003). Comparative Enzyme Kinetics. (V. Leskovac, Ed.) *Journal Serb. Chem. Soc*, *68*(12), 911–1022.

Lesniewski, R. A., Jain, S., Anantharaman, K., Schloss, P. D., & Dick, G. J. (2012). The metatranscriptome of a deep-sea hydrothermal plume is dominated by water column methanotrophs and lithotrophs. *The ISME Journal*, *6*(12), 2257–2268.

Lilley, M. D., Butterfield, D. A., Lupton, J. E., & Olson, E. J. (2003). Magmatic events can produce rapid changes in hydrothermal vent chemistry. *Nature*, *422*, 878–881.

Lin, Y.-S., Biddle, J. F., Lipp, J. S., Orcutt, B. N., Holler, T., Teske, A., & Hinrichs, K. U. (2010). Effect of Storage Conditions on Archaeal and Bacterial Communities in Subsurface Marine Sediments. *Geomicrobiology Journal*, *27*(3), 261–272.

Ljungdahl, L. G. (1986). The autotrophic pathway of acetate synthesis in acetogenic bacteria. *Annual Review of Microbiology*, *40*, 415–450.

Lloyd, K G, Edgcomb, V. P., Molyneaux, S. J., Boer, S., Wirsen, C. O., Atkins, M. S., & Teske, A. (2005). Effects of dissolved sulfide, pH, and temperature on growth and survival of marine hyperthermophilic archaea. *Applied and Environmental Microbiology*, *71*(10), 6383–6387.

Lloyd, Karen G, Albert, D. B., Biddle, J. F., Chanton, J. P., Pizarro, O., & Teske, A. (2010). Spatial Structure and Activity of Sedimentary Microbial Communities Underlying a Beggiatoa spp. Mat in a Gulf of Mexico Hydrocarbon Seep. *Plos One*, *5*(1), e8738.

Lovley, D R. (1993). Dissimilatory metal reduction. *Annual Review of Microbiology*, *47*, 263–90.

Lovley, D R, Dwyer, D. F., & Klug, M. J. (1982). Kinetic analysis of competition between sulfate reducers and methanogens for hydrogen in sediments. *Applied and Environmental Microbiology*, *43*(6), 1373–1379.

Lovley, D R, & Phillips, E. J. (1987). Competitive mechanisms for inhibition of sulfate reduction and methane production in the zone of ferric iron reduction in sediments. *Applied and Environmental Microbiology*, *53*(11), 2636–2641.

Lovley, Derek R, & Goodwin, S. (1988a). Hydrogen concentrations as an indicator of the predominant terminal. *Geochimica et Cosmochimica Acta*, *52*, 2993–3003.

Lovley, Derek R, & Phillips, E. J. P. (1988b). Novel Mode of Microbial Energy Metabolism: Organic Carbon Oxidation Coupled to Dissimilatory Reduction of Iron or Manganese Novel Mode of Microbial Energy Metabolism: Organic Carbon Oxidation Coupled to Dissimilatory Reduction of Iron or Manganese, *54*(6), 1472-1480.

Lovley, R., & Klug, M. J. (1986). Model for the distribution of sulfate reduction and methanogenesis in freshwater sedimentst. *Geochimica et Cosmochimica Acta*, *50*, 11–18.

Luton, P. E., Wayne, J. M., Sharp, R. J., & Riley, P. W. (2002). The mcrA gene as an alternative to 16S rRNA in the phylogenetic analysis of methanogen populations in landfill. *Microbiology*, *148*, 3521–3530.

MacLeod, F. A., Guiot, S. R., & Costerton, J. W. (1990). Layered structure of bacterial aggregates produced in an upflow anaerobic sludge bed and filter reactor. *Applied and environmental microbiology*, *56*(6), 1598–1607.

Maidak, B. L., Olsen, G. J., Larsen, N., Overbeek, R., McCaughey, M. J., & Woese, C. R. (1997). The RDP (Ribosomal Database Project). *Nucleic acids research*, *25*(1), 109–111.

Manefield, M., Whiteley, A. S., Griffiths, R. I., & Bailey, M. J. (2002). RNA Stable Isotope Probing, a Novel Means of Linking Microbial Community Function to Phylogeny. *Applied and Environmental Microbiology*, *68*(11), 5367–5373.

Marteinsson, V. T., Birrien, J. L., Reysenbach, A. L., Vernet, M., Marie, D., Gambacorta, A., Me, P. (1999). Thermococcus barophilus sp. nov., a new barophilic and hyperthermophilic archaeon isolated under high hydrostatic pressure from a deep-sea hydrothermal vent. *International Journal of Systematic and Evolutionary Microbiology*, *49*(2), 351–359.

Martin, W., Baross, J., Kelley, D., & Russell, M. J. (2008). Hydrothermal vents and the origin of life. *Nature Reviews. Microbiology*, *6*(11), 805–814.

McCliment, E. A., Voglesonger, K. M., O'Day, P. A., Dunn, E. E., Holloway, J. R., & Cary, S. C. (2006). Colonization of nascent, deep-sea hydrothermal vents by a novel Archaeal and Nanoarchaeal assemblage. *Environmental Microbiology*, *8*(1), 114–125.

McCollom, T. M., & Shock, E. L. (1997). Geochemical constraints on chemolithoautotrophic metabolism by microorganisms in seafloor hydrothermal systems. *Geochimica et Cosmochimica Acta*, *61*(20), 4375–4391.

Mehta, M. P., & Baross, J. A. (2006). Nitrogen fixation at 92 degrees C by a hydrothermal vent archaeon. *Science*, *314*, 1783–1786.

Merkel, A. Y., Huber, J. A., Chernyh, N. A., Bonch-Osmolovskaya, E. A., & Lebedinsky, A. V. (2013). Detection of putatively thermophilic anaerobic methanotrophs in diffuse hydrothermal vent fluids. *Applied and Environmental Microbiology*, *79*(3), 915–923.

Mevel, G., Faidy, C., & Prieur, D. (1987). Distribution, activity, and diversity of heterotrophic nitrifiers originating from East Pacific deep-sea hydrothermal vents. *Canadian Journal of Microbiology*, *42*, 162–171.

Meyer, B., & Kuever, J. (2007). Molecular analysis of the distribution and phylogeny of dissimilatory adenosine-5'-phosphosulfate reductase-encoding genes (aprBA) among sulfuroxidizing bacteria and archaea. *Microbiology*, *153*, 3478–3498.

Meyer, F., Paarmann, D., D'Souza, M., Olson, R., Glass, E. M., Kubal, M., Edwards, R. A. (2008). The metagenomics RAST server - a public resource for the automatic phylogenetic and functional analysis of metagenomes. *BMC bioinformatics*, *9*, 386.

Milucka, J., Ferdelman, T. G., Polerecky, L., Franzke, D., Wegener, G., Schmid, M., Kuypers, M. M. M. (2012). Zero-valent sulphur is a key intermediate in marine methane oxidation. *Nature*, *491*(7425), 541–546.

Minic, Z., & Thongbam, P. D. (2011). The biological deep sea hydrothermal vent as a model to study carbon dioxide capturing enzymes. *Marine Drugs*, *9*(5), 719–738.

Miroshnichenko, M. L., L'Haridon, S., Schumann, P., Spring, S., Bonch-Osmolovskaya, E. A., Jeanthon, C., & Stackebrandt, E. (2004). Caminibacter profundus sp. nov., a novel thermophile of Nautiliales ord. nov. within the class "Epsilonproteobacteria", isolated from a deep-sea hydrothermal vent. *International Journal of Systematic and Evolutionary Microbiology*, *54*(1), 41–45.

Mori, K., & Suzuki, K. (2008). Thiofaba tepidiphila gen. nov., sp nov., a novel obligately chemolithoautotrophic, sulfur-oxidizing bacterium of the Gammaproteobacteria isolated from a hot spring. *International Journal of Systematic and Evolutionary Microbiology*, *58*, 1885–1891.

Morse, J., Millero, F., Cornwell, J., & Rickard, D. (1987). The chemistry of the hydrogen sulfide and iron sulfide systems in natural waters. *Earth-Science Reviews*, *24*(1), 1–42.

Mottl, M. J., & Wheat, C. G. (1994). Hydrothermal circulation through mid-ocean ridge flanks: Fluxes of heat and magnesium. *Geochimica et Cosmochimica Acta*, *58*(10), 2225–2237.

Mussmann, M., Hu, F. Z., Richter, M., de Beer, D., Preisler, A., Jørgensen, B. B., Ehrlich, G. D. (2007). Insights into the genome of large sulfur bacteria revealed by analysis of single filaments. *Plos Biology*, *5*(9), 1923–1937.

Muyzer, G., & Stams, A. J. (2008). The ecology and biotechnology of sulphate-reducing bacteria. *Nature Reviews Microbiology*, *6*(6), 441–544.

Nakagawa, S., Inagaki, F., Takai, K., Horikoshi, K., & Sako, Y. (2005a). Thioreductor micantisoli gen. nov., sp. nov., a novel mesophilic, sulfur-reducing chemolithoautotroph within the epsilon-Proteobacteria isolated from hydrothermal sediments in the Mid-Okinawa Trough. *International journal of systematic and evolutionary microbiology*, *55*, 599–605.

Nakagawa, S., Nakamura, S., Inagaki, F., Takai, K., Shirai, N., & Sako, Y. (2004a). Hydrogenivirga caldilitoris gen. nov., sp. nov., a novel extremely thermophilic, hydrogen- and sulfur-oxidizing bacterium from a coastal hydrothermal field. *International Journal of Systematic and Evolutionary Microbiology*, *54*(Pt 6), 2079–2084.

Nakagawa, S., & Takai, K. (2008). Deep-sea vent chemoautotrophs: diversity, biochemistry and ecological significance. *FEMS Microbiology Ecology*, *65*(1), 1–14.

Nakagawa, S., Takai, K., Inagaki, F., Hirayama, H., Nunoura, T., Horikoshi, K., & Sako, Y. (2005b). Distribution, phylogenetic diversity and physiological characteristics of epsilon-Proteobacteria in a deep-sea hydrothermal field. *Environmental Microbiology*, *7*(10), 1619–1632.

Nakagawa, S., Takai, K., Inagaki, F., Horikoshi, K., & Sako, Y. (2005c). Nitratiruptor tergarcus gen. nov., sp. nov. and Nitratifractor salsuginis gen. nov., sp. nov., nitrate-reducing chemolithoautotrophs of the epsilon-Proteobacteria isolated from a deep-sea hydrothermal system in the Mid-Okinawa Trough. *International Journal of Systematic and Evolutionary Microbiology*, *55*, 925–933.

Nakagawa, T., Nakagawa, S., Inagaki, F., Takai, K., & Horikoshi, K. (2004b). Phylogenetic diversity of sulfate-reducing bacteria and archaea in active deep-sea hydrothermal vent chimney structures. *FEMS Microbiology Letters*, *232*(2), 145–152.

Nercessian, O, Bienvenu, N., Moreira, D., Prieur, D., & Jeanthon, C. (2005). Diversity of functional genes of methanogens, methanotrophs and sulfate reducers in deep-sea hydrothermal environments. *Environmental Microbiology*, *7*(1), 118–132.

Nercessian, Olivier, Reysenbach, A.-L., Prieur, D., & Jeanthon, C. (2003). Archaeal diversity associated with in situ samplers deployed on hydrothermal vents on the East Pacific Rise (13 degrees N). *Environmental Microbiology*, *5*(6), 492–502.

Newman, D. K., & Ahmann, D. (2009). A brief review of microbial arsenate respiration. *Geobiology, 15(4)*, 255-268.

Newport, P. J., & Nedwell, D. B. (1988). The mechanisms of inhibition of Desulfovibrio and Desulfotomaculum species by selenate and molybdate. *Journal of Applied Microbiology*, *65*(5), 419–423.

Novitsky, J. A. (1986). Degradation of Dead Microbial Biomass in a Marine Sediment. *Applied and Environmental Microbiology*, *52*(3), 504–509.

Nunoura, T., Oida, H., Nakaseama, M., Kosaka, A., Ohkubo, S. B., Kikuchi, T., Takai, K. (2010). Archaeal diversity and distribution along thermal and geochemical gradients in hydrothermal sediments at the Yonaguni Knoll IV hydrothermal field in the Southern Okinawa trough. *Applied and Environmental Microbiology*, *76*(4), 1198–1211.

Nunoura, T., & Takai, K. (2009). Comparison of microbial communities associated with phase-separation-induced hydrothermal fluids at the Yonaguni Knoll IV hydrothermal field, the Southern Okinawa Trough. *FEMS Microbiology Ecology*, *67*(3), 351–370.

Oakley, B. B., Carbonero, F., Dowd, S. E., Hawkins, R. J., & Purdy, K. J. (2011). Contrasting patterns of niche partitioning between two anaerobic terminal oxidizers of organic matter. *The ISME Journal*, *6*(5), 905–914.

Okabe, S., Nielsen, P. H., Jones, W. L., & Characklis, W. G. (1995). Sulfide product inhibition of Desulfovibrio desulfuricans in batch and continuous cultures. *Water Research*, *29*(2), 571–578.

Oleszkiewicz, J. A., Marstaller, T., & McCartney, D. M. (1989). Effects of pH on sulfide toxicity to anaerobic processes. *Environmental Technology Letters*, *10*(9), 815–822.

Olins, H. C., Rogers, D. R., Frank, K. L., Vidoudez, C., & Girguis, P. R. (2013). Assessing the influence of physical, geochemical and biological factors on anaerobic microbial primary productivity within hydrothermal vent chimneys. *Geobiology*, *11*(3), 279-293.

Opatkiewicz, A. D., Butterfield, D. A., & Baross, J. A. (2009). Individual hydrothermal vents at Axial Seamount harbor distinct subseafloor microbial communities. *FEMS Microbiology Ecology*, *70*(3), 413–424.

Orcutt, B., Boetius, A., Elvert, M., Samarkin, V., & Joye, S. B. (2005). Molecular biogeochemistry of sulfate reduction, methanogenesis and the anaerobic oxidation of methane at Gulf of Mexico cold seeps. *Geochimica et Cosmochimica Acta*, *69*(17), 4267–4281.

Oremland, R S, & Polcin, S. (1982). Methanogenesis and sulfate reduction: competitive and noncompetitive substrates in estuarine sediments. *Applied and Environmental Microbiology*, *44*(6), 1270–1276.

Oremland, Ronald S, & Taylor, B. F. (1977). Sulfate reduction and methanogenesis in marine sediments. *Geochimica et Cosmochimica*, *42*(2), 209–214.

Page, A., Tivey, M. K., Stakes, D. S., & Reysenbach, A. L. (2008). Temporal and spatial archaeal colonization of hydrothermal vent deposits. *Environmental Microbiology*, *10*(4), 874–884.

Pallud, C., & Van Cappellen, P. (2006). Kinetics of microbial sulfate reduction in estuarine sediments. *Geochimica et Cosmochimica Acta*, *70*(5), 1148–1162.

Peinemann-simon, B. J. S., Völker, H., Stüben, D., Botz, R., Stoffers, P., Dando, P. R., & Thomm, M. (1997). Stetteria hydrogenophila, gen. nov. and sp. nov., a novel mixotrophic sulfur-dependent crenarchaeote isolated from Milos , Greece. *Extremophiles*, *1*, 67–73.

Perner, M., Kuever, J., Seifert, R., Pape, T., Koschinsky, A., Schmidt, K., Imhoff, J. F. (2007). The influence of ultramafic rocks on microbial communities at the Logatchev hydrothermal field, located 15 °N on the Mid-Atlantic Ridge. *FEMS Microbiology Ecology*, *61*(1), 97–109.

Perner, M., Seifert, R., Weber, S., Koschinsky, A., Schmidt, K., Strauss, H., Imhoff, J. F. (2007). Microbial CO(2) fixation and sulfur cycling associated with low-temperature emissions at the Lilliput hydrothermal field, southern Mid-Atlantic Ridge (9 °S). *Environmental Microbiology*, *9*(5), 1186–201.

Pernthaler, A., Dekas, A. E., Brown, C. T., Goffredi, S. K., Embaye, T., & Orphan, V. J. (2008). Diverse syntrophic partnerships from-deep-sea methane vents revealed by direct cell capture and metagenomics. *Proceedings of the National Academy of Sciences of the United States of America*, *105*(19), 7052–7057.

Piłsyk, S., & Paszewski, A. (2009). Sulfate permeases — phylogenetic diversity of sulfate transport. *Acta Biochimica Polonica*, *56*(3), 375–384.

Pimenov, N. V, Lein, Ai., Sagalevich, A. M., & Ivanov, M. V. (2000). Assimilation of carbon dioxide and oxidation of methane in various zones of the Rainbow hyperthermophilic field zones. *Mikrobiologiia*, *69*(6), 810–818.

Pond, D. W., Bell, M. V, Dixon, D. R., Fallick, a E., Segonzac, M., & Sargent, J. R. (1998). Stable-carbon-isotope composition of Fatty acids in hydrothermal vent mussels containing methanotrophic and thiotrophic bacterial endosymbionts. *Applied and Environmental Microbiology*, *64*(1), 370–375.

Rabus, R., Hansen, T. A., & Widdel, F. (2006). Dissimilatory Sulfate and Sulfur Reducing Bacteria and archaea. *Bacteria and archaea*, *2*, 659–768.

Raghoebarsing, A. A., Pol, A., van de Pas-Schoonen, K. T., Smolders, A. J., Ettwig, K. F., Rijpstra, W. I., Strous, M. (2006). A microbial consortium couples anaerobic methane oxidation to denitrification. *Nature*, *440*(7086), 918–21.

Ragsdale, S. W., & Pierce, E. (2008). Acetogenesis and the Wood-Ljungdahl pathway of CO2 fixation. *Biochimica et Biophysica Acta*, *1784*(12), 1873–98.

Ran, B., & Simoneit, B. R. T. (1994). Dissolved organic carbon in interstitial waters from sediments of Middle Valley, Leg 1391. *Proc ODP Sci Res*, *139*, 441–446.

Reis, M. a, Almeida, J. S., Lemos, P. C., & Carrondo, M. J. (1992). Effect of hydrogen sulfide on growth of sulfate reducing bacteria. *Biotechnology and Bioengineering*, *40*(5), 593–600.

Reysenbach, A. L., Longnecker, K., & Kirshtein, J. (2000). Novel bacterial and archaeal lineages from an in situ growth chamber deployed at a Mid-Atlantic Ridge hydrothermal vent. *Applied and Environmental Microbiology*, *66*(9), 3798–3806.

Reysenbach, A., & Longnecker, K. (2000). Novel Bacterial and Archaeal Lineages from an In Situ Growth Chamber Deployed at a Mid-Atlantic Ridge Hydrothermal Vent Novel Bacterial and

Archaeal Lineages from an In Situ Growth Chamber Deployed at a Mid-Atlantic Ridge Hydrothermal Vent. *Applied and Environmental Microbiology*, *66*(9), 3768–3806.

Robador, A., Brüchert, V., & Jørgensen, B. B. (2009). The impact of temperature change on the activity and community composition of sulfate-reducing bacteria in arctic versus temperate marine sediments. *Environmental Microbiology*, *11*(7), 1692–1703.

Robigou, V., Delaney, J. R., & Stakes, D. S. (1993). Large massive sulfide deposits in a newly disocvered active hydrothermal system, the high rise field, endeavour segment Juan de Fuca ridge. *Geophysical Research Letters*, *20*(17), 1887–1890.

Rogers, K. L., & Amend, J. P. (2006). Energetics of potential heterotrophic metabolisms in the marine hydrothermal system of Vulcano Island, Italy. *Geochimica et Cosmochimica Acta*, *70*(24), 6180–6200.

Rogers, K. L., & Schulte, M. D. (2012). Organic Sulfur Metabolisms in Hydrothermal Environments. *Geobiology*, 1–13.

Roychoudhury, A. N. (2004). Sulfate Respiration in Extreme Environments: A Kinetic Study. *Geomicrobiology Journal*, *21*(1), 33–43.

Roychoudhury, A. N., Van Cappellen, P., Kostka, J. E., & Viollier, E. (2003). Kinetics of microbially mediated reactions: dissimilatory sulfate reduction in saltmarsh sediments (Sapelo Island, Georgia, USA). *Estuarine, Coastal and Shelf Science*, *56*(5-6), 1001–1010.

Sako, Y., Takai, K., Ishida, Y., Uchida, A., & Katayama, Y. (1996). Rhodothermus obamensis sp. nov., a modern lineage of extremely thermophilic marine bacteria. *International Journal of Systematic Bacteriology*, *46*(4), 1099–104.

Saleh, A. M., Macpherson, R., & Miller, J. D. (1964). The Effect of Inhibitors on Sulphate Reducing Bacteria: a Compilation. *Journal of Applied Microbiology*, *27*(2), 281–293.

Santelli, C. M., Orcutt, B. N., Banning, E., Bach, W., Moyer, C. L., Sogin, M. L., Edwards, K. J. (2008). Abundance and diversity of microbial life in ocean crust. *Nature*, *453*(7195), 653–657.

Schimel, J., Balser, T. C., & Wallenstein, M. (2007). Microbial stress reponse physiology and its implications. *Ecology*, *88*(6), 1386–1394.

Schloss, P. D. (2009). A high-throughput DNA sequence aligner for microbial ecology studies. *PloS One*, *4*(12), e8230.

Schloss, P. D., Westcott, S. L., Ryabin, T., Hall, J. R. A., Hartmann, M., Hollister, E. B., Weber, C. F. (2009). Introducing mothur: open-source, platform-independent, community-supported

software for describing and comparing microbial communities. *Applied and Environmental Microbiology*, *75*(23), 7537–7541.

Schrenk, M. O., Kelley, D. S., Delaney, J. R., & Baross, J. A. (2003). Incidence and Diversity of Microorganisms within the Walls of an Active Deep-Sea Sulfide Chimney. *Applied and Environmental Microbiology*, *69*(6), 3580–3592.

Sekiguchi, Y., Muramatsu, M., Imachi, H., Narihiro, T., Ohashi, A., Harada, H., … Kamagata, Y. (2008). Thermodesulfovibrio aggregans sp. nov. and Thermodesulfovibrio thiophilus sp. nov., anaerobic, thermophilic, sulfate-reducing bacteria isolated from thermophilic methanogenic sludge, and emended description of the genus Thermodesulfovibrio. *International Journal of Systematic Bacteriology*, *58*(Pt 11), 2541–2548.

Sergerer, A., Neuner, A., Kristjansson, J. K., & Stetter, K. O. (1986). Acidianus-Infernus gen nov., sp nov, and Acidianus brierley comb nov. facultatively aerobic, extremely acidophilic thermophilic sulfur metabolizing archaebacteria. *International Journal of Systematic Bacteriology*, *36*(4), 559–564.

Shock, E. L., Mccollom, T., & Schulte, M. D. (1995). Geochemical constraints on chemolithoautotrophic reactions in hydrothermal systems. *Origins of Life and Evolution of the Biosphere*, *25*(1-3), 141–159.

Shock, E. L., & Schulte, M. D. (1998). Organic synthesis during fluid mixing in hydrothermal systems. *Journal of Geophysical Research*, *103*(E12), 28513-28526.

Simon, C., Wiezer, A., Strittmatter, A. W., & Daniel, R. (2009). Phylogenetic Diversity and Metabolic Potential Revealed in a Glacier Ice Metagenome. *Applied and Environmental Microbiology*, *75*(23), 7519–7526.

Slobodkina, G. B., Kolganova, T. V, Querellou, J., Bonch-Osmolovskaya, E. A., & Slobodkin, a I. (2009). Geoglobus acetivorans sp. nov., an iron(III)-reducing archaeon from a deep-sea hydrothermal vent. *International Journal of Systematic and Evolutionary Microbiology*, *59*, 2880–2883.

Smith, J. L., Campbell, B. J., Hanson, T. E., Zhang, C. L., & Cary, S. C. (2008). Nautilia profundicola sp. nov., a thermophilic, sulfur-reducing epsilonproteobacterium from deep-sea hydrothermal vents. *International Journal of Systematic and Evolutionary Microbiology*, *58*, 1598–1602.

Sogin, M. L., Morrison, H. G., Huber, J. A., Welch, D. M., Huse, S. M., Neal, P. R., Herndl, G. J. (2006). Microbial diversity in the deep sea and the underexplored “rare biosphere.” *Proceedings of the National Academy of Sciences*, *103*(32), 12115–12120.

Sokolova, T., Hanel, J., Onyenwoke, R. U., Reysenbach, A.-L., Banta, A., Geyer, R., Wiegel, J. (2007). Novel chemolithotrophic, thermophilic, anaerobic bacteria Thermolithobacter ferrireducens gen. nov., sp. nov. and Thermolithobacter carboxydivorans sp. nov. *Extremophiles*, *11*(1), 145–157.

Sonne-hansen, J., & Westermann, P. (1999). Kinetics of Sulfate and Hydrogen Uptake by the Thermophilic Sulfate-Reducing Bacteria Thermodesulfobacterium sp. Strain. *Applied and Environmental Microbiology*, *65*(3), 1304–1307.

Stolz, J. F., & Oremland, R. S. (1999). Bacterial respiration of arsenic and selenium. *FEMS Microbiology Reviews*, *23*(5), 615–627.

Strauss, G., & Fuchs, G. (1993). Enzymes of a novel autotrophic CO2 fixation pathway in the phototrophic bacterium Chloroflexus aurantiacus, the 3-hydroxypropionate cycle. *European journal of biochemistry/FEBS*, *215*(3), 633–643.

Strous, M., Heijnen, J. J., Kuenen, J. G., & Jetten, M. S. M. (1998). The sequencing batch reactor as a powerful tool for the study of slowly growing anaerobic ammonium-oxidizing microorganisms. *Applied Microbiology and Biotechnology*, *50*(5), 589–596.

Stults, J. R., Snoeyenbos-west, O., Methe, B., Lovley, D. R., & Chandler, D. P. (2001). Application of the 5 ′ Fluorogenic Exonuclease Assay (TaqMan) for Quantitative Ribosomal DNA and rRNA Analysis in Sediments. *Applied and Environmental Microbiology*, *67*(6), 2781–2789.

Suzuki, M. T., Beja, O., Taylor, L. T., & DeLong, E. F. (2001). Phylogenetic analysis of ribosomal RNA operons from uncultivated coastal marine bacterioplankton. *Environmental Microbiology*, *3*(5), 323–331.

Suzuki, Y., Inagaki, F., Takai, K., Nealson, K. H., & Horikoshi, K. (2004). Microbial diversity in inactive chimney structures from deep-sea hydrothermal systems. *Microbial Ecology*, *47*(2), 186–196.

Sylvan, J. B., Toner, B. M., & Edwards, K. J. (2012). Life and Death of Deep-Sea Vents : Bacterial Diversity and Ecosystem Succession on Inactive Hydrothermal Sulfides. *mBio*, *3*(1), e00279–11.

Takai, K, Komatsu, T., Inagaki, F., & Horikoshi, K. (2001). Distribution of archaea in a black smoker chimney structure. *Applied and Environmental Microbiology*, *67*(8), 3618–3629.

Takai, K, Miyazaki, M., Nunoura, T., Hirayama, H., Oida, H., Furushima, Y., Horikoshi, K. (2006a). Sulfurivirga caldicuralii gen. nov., sp nov., a novel microaerobic, thermophilic, thiosulfate-oxidizing chemolithoautotroph, isolated from a shallow marine hydrothermal system occurring in a coral reef, Japan. *International Journal of Systematic and Evolutionary Microbiology*, *56*, 1921–1929.

Takai, K. (2003). Deferribacter desulfuricans sp. nov., a novel sulfur-, nitrate- and arsenate-reducing thermophile isolated from a deep-sea hydrothermal vent. *International Journal of Systematic and Evolutionary Microbiology*, *53*(3), 839–846.

Takai, K. (2004a). Hydrogenimonas thermophila gen. nov., sp. nov., a novel thermophilic, hydrogen-oxidizing chemolithoautotroph within the -Proteobacteria, isolated from a black smoker in a Central Indian Ridge hydrothermal field. *International Journal of Systematic and Evolutionary Microbiology*, *54*(1), 25–32.

Takai, K., & Horikoshi, K. (2000a). Rapid Detection and Quantification of Members of the Archaeal Community by Quantitative PCR Using Fluorogenic Probes. *Applied and Environmental Microbiology*, *66*(11), 5066–5072.

Takai, K., Campbell, B. J., Cary, S. C., Suzuki, M., Oida, H., Nunoura, T., Horikoshi, K. (2005a). Enzymatic and Genetic Characterization of Carbon and Energy Metabolisms by Deep-Sea Hydrothermal Chemolithoautotrophic Isolates of Epsilonproteobacteria. *Applied and Environmental Microbiology*, *71*(11), 7310–7320.

Takai, K., Hirayama, H., Nakagawa, T., Suzuki, Y., Nealson, K. H., & Horikoshi, K. (2005b). Lebetimonas acidiphila gen. nov., sp. nov., a novel thermophilic, acidophilic, hydrogen-oxidizing chemolithoautotroph within the “Epsilonproteobacteria”, isolated from a deep-sea hydrothermal fumarole in the Mariana Arc. *International Journal of Systematic and Evolutionary Microbiology*, *55*(Pt 1), 183–189.

Takai, K., Inoue, A., & Horikoshi, K. (2002). Methanothermococcus okinawensis sp. nov., a thermophilic, methane-producing archaeon isolated from a Western Pacific deep-sea hydrothermal vent system. *International Journal of Systematic and Evolutionary Microbiology*, *52*, 1089–1095.

Takai, K., & Nakamura, K. (2011). Archaeal diversity and community development in deep-sea hydrothermal vents. *Current Opinion in Microbiology*, *14*(3), 282–291.

Takai, K., Nealson, K. H., & Horikoshi, K. (2004b). Methanotorris formicicus sp. nov., a novel extremely thermophilic, methane-producing archaeon isolated from a black smoker chimney in the Central Indian Ridge. *International Journal of Systematic and Evolutionary Microbiology*, *54*, 1095–1100.

Takai, K., Sugai, A., Itoh, T., & Horikoshi, K. (2000b). Palaeococcus ferrophilus gen. nov., sp. nov., a barophilic , hyperthermophilic archaeon from a deep-sea hydrothermal vent chimney. *International Journal of Systematic and Evolutionary Microbiology*, *50*, 489–500.

Takai, K., Suzuki, M., Nakagawa, S., Miyazaki, M., Suzuki, Y., Inagaki, F., & Horikoshi, K. (2006b). Sulfurimonas paralvinellae sp. nov., a novel mesophilic, hydrogen- and sulfur-oxidizing chemolithoautotroph within the Epsilonproteobacteria isolated from a deep-sea

hydrothermal vent polychaete nest, reclassification of Thiomicrospira denitrificans as Su. *International Journal of Systematic and Evolutionary Microbiology*, *56*, 1725–1733.

Tarpgaard, I. H., Roy, H., & Jørgensen, B. B. (2011). Concurrent low- and high-affinity sulfate reduction kinetics in marine sediment. *Geochimica et Cosmochimica Acta*, *75*(11), 2997–3010.

Templeton, A. S., Staudigel, H., & Tebo, B. M. (2005). Diverse Mn(II)-Oxidizing Bacteria Isolated from Submarine Basalts at Loihi Seamount. *Geomicrobiology Journal*, *22*(3-4), 127–139.

Teske, A. P. (2006). Microbial communities of deep marine subsurface sediments: Molecular and cultivation surveys. *Geomicrobiology Journal*, *23*(6), 357–368.

Teske, A. P., & Sorensen, K. B. (2008). Uncultured archaea in deep marine subsurface sediments: have we caught them all? *The ISME Journal*, *2*(1), 3–18.

Tivey, M. A., Johnson, H. P., & Hole, W. (2002). Crustal magnetization reveals subsurface structure of Juan de Fuca Ridge hydrothermal vent fields. *Geology*, *30*(11), 979–982.

Tivey, Margaret K., & Delaney, J. R. (1986). Growth of large sulfide structures on the endeavour segment of the Juan de Fuca ridge. *Earth and Planetary Science Letters*, *77*(3-4), 303–317.

Tivey, Margaret Kingston. (1995). The influence of hydrothermal fluid composition and advection rates on black smoker chimney mineralogy: Insights from modeling transport and reaction. *Geochimica et Cosmochimica Acta*, *59*(10), 1933–1949.

Tivey, Margaret Kingston. (2000). Environmental Conditions Within Active Seafloor Vent Structures : Sensitivity to Vent Fluid Composition and Fluid Flow. *Geophysical Monograph*, 137–152.

Tivey, Margaret Kingston, Stakes, D. S., Cook, T. L., Hannington, M. D., & Petersen, S. (1999). A model for growth of steep-sided vent structures on the Endeavour Segment of the Juan de Fuca Ridge: Results of a petrologic and geochemical study. *Journal of Geophysical Research*, *104*(B10), 22859–22883.

Toner, B. M., Lesniewski, R. a., Marlow, J. J., Briscoe, L. J., Santelli, C. M., Bach, W., Edwards, K. J. (2013). Mineralogy Drives Bacterial Biogeography of Hydrothermally Inactive Seafloor Sulfide Deposits. *Geomicrobiology Journal*, *30*(4), 313–326.

Treude, T., Smith, C., Wenzhöfer, F., Carney, E., Bernardino, A., Hannides, A., Boetius, A. (2009). Biogeochemistry of a deep-sea whale fall: sulfate reduction, sulfide efflux and methanogenesis. *Marine Ecology Progress Series*, *382*, 1–21.

Utgikar, V., Harmon, S. M., Chaudhary, N., Tabak, H. H., Govind, R., & Haines, J. R. (2002). Inhibition of Sulfate-Reducing Bacteria by Metal Sulfide Formation in Bioremediation of. *Environmental Toxicology*, *17*(1), 40–48.

Utgikar, V. P., Tabak, H. H., Haines, J. R., & Govind, R. (2003). Quantification of toxic and inhibitory impact of copper and zinc on mixed cultures of sulfate-reducing bacteria. *Biotechnology and Bioengineering*, *82*(3), 306–312.

Valentine, D. L., Reeburgh, W. S., & Hall, R. (2000). New perspectives on anaerobic methane oxidation. *Environmental Microbiology*, *2*(5), 477–484.

Van de Graaf, A. A., de Bruijn, P., Robertson, L. A., Jetten, M. M., & Kuenen, J. G. (1996). Autotrophic growth of anaerobic ammonium oxidizing microorganisms in a fluidized bed reactor. *Microbiology*, *142*, 2187–2196.

Venter, J. C., Remington, K., Heidelberg, J. F., Halpern, A. L., Rusch, D., Eisen, J. A., Smith, H. O. (2004). Environmental genome shotgun sequencing of the Sargasso Sea. *Science*, *304*(5667), 66–74.

Ver Eecke, H. C., Kelley, D. S., & Holden, J. F. (2009). Abundances of hyperthermophilic autotrophic Fe(III) oxide reducers and heterotrophs in hydrothermal sulfide chimneys of the northeastern Pacific Ocean. *Applied and Environmental Microbiology*, *75*(1), 242–245.

Vetriani, C., Speck, M. D., Ellor, S. V., Lutz, R. A., & Starovoytov, V. (2004). Thermovibrio ammonificans sp. nov., a thermophilic, chemolithotrophic, nitrate-ammonifying bacterium from deep-sea hydrothermal vents. *International Journal of Systematic and Evolutionary Microbiology*, *54*, 175–181.

Von Damm, K. L. (1988). Systematics of and postulated controls on submarine hydrothermal solution chemistry. *Journal of Geophysical Research*, *93*(B5), 4551.

Von Damm, K. L., Buttermore, L. G., Oosting, S. E., Bray, A. M., Fornari, D. J., Lilley, M. D., & Shanks, W. C. (1997). Direct observation of the evolution of a seafloor “black smoker” from vapor to brine. *Earth and Planetary Science Letters*, *149*(1-4), 101–111.

Von Damm, K., Oosting, S.., Kozlowski, R., Buttermore, L. G., Colodner, D. C., Edmonds, H.., Grebmeier, J. M. (1995). Evolution of East Pacific Rise hydrothermal vent fluids following a volcanic eruption. *Nature*, *375*(4), 47–50.

Voordeckers, J. W., Starovoytov, V., & Vetriani, C. (2005). Caminibacter mediatlanticus sp. nov., a thermophilic, chemolithoautotrophic, nitrate-ammonifying bacterium isolated from a deep-sea hydrothermal vent on the Mid-Atlantic Ridge. *International Journal of Systematic and Evolutionary Microbiology*, *55*, 773–779.

Wagner, M., Roger, A. J., Flax, J. L., Brusseau, G. A., & Stahl, D. A. (1998). Phylogeny of dissimilatory sulfite reductases supports an early origin of sulfate respiration. *Journal of Bacteriology*, *180*(11), 2975–2982.

Wang, S., Xiao, X., Jiang, L., Peng, X., Zhou, H., Meng, J., & Wang, F. (2009). Diversity and Abundance of Ammonia-Oxidizing Archaea in Hydrothermal Vent Chimneys of the Juan de Fuca Ridge Diversity and Abundance of Ammonia-Oxidizing Archaea in Hydrothermal Vent Chimneys of the Juan de Fuca Ridge. *Applied and Environmental Microbiology*, *75*(12) 4216–4220.

Wankel, S. D., Germanovich, L. N., Lilley, M. D., Genc, G., DiPerna, C. J., Bradley, A. S., Girguis, P. R. (2011). Influence of subsurface biosphere on geochemical fluxes from diffuse hydrothermal fluids. *Nature Geoscience*, *4*(7), 461–468.

Wankel, S. D., Joye, S. B., Samarkin, V. a., Shah, S. R., Friederich, G., Melas-Kyriazi, J., & Girguis, P. R. (2010). New constraints on methane fluxes and rates of anaerobic methane oxidation in a Gulf of Mexico brine pool via in situ mass spectrometry. *Deep Sea Research Part II: Topical Studies in Oceanography*, *57*(21-23), 2022–2029.

Weber, A., & Jørgensen, B. B. (2002). Bacterial sulfate reduction in hydrothermal sediments of the Guaymas Basin, Gulf of California, Mexico. *Deep-Sea Research Part I-Oceanographic Research Papers*, *49*(5), 827–841.

Weijma, J., Stams, A. J., Hulshoff Pol, L. W., & Lettinga, G. (2000). Thermophilic sulfate reduction and methanogenesis with methanol in a high rate anaerobic reactor. *Biotechnology and Bioengineering*, *67*(3), 354–363.

Wery, N., Cambon-Bonavita, M. A., Lesongeur, F., & Barbier, G. (2002). Diversity of anaerobic heterotrophic thermophiles isolated from deep-sea hydrothermal vents of the Mid-Atlantic Ridge. *FEMS Microbiology Ecology*, *41*(2), 105–114.

Westrich, J. T., & Berner, R. A. (1984). The role of sedimentary organic matter in bacterial sulfate reduction: The G model tested. *Limnology and Oceanography*, *29*(2), 236–249.

Wheat, C. G., McManus, J., Mottl, M. J., & Giambalvo, E. (2003). Oceanic phosphorus imbalance: Magnitude of the mid-ocean ridge flank hydrothermal sink. *Geophysical Research Letters*, *30*(17).

Wilmes, P., & Bond, P. L. (2009). Microbial community proteomics: elucidating the catalysts and metabolic mechanisms that drive the Earth's biogeochemical cycles. *Current Opinion in Microbiology*, *12*(3), 310–317.

Wirsen, C. O., & Molyneaux, J. (1993). Chemosynthetic Microbial Activity at Mid-Atlantic Ridge Hydrothermal Vent Sites the Atlantic. *Journal of Geophysical Research*, *98*(B6), 9693–9703.

Wolfaardt, G. M., Lawrence, J. R., Robarts, R. D., & Caldwell, D. E. (1994). The role of interactions , sessile growth , and nutrient amendments on the degradative efficiency of a microbial consortium more I4co2. *Canadian Journal of Microbiology*, *40*, 331–340.

Xie, W., Wang, F., Guo, L., Chen, Z., Sievert, S. M., Meng, J., Xu, A. (2011). Comparative metagenomics of microbial communities inhabiting deep-sea hydrothermal vent chimneys with contrasting chemistries. *The ISME Journl*, *5*(3), 414–426.

Xu, N., Christodoulatos, C., & Braida, W. (2006). Adsorption of molybdate and tetrathiomolybdate onto pyrite and goethite: effect of pH and competitive anions. *Chemosphere*, *62*(10), 1726–1735.

Yue, J. C., & Clayton, M. K. (2005). A similarity measure based on species proportions. *Communications in Statistics-Theory and Methods*, *34*(11), 2123–2131.

Zarzycki, J., Brecht, V., Müller, M., & Fuchs, G. (2009). Identifying the missing steps of the autotrophic 3-hydroxypropionate CO2 fixation cycle in Chloroflexus aurantiacus. *Proceedings of the National Academy of Sciences of the United States of America*, *106*(50), 21317–21322.

Zhang, Y., Zhao, Z., Chen, C.-T. A., Tang, K., Su, J., & Jiao, N. (2012). Sulfur metabolizing microbes dominate microbial communities in Andesite-hosted shallow-sea hydrothermal systems. *PloS One*, *7*(9), e44593.

Zhou, H. Y., Li, J. T., Peng, X. T., Meng, J., Wang, F. P., & Ai, Y. C. (2009). Microbial diversity of a sulfide black smoker in main endeavour hydrothermal vent field, Juan de Fuca Ridge. *Journal of Microbiology*, *47*(3), 235–247.

Zhu, W., Tivey, M. K., Gittings, H., & Craddock, P. R. (2007). Permeability-porosity relationships in seafloor vent deposits: Dependence on pore evolution processes. *Journal of Geophysical Research*, *112*(B5), 1–15.

APPENDIX A:

Supplemental Information for Chapter two

Supplemental Table A2.1: Primers used for the enumeration of 16S rRNA genes

Supplemental Table A2.1: Primers used for the enumeration of 16S rRNA genes

Target gene	Forward Primer	Conc [nM]	T (°C)*	Reverse Priemr	Conc [nM]	T (°C) *	Reference
Bacterial 16S	**Bact1369F-** CGGTGAATACGTTCYCGG	1000	59	**Prok1541R-** AAGGAGGTGATCC RGCCGCA	1000	59	(Suzuki *et al.* 2001)
Bacterial 16S[1]	**Gray28F –** GAGTTTGATCNTGGCTCAG	500	54	**Gray519R**- GTNTTACNGCGGCKGCTG	500	54	(modified from *Frias-lopez et al*., 2002; modified from Manefield *et al*., 2002)
Archaeal 16S	**Arch1-1369F-** CGGTGAATACGTCCCTGC **Arch2- 1369F**- CGGTGAATATGCCCCTGC	500 (1:1 Mix)	59	**Prok1541R**- AAGGAGGTGATCC RGCCGCA	1000	59	(Suzuki *et al.* 2001)
Archaeal 16S[1]	**Arch349F**- GYGCASCAGKCGMGAAW	500	54	**Arch806R**- GGACTACVSGGGTATCTAAT	500	54	(Takai & Horikoshi, 2000)

*Annealing temperature

1. Primers used for 454-pytrotag sequencing, all other primers used for qPCR.

APPENDIX B:

Supplemental Information for Chapter three

Supplemental Information-Methods: Detailed methods of chromium distillation, qPCR plasmid cloning and 454 sequence processing via mother.

Supplemental Table B3.1: *dsrB* sequence tag and alpha diversity characteristics

B.3 Supplemental Information Methods

B.3.1 Chromium distillation for determining rates of sulfate reduction

Using this method, 1 gram (wet weight) of crushed mineral (about 60% mineral, 30% interstitial fluid) was added to 10 mL of a 1:1 ethanol to water solution in the chromium distillation apparatus, and then degassed with nitrogen for 15 minutes to achieve anaerobicity. 8 mL of 12 N HCl and 16 mL of 1 M reduced chromium chloride was added anaerobically to the chamber and gently heated to a slow boil for 3 hours to evolve hydrogen sulfide gas. The resulting sulfide gas was carried via nitrogen gas through a condenser to remove any ethanol or water vapor, and was then trapped as zinc sulfide in a 25% zinc acetate solution. The radioactivity of the resulting sulfide ($Zn^{35}S$) and the remaining sulfate from the supernatant ($^{35}SO_4^{2-}$) were measured via liquid scintillation counter in Ultima Gold scintillation cocktail (ThermoFisher Inc., Waltham, MA).

B.3.2 Conversion of rates previously described in sediments.

Conventionally, published sulfate reduction rates from sediment systems are reported as volumetric rates in units of nmol S $cm^{3\ -1}$ day^{-1}. Due to the challenges associated with working with crushed mineral, accurate volumetric subsampling for each sample was difficult to replicate. Because of this, each incubation was subsampled by mass (wet weight). Published volumetric rates (mol/cm^3day) were converted to units of mol g^{-1} day^{-1} using either published density values of associated sediment samples or assuming an average sediment density of approximately 2 g/cm^3.

B.3.3 Plasmid generation for qPCR standard curves

Standard curves for total bacterial and archaeal 16S rRNA genes were constructed as above from serial dilutions (10^8 to 10^1 copies μl^{-1} TE) of plasmids containing inserts of the 16S rRNA gene from *Arcobacter nitrofigulis* (ATCC 33309) and *Methanosarcina acidovorans* respectively. Standards for functional genes of interest were generated using *Desulfovibrio vulgaris* Hildenborough (ATCC 29579/ NCIMB 8303/ AE017285) as template for amplification of target genes, which were then cloned using the Strataclone vector (Agilent Technologies Inc.) following the manufacturer's instructions. Plasmids were extracted using the Qiaprep Minispin™ kit (Qiagen Inc), quantified with Quanti-iT™ PicoGreen (Life Technologies) on a Spectramax™ Gemini XS fluorometer (Molecular Devices Inc.), linearized and serially diluted into aliquots from 10^8 to 10^1 copies μL^{-1} in 10 mM Tris-EDTA buffer.

B.3.4 Sequencing and Phylogenetic Analysis via 454 pyrosequencing

The resulting 454 datasets were processed via Mothur (Schloss et al., 2009). Sequencing error was reduced by running the Mothur implementation of the AmpliconNoise algorithm (shhh.seqs). The 16S rRNA gene sequence data was aligned to the SILVA-compatible alignment database reference alignment (Schloss, 2009). Sequences were screened and selected to start at the same position, then those sequences within 2 bp of a more abundant sequence were merged in a pre clustering step, in which a difference of 1 bp per 100 bp of sequence length was allowed. Chimeric sequences were identified and removed using the command chimera.uchime, which uses the abundant sequences in the sample set as a reference database. Sequences were classified using the Mothur version of the "Bayesian" classifier

against the Grenegenes99 database (Werner et al., 2012). Contaminating sequences, those affiliated with organelles such as chloroplasts and mitochondria, were removed. Operational taxanomic units (OTUs) were built by generating a distance matrix with pairwise distance lengths smaller than 0.15. The data were then clustered and each OTU was classified.

Supplementary Table B3.1: *dsrB* sequence tag and alpha diversity characteristics

Sample	Sampled Reads	OTU (97%)	coverage	npshannon	simpson	chao
ChowderHill_dsr	1342	312	0.83234	4.447181	0.054399	942
DeadDog_dsr	1342	270	0.859911	4.445753	0.035912	973.12
Needles_dsr	1342	293	0.842027	4.404188	0.053839	1121.37

Supplemental References:

Schloss, P. D. (2009). A high-throughput DNA sequence aligner for microbial ecology studies. *PloS one*, *4*(12), e8230.

Schloss, P. D., Westcott, S. L., Ryabin, T., Hall, J. R. A., Hartmann, M., Hollister, E. B., Lesniewski, R. a, et al. (2009). Introducing mothur: open-source, platform-independent, community-supported software for describing and comparing microbial communities. *Appl. Environ. Microbiol.*, *75*(23), 7537-7541.

Werner, J. J., Koren, O., Hugenholtz, P., DeSantis, T. Z., Walters, W. a, Caporaso, J. G., Angenent, L. T., et al. (2012). Impact of training sets on classification of high-throughput bacterial 16s rRNA gene surveys. *ISME J*, *6*(1), 94-103.

APPENDIX C:

Supplemental Information for Chapter four

Supplemental Figure C4.1: Scanning electron microscope (SEM) images of crushed Grotto flange

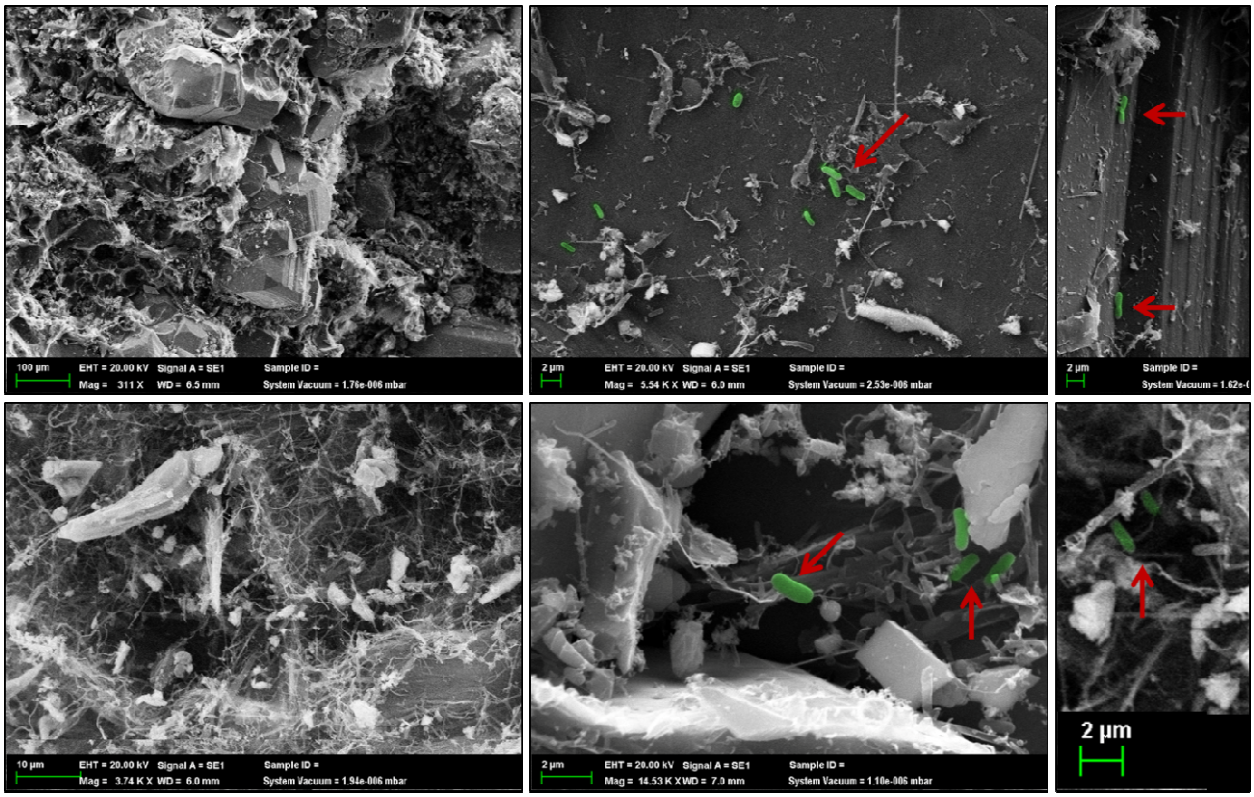

Supplemental Figure C4.1: Scanning electron microscope (SEM) images of crushed Grotto flange with a fine layer of gold palladium on the EVO SEM. Scale bars represent (a) 100µm, (b) 10µm and (c-f) 2µm. Microbes (confirmed with EDAX scan of consisting primarily of carbon) are highlighted in green.